2

PAGES -99
CAT. 31

UNIDEV, INC. HOLIDAY OFFICE CENTER, HUNTSVILLE, ALABAMA

EVALUATION OF SKYLAB IB SENSITIVITY TO ON-PAD WINDS WITH TURBULENCE

CR-123564

by
T. Coffin

UNIDEV, INC.
HUNTSVILLE, ALABAMA

January 1972

CONTRACT NO. NAS8-26702
UNIDEV REPORT NO. UR-72-00014

Submitted to:

GEORGE C. MARSHALL SPACE FLIGHT CENTER
NATIONAL AERONAUTICS & SPACE ADMINISTRATION
HUNTSVILLE, ALABAMA 35812

EVALUATION OF SKYLAB IB SENSITIVITY TO ON-PAD WINDS WITH TURBULENCE

by
T. Coffin

UNIDEV, INC.
HUNTSVILLE, ALABAMA

January 1972

CONTRACT NO. NAS8-26702
UNIDEV REPORT NO. UR-72-00014

Submitted to:

GEORGE C. MARSHALL SPACE FLIGHT CENTER
NATIONAL AERONAUTICS & SPACE ADMINISTRATION
HUNTSVILLE, ALABAMA 35812

FOREWORD

This report presents an evaluation of SKYLAB IB vehicle response to the pre-launch wind environment. The report was prepared by UNIDEV, Inc., for the George C. Marshall Space Flight Center, National Aeronautics and Space Administration, under Contract NAS8-26702 entitled "Assessment of Wind Induced Oscillation of the SKYLAB IB/LC-39 Configuration". The work was administered under technical direction of the Aero-Astrodynamics Laboratory with Messrs. R. Beranek and J. Poe acting as technical monitors.

Dr. L. L. Fontenot, Technical Director, performed as Program Manager. The study was executed by the Research and Development Division, directed by Mr. T. Coffin, who served as Principal Investigator. Computer programming support was provided by Mr. Y. C. Lee.

ABSTRACT

Computer simulation was performed to estimate displacements and bending moments experienced by the SKYLAB IB vehicle on the launch pad due to atmospheric winds. The vehicle was assumed a beam-like structure represented by a finite number of generalized coordinates. Wind flow across the vehicle was treated as a non-homogeneous, stationary random process. Response computations were performed by the assumption of simple "strip theory" and application of generalized harmonic analysis. Displacement and bending moment statistics were obtained for six vehicle propellant loading conditions and four representative reference wind profile and turbulence levels. Means, variances and probability distributions are presented graphically for each case. A separate analysis was performed to indicate the influence of wind gradient variations on vehicle response statistics.

TABLE OF CONTENTS

LIST OF ILLUSTRATIONS

LIST OF TABLES

Section I

INTRODUCTION

The SKYLAB IB vehicle is to be launched from a pedestal constructed on the Launch Umbilical Tower (LUT) base platform. During the period of launch preparation and count-down, various propellant loading conditions are sequenced, resulting in a concurrent variation in vehicle aeroelastic characteristics. At the same time the vehicle is exposed to the atmospheric wind environment dictated by Nature. This report presents an evaluation of displacements and bending moments experienced by the SKYLAB IB supported on its launch pedestal. The results provide an indication of structural integrity and clearance requirements with respect to the ground wind environment.

The Saturn IB vehicles assigned the SKYLAB project are AS-206, AS-207 and AS-208. Available information/1,2,3,4,5/ indicates that the three configurations are very similar in structural dynamic characteristics. All results reported in this document are based on AS-207 structural dynamic parameters as defined in /4/.

Six propellant loading configurations were analyzed for fill conditions ranging from all tanks empty to the completely fueled vehicle at ignition. For each configuration, four reference wind speeds at the 18.3m (60 ft.) level ranging from 10.3 meters/second (20 knots) to 41.2 meters/second (80 knots), were considered. In the above cases the three sigma wind speed profile based on /6/ was utilized. A separate analysis was performed to indicate the influence of wind speed gradient with a fixed reference wind speed.

Section II

DESCRIPTION OF MATHEMATICAL MODEL

2.1 VEHICLE DESCRIPTION

A sketch of the SKYLAB IB and support system is illustrated in Figure 2.1. The launch pedestal is 39 meters (128 ft.) high, bringing the vehicle tip 107 meters (351 ft) above the LUT base. Vehicle station zero is located approximately 53.7 meters (176 ft.) above mean grade.

Bending characteristics utilized to synthesize the system are based on a multibeam lateral vibration analysis reported in /4/. The model includes two explicit degrees of freedom for the launch pedestal, one in translation and one in rotation. The pedestal was considered unattached to the LUT (tie structure sliding) and the external damper system assumed inactive.

Structural dynamic characteristics representing the following six propellant loading conditions were analyzed.

Table 2.1. PROPELLANT LOADING CONDITIONS

Case	Service Module	S-IB RP-1	S-IB LOX	S-IVB LOX	S-IVB LH_2
1	empty	empty	empty	empty	empty
2	full	empty	empty	empty	empty
3	full	full	empty	empty	empty
4	full	full	full	empty	empty
5	full	full	full	full	empty
6	full	full	full	full	full

2.2 RESPONSE SIMULATION

Response simulation was performed utilizing ground wind profiles based on /6/. Mean-square density spectra of the atmospheric turbulence at Cape Kennedy were obtained from /7,8/. Each propellant loading condition was analyzed assuming four representative reference wind speeds at the 18.3 meter (60 ft.)

level and associated turbulence characteristics. Reference wind speeds selected are summarized in Table 2.2.

Table 2.2. SUMMARY OF REFERENCE WIND SPEEDS

REFERENCE PEAK WIND		REFERENCE MEAN WIND	
meters/sec.	knots	meters/sec.	knots
10.30	20	6.54	12.713
20.58	40	13.6	26.436
30.87	60	20.5	39.84
41.16	80	27.35	53.156

A separate simulation was performed to illustrate the influence of wind speed gradient on response statistics for a fixed reference wind speed. In this analysis a single propellant loading configuration was simulated with a fixed reference peak wind speed of 41.16 M/S and four profile shapes representing varying probabilities of occurrence based on /6/.

Displacement and bending moment statistics were computed by modification and extension of a digital program developed previously /9/. The local wind-induced load intensity was assumed proportional to the square of local relative wind speed directed as the relative velocity plus an "inertia load" proportional to, and directed as local relative acceleration. Generalized harmonic analysis was performed, assuming the load distribution representative of a stationary, non-homogeneous process. Lift and drag response estimates were obtained separately, assuming statistical independence. By assuming lift and drag responses jointly normal (which implies the same of the excitation), density and distribution functions representing resultant (vector sum) response at selected vehicle locations were obtained.

In the above analysis, the SKYLAB IB was synthesized by 53 discrete elements assigned appropriate local geometric and modal characteristics. A structural damping ratio of (1.5%) critical (viscous) was assumed for all modes. Three vehicle modes were used in the response expansion. A summary of results is presented in the following Section.

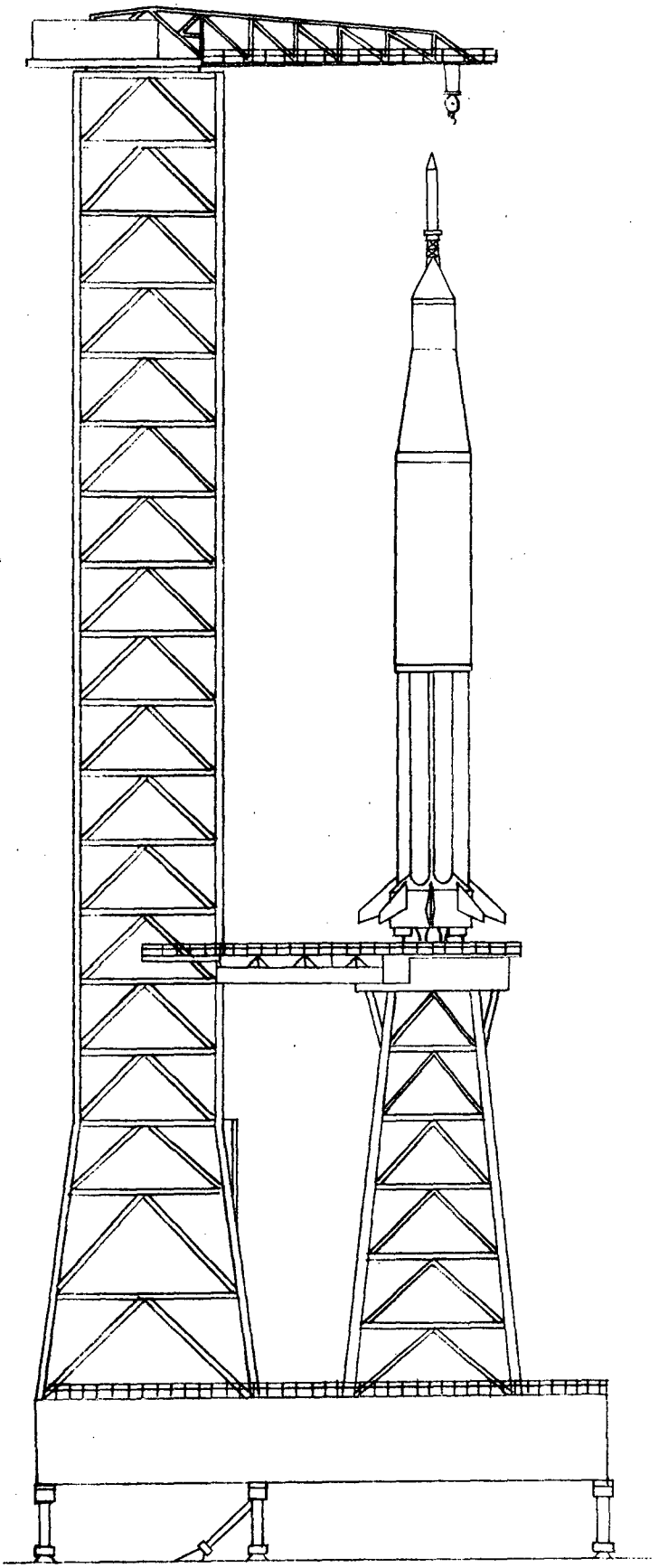

FIG. 2.1 SKYLAB IB LAUNCH CONFIGURATION

Section III

DISCUSSION AND SUMMARY OF RESULTS

3.1 INTRODUCTORY REMARKS

Displacement and bending moment mean values, variances and joint statistics are illustrated in Sections V and VI. Section V indicates results for six propellant loading conditions and four representative reference wind speeds. For all propellant loading conditions the "three sigma" peak /6/ wind profile was assumed. Section VI indicates the influence of wind speed gradients on vehicle response statistics for a fixed reference wind speed.

The analysis performed herein is based on the vehicle being representative of a "beam-like" structure. In reality, the SIB stage consists of a cluster of eight tanks surrounding a center barrel. Moments and resulting stresses experienced at a specific tank location must be evaluated utilizing appropriate tank modes. For each vehicle and wind condition considered, 12 statistical parameters were computed and are illustrated in Sections V and VI:

Mean drag displacement and bending moment

Lift and drag displacement and bending moment variances

Absolute displacement and bending moment associated with concurrent lift and drag response

Probability density and distribution functions for resultant tip displacement and base bending moment.

By "drag" and "lift" are meant the directions parallel to mean grade in-line with, and orthogonal to the mean wind vector, respectively. As a gross indicator of wind sensitivity, the figures illustrating displacement and bending moment associated with concurrent three sigma lift and drag response as a function of vehicle station permit a quick-look assessment of each condition.

3.2 RESPONSE FOR VARYING PROPELLANT FILL CONDITIONS AND WIND SPEEDS

Response statistics for six propellant fill conditions and four reference wind speeds are presented in Section V. Absolute tip displacement and base bending moment (assuming 3 sigma lift and drag response) are summarized in

Table 3-1 for the six propellant fill conditions analyzed and peak reference wind speeds of 80 kt. and 20 kt. It may be observed that a maximum base bending moment of 8.65 x 10^6 N.M. occurred for Cases 5 and 6 and a maximum tip displacement of 76.5 cm (Case 6). The trend of increasing response with Case number appears reasonable since concurrently the natural frequencies are reduced and the turbulence spectra are concentrated in the low frequency range. The Case 2 results appear suspect, since a decrease in tip deflection is accompanied by an increase in base bending moment. This discrepancy is most likely due to variability in structural dynamic parameter computations (bending moment mode shapes?).

Table 3-1. ABSOLUTE DISPLACEMENT AND BENDING MOMENT FOR 80 KT AND 20 KT REFERENCE WINDS

CASE	TIP DISPLACEMENT (cm)		BASE BENDING MOMENT (N.M. x 10^{-6})	
	41.16 m/s (80 kt)	10.3 m/s (20 kt)	41.16 m/s 80 kt)	10.3 m/s (20 kt)
1	68.92	5.37	6.99	0.565
2	68.84	5.307	7.07	0.565
3	71.39	5.53	7.48	0.592
4	72.75	5.604	7.89	0.603
5	76.19	5.793	8.65	0.651
6	76.52	5.772	8.65	0.644

A brief comparison was performed to estimate the relative contribution of fluctuating lift and drag forces. Figure 3-2 illustrates R.M.S. lift to drag ratios of tip displacement and base bending moment for the Cases and peak reference wind speeds noted. (The term "R.M.S." is used loosely to define the square root of variance, i.e., no mean contribution is included.)

At the higher wind speed the drag contribution is seen to be highly dominant and increasing with case number. This appears consistent with /7, 8/ which indicates the drag turbulence more highly correlated in space for neutral winds. Also, spacial correlation increases with decreasing frequency and vehicle natural frequencies reduce with increasing Case number, as noted previously. For the lower wind speed the drag contribution is far less dominant

Table 3-2. COMPARISON OF FLUCTUATING LIFT AND DRAG CONTRIBUTIONS TO TIP DISPLACEMENT AND BASE BENDING MOMENT

CASE	R.M.S. LIFT DISPLACEMENT / R.M.S. DRAG DISPLACEMENT		R.M.S. LIFT BENDING MOMENT / R.M.S. DRAG BENDING MOMENT	
	41.16 m/s (80 kt)	10.3 m/s (20 kt)	41.16 m/s (80 kt)	10.3 m/s (20 kt)
1	0.730	0.940	0.730	0.970
2	0.719	0.930	0.719	0.930
3	0.716	0.929	0.715	0.929
4	0.680	0.870	0.678	0.866
5	0.669	0.840	0.667	0.835
6	0.652	0.817	0.649	0.812

although the same trend with Case number occurs. The results indicate a shift in dominant excitation from drag towards lift turbulence with decreasing wind speed. This is again consistent with /7,8/.

3.3 SUMMARY OF RESULTS FOR A FIXED REFERENCE WIND SPEED AND VARYING GRADIENT

Response statistics for the Case 5 vehicle configuration subjected to a fixed reference wind with varying profile statistics are illustrated in Section VI. Absolute tip displacements and base bending moments for the four profiles considered are summarized in Table 3-3. It should be noted that in this section and Section VI the term "mean" denotes the average peak wind. It is interesting to note that over the range of confidence levels selected a considerably larger spread in response statistics may be obtained than through variation in propellant loading; compare Tables 3-1 and 3-3.

Table 3-3. ABSOLUTE DISPLACEMENT AND BENDING MOMENT FOR A FIXED REFERENCE WIND WITH VARYING GRADIENT

PEAK WIND PROFILE STATISTICS	TIP DISPLACEMENT (cm) 41.16 m/s (80 kt)	BASE BENDING MOMENT (N.M. x 10^{-6}) 41.16 m/s (80 kt)
Mean + 3σ	76.19	8.653
Mean + 2σ	71.45	8.124
Mean + σ	67.02	7.630
Mean	62.78	7.156

A brief comparison of fluctuating lift and drag contribution to response was performed for the four confidence levels evaluated and an 80 kt. reference wind. The ratio (R.M.S. lift/R.M.S. drag) did not vary significantly from approximately 0.67. However, a definite trend of increasing ratio with decreasing confidence level was observed. This trend is consistent with results of the previous sub-section since a decreasing confidence level results in a decreasing wind speed at elevations above the reference level.

Section IV

REFERENCES

1. Cobb, W. A.; "Projected Mass Characteristics SL-2(AS-206/CSM 116)", Memorandum S&E-ASTN-SAE 71-20, Marshall Space Flight Center, March, 1971.

2. Isbell, T. B.; "Mass Characteristics, AAP-3(AS-207/CSM 117)", Memorandum S&E-ASTN-SAE-69-96, Marshall Space Flight Center, November, 1969.

3. Isbell, T. B.; "Mass Characteristics, AAP(AS-208/CSM 118)", Memorandum S&E-ASTN-SAE-69-97, Marshall Space Flight Center, November, 1969.

4. de la Garza, E.; "Summary of Saturn IB SKYLAB 2 Coupled Vehicle/Pedestal Bending Characteristics", Technical Bulletin TB-AP-71-180, Chrysler Corporation, Space Division, New Orleans, La., March, 1971.

5. Lee, T. N., and Sato, T.; "Dynamic Characteristic, Saturn-IB-Pedestal and Launch Umbilical-Tower with Damper Connected and Tie-Structure Sliding", Technical Report HSM-R5-71, Chrysler Corporation Huntsville Division, April, 1971.

6. Fichtl, G. H.; "Distribution of Peak Ground Wind Profile Shapes for Mission Planning and Operations", Marshall Space Flight Center Memorandum R-AERO-YE-176-69, January 1969.

7. Fichtl, G. H.; "Design Ground Wind Spectra of Atmospheric Turbulence", Marshall Space Flight Center Memorandum S&E-AERO-YE-185-69, March 1969.

8. Fichtl, G. H. and McVehil, G. E.; "Longitudinal and Lateral Spectra of Turbulence in the Atmospheric Boundary Layer", NASA TN D5584, February 1970.

9. Coffin, T.,; "Computer Simulation of Saturn V Response to Pre-Launch Wind Loads", Report UR-00012, UNIDEV, Inc., November, 1970.

Section V

RESULTS OF SIMULATION FOR VARYING PROPELLANT LOAD CONDITIONS AND REFERENCE WIND SPEEDS

In this section, drag, lift and resultant statistics are presented for six propellant loading conditions and four representative reference wind speeds. By "drag" is meant the direction parallel to the quasi-mean wind vector, "lift" being perpendicular, both components parallel to mean grade. All results are based on "three sigma" wind profiles derived from /6/. Propellant loading condition and structural dynamic characteristics are summarized with data for each case. Assumed wind conditions are noted on each Figure.

5.1 SUMMARY OF PROPELLANT LOAD CONDITIONS AND STRUCTURAL DYNAMIC CHARACTERISTICS FOR CASE 1

Propellant Loading Configuration

Service Module	S-IB RP-1	S-IB LOX	S-IVB LOX	S-IVB LH_2
empty	empty	empty	empty	empty

Structural Dynamic Characteristics

Mode No.	Natural Frequency Hz	Generalized Mass kg.(lb.sec.^{2}/in)	Structural Damping Ratio
1	0.510748	10609.18(60.5830)	0.015
2	1.75214	3020.79(17.2499)	0.015
3	2.70250	6976.71(39.8411)	0.015

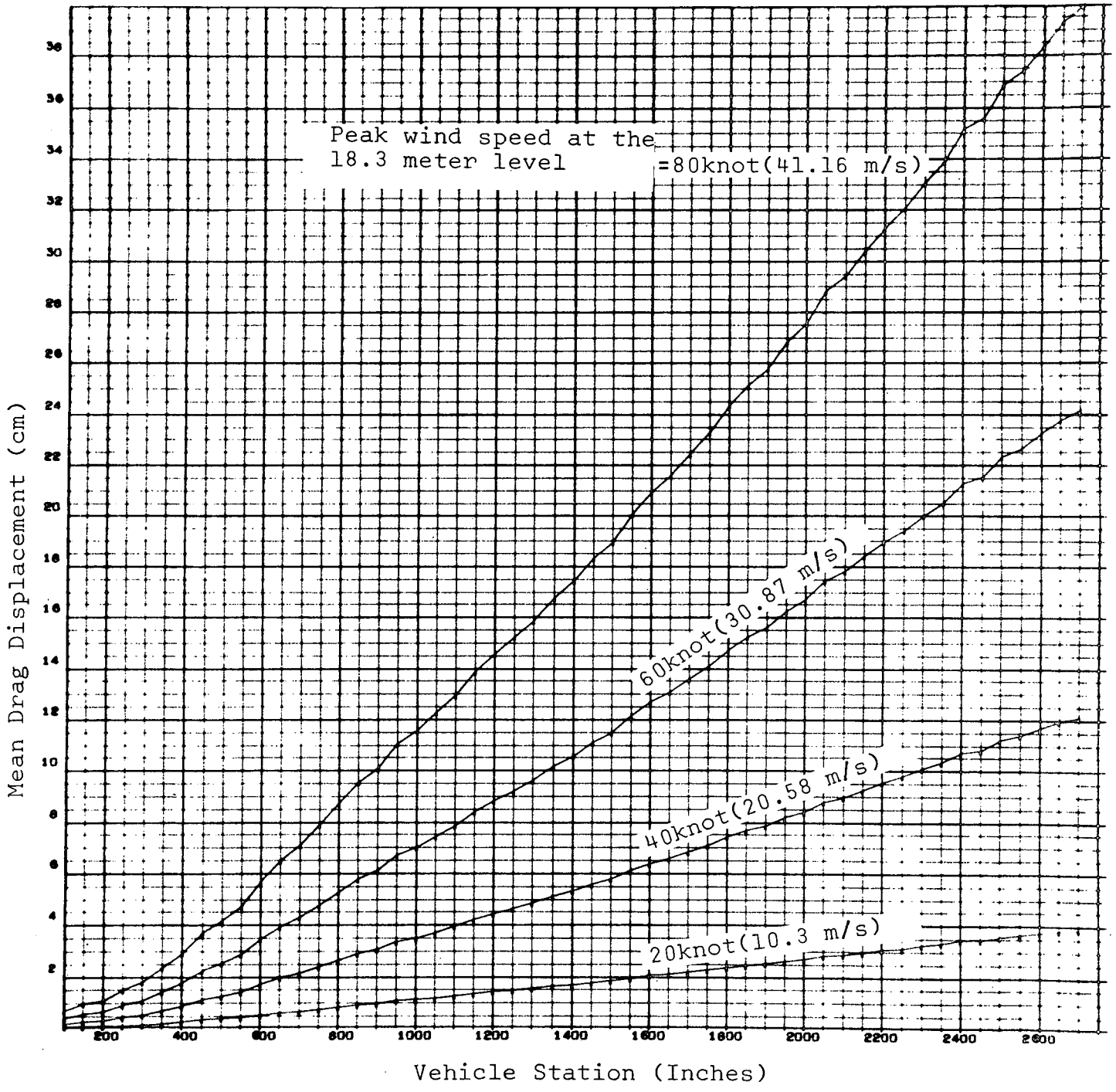

FIG. 5.1.1 MEAN DRAG DISPLACEMENT VERSUS VEHICLE STATION

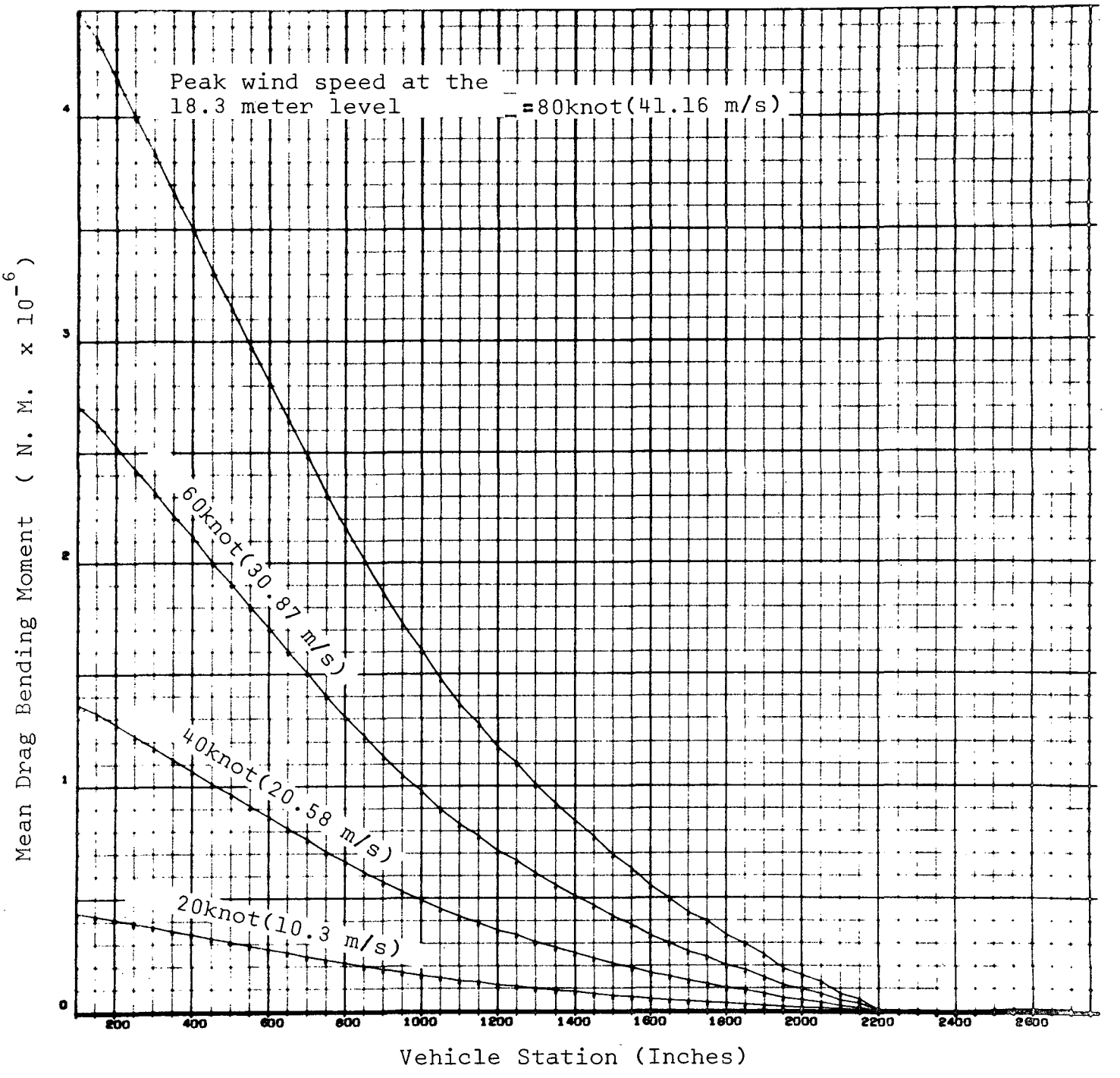

FIG. 5.1.2 MEAN DRAG BENDING MOMENT VERSUS VEHICLE STATION

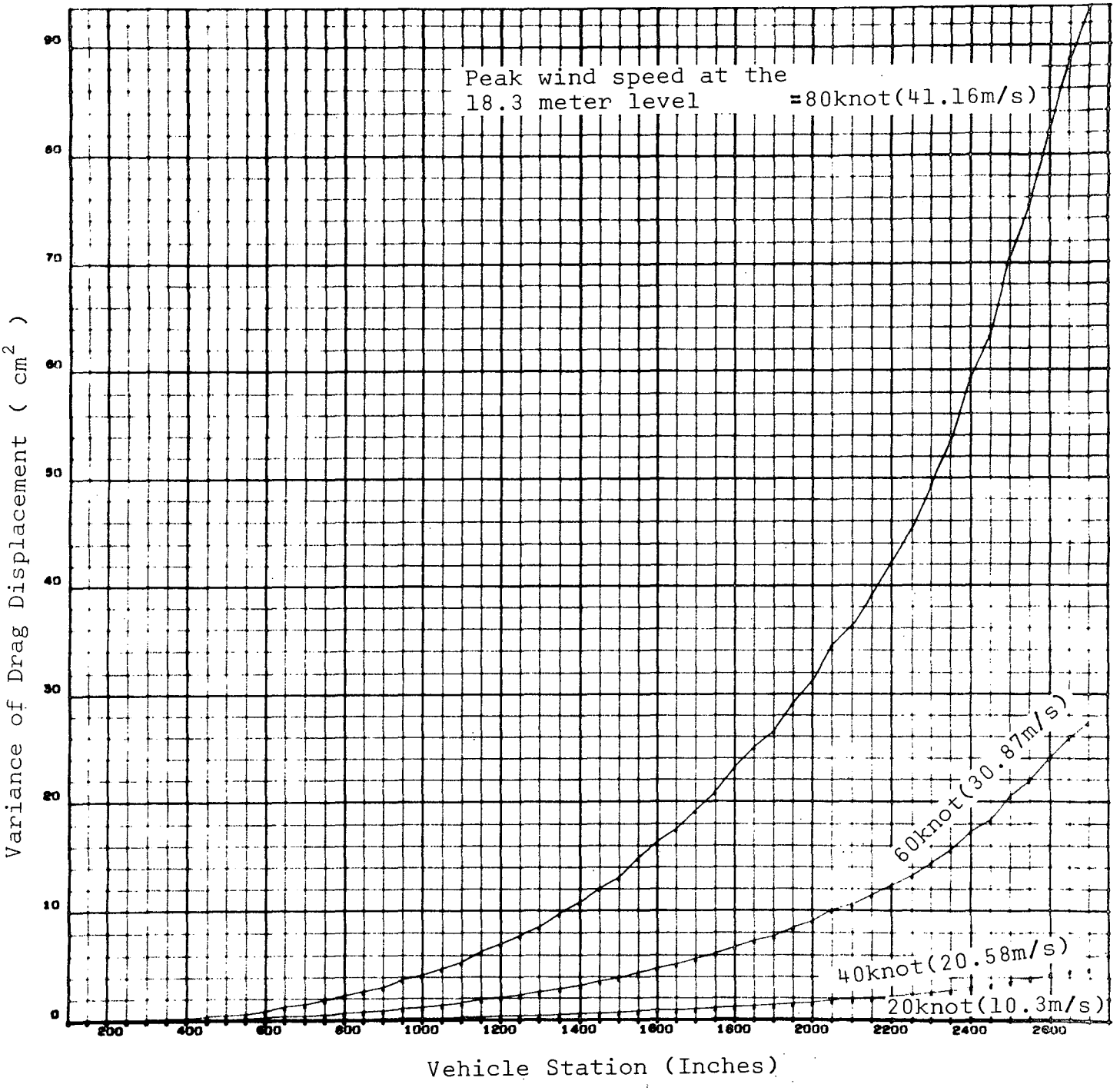

FIG. 5.1.3 VARIANCE OF DRAG DISPLACEMENT VERSUS VEHICLE STATION

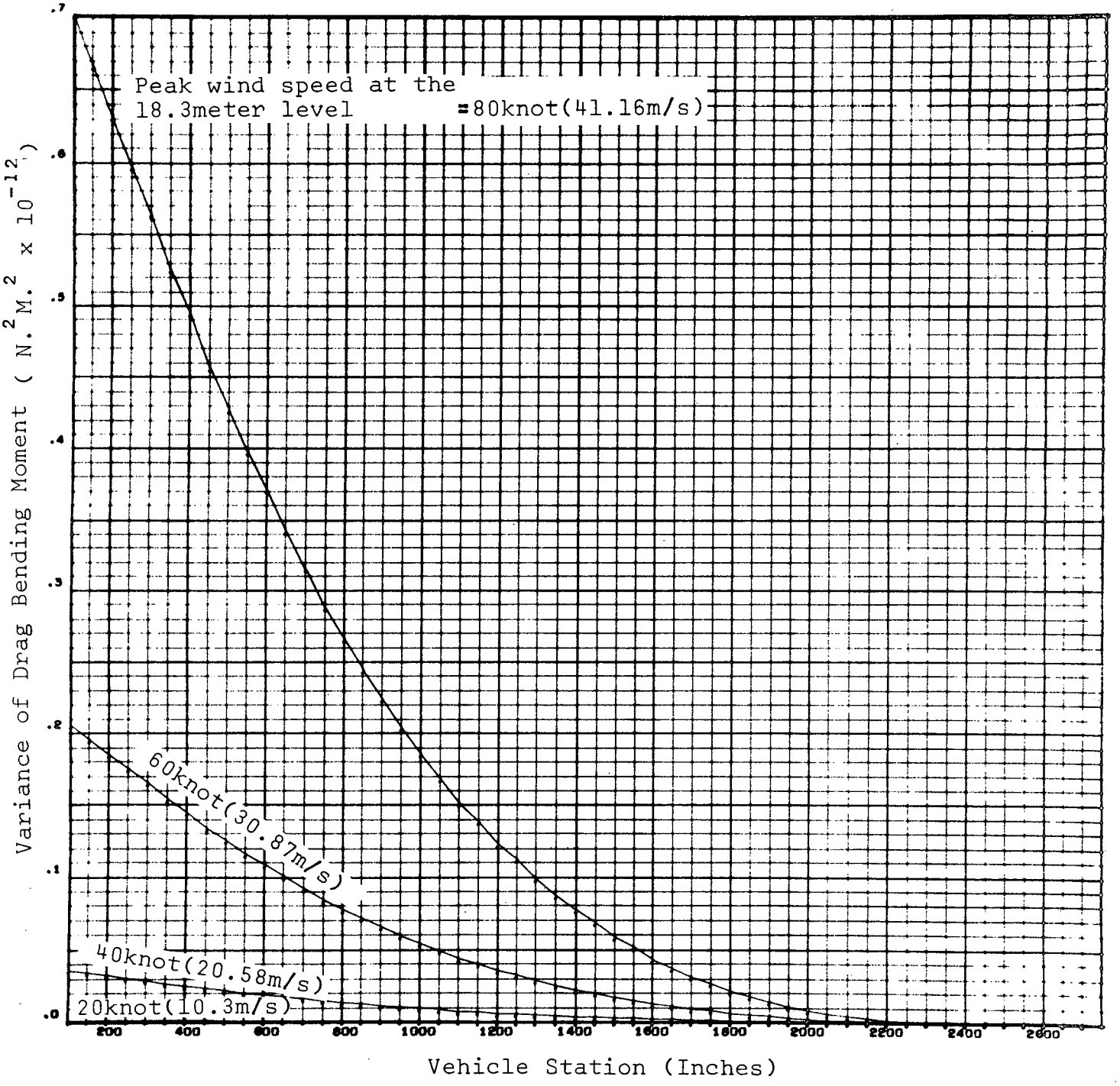

FIG. 5.1.4 VARIANCE OF DRAG BENDING MOMENT VERSUS VEHICLE STATION

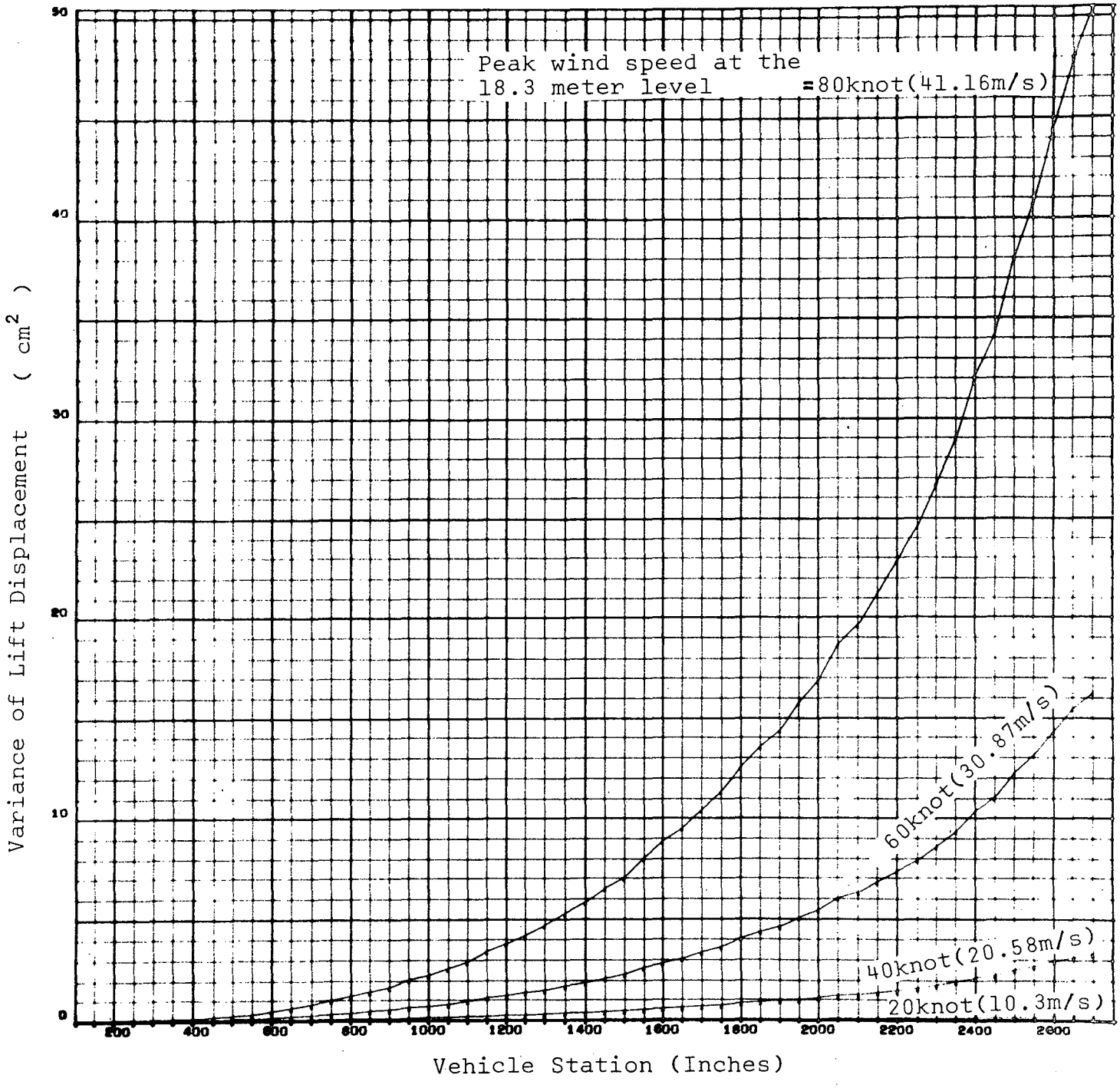

FIG. 5.1.5 VARIANCE OF LIFT DISPLACEMENT VERSUS VEHICLE STATION

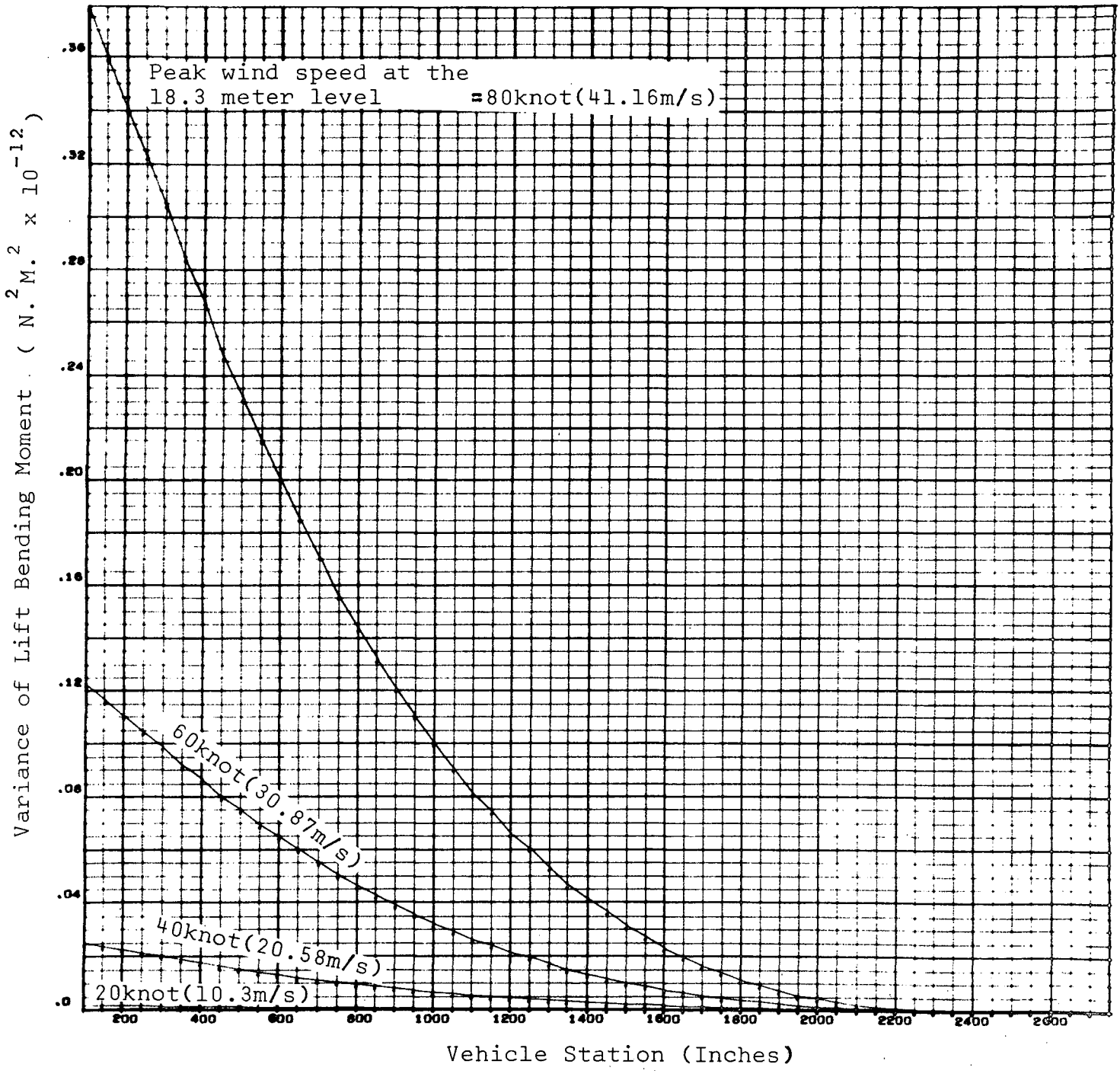

FIG. 5.1.6 VARIANCE OF LIFT BENDING MOMENT VERSUS VEHICLE STATION

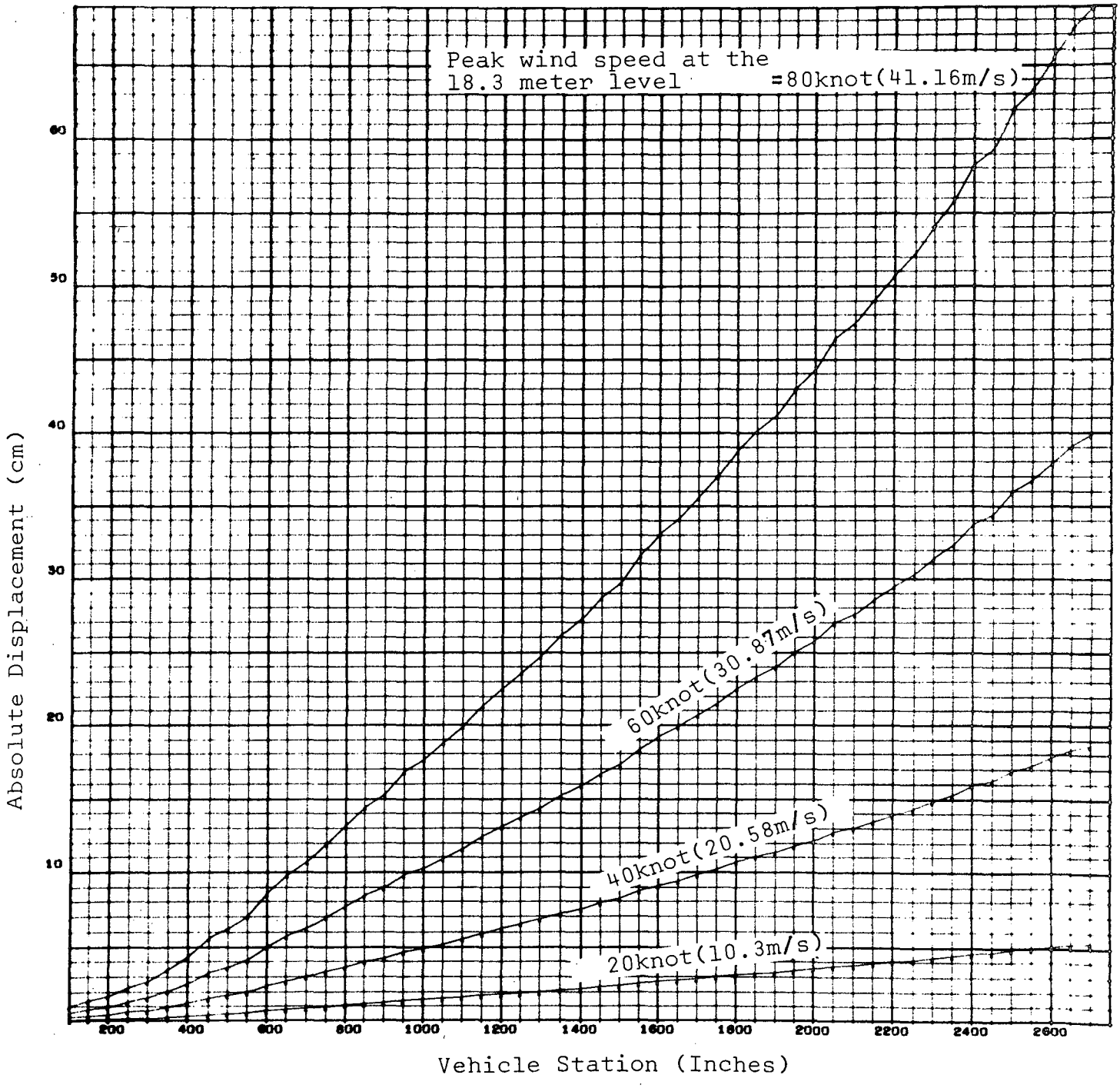

FIG. 5.1.7 ABSOLUTE DISPLACEMENT VERSUS VEHICLE STATION FOR CONCURRENT 3 SIGMA LIFT AND DRAG RESPONSE

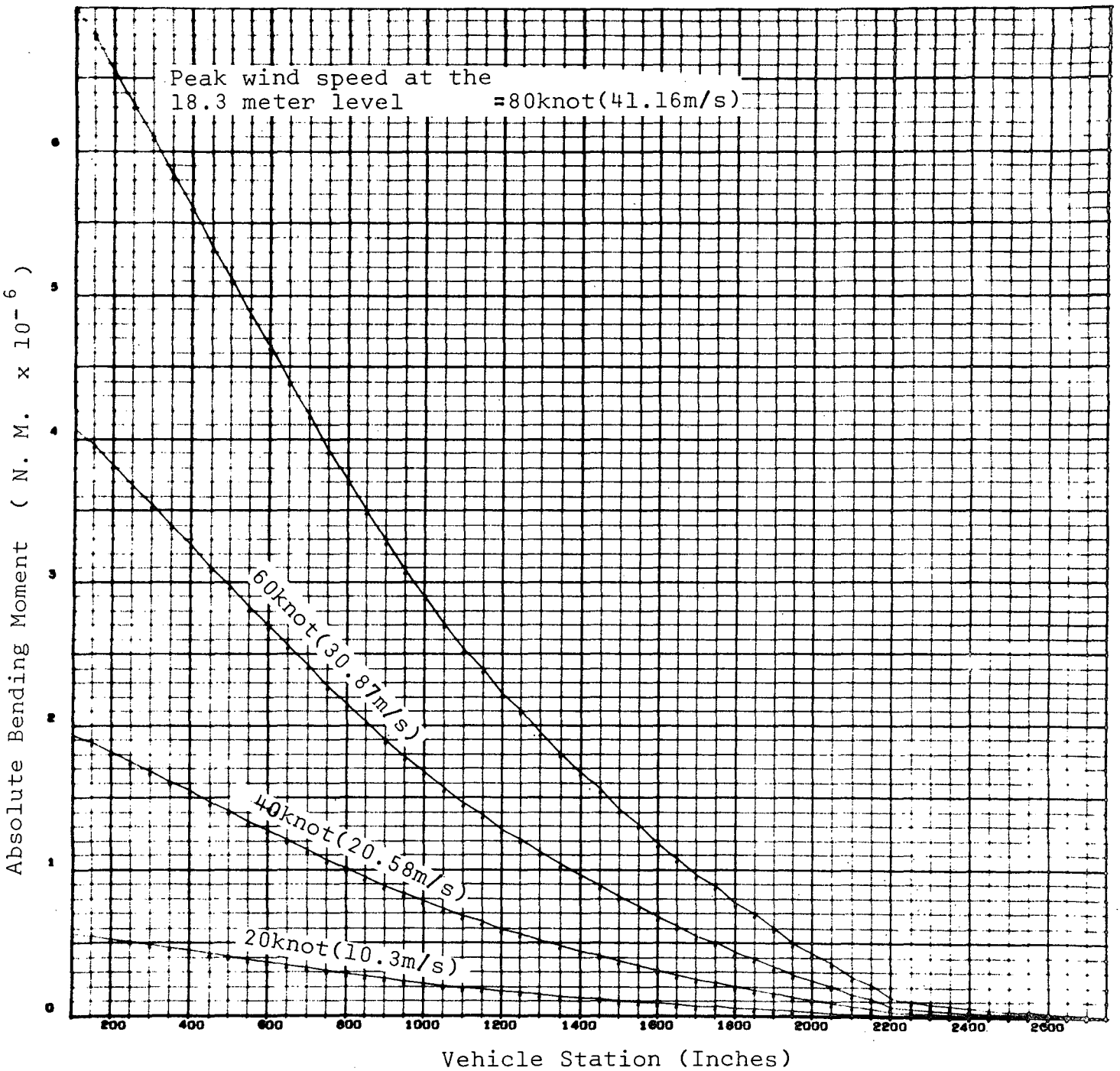

FIG. 5.1.8 ABSOLUTE BENDING MOMENT VERSUS VEHICLE STATION FOR CONCURRENT 3 SIGMA LIFT AND DRAG RESPONSE

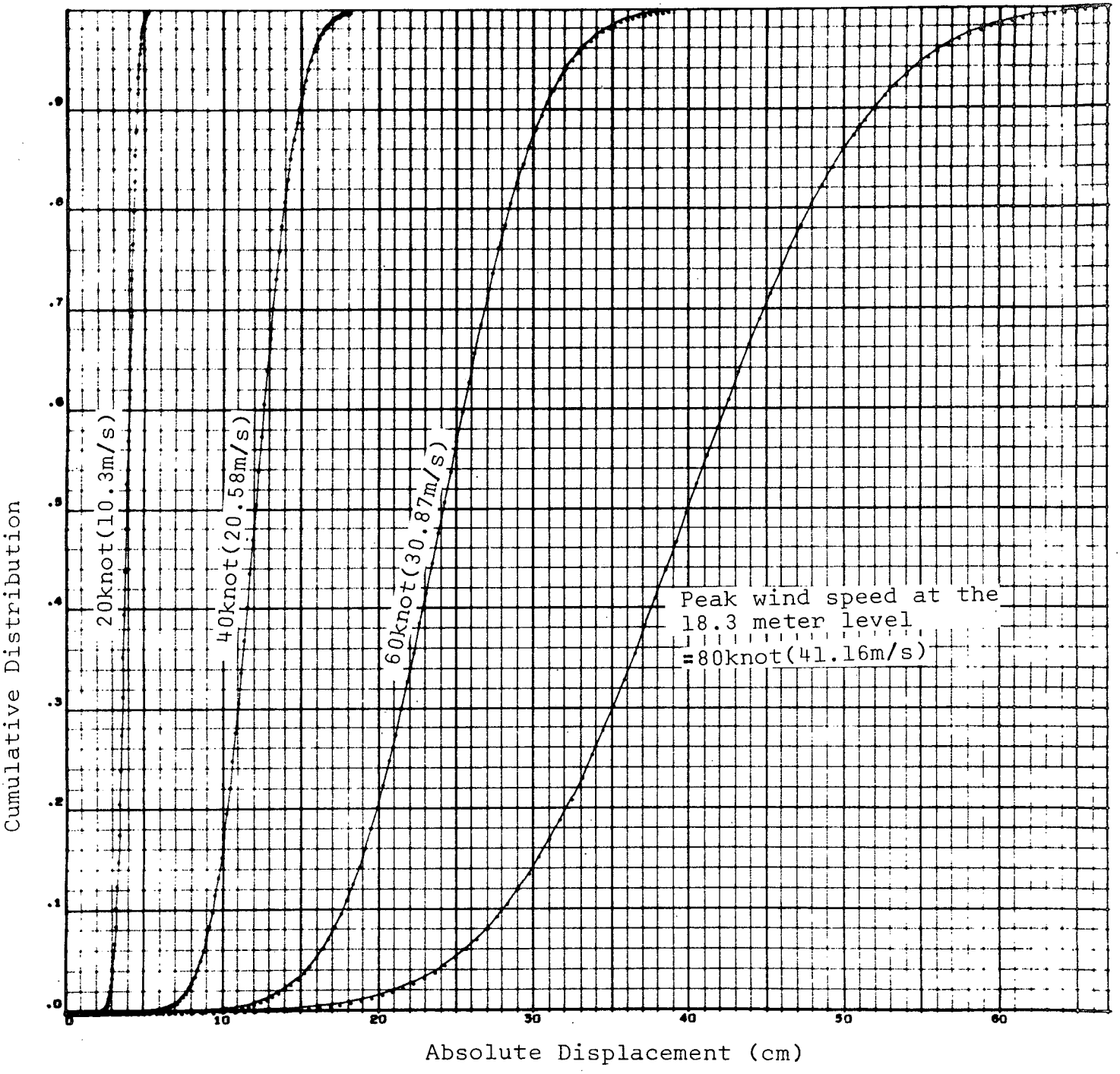

FIG. 5.1.9 CUMULATIVE DISTRIBUTION VERSUS TIP DISPLACEMENT

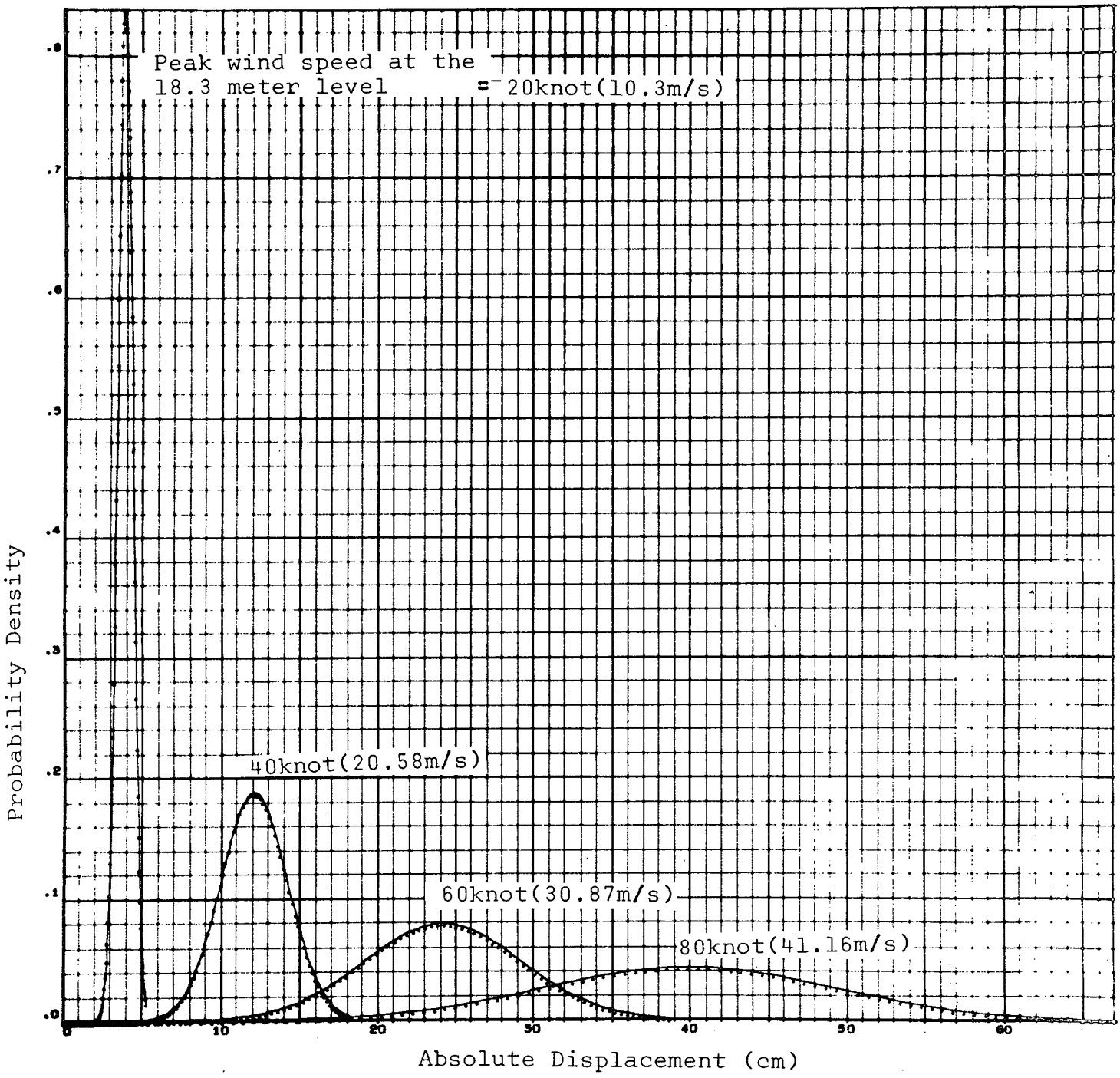

FIG. 5.1.10 PROBABILITY DENSITY VERSUS TIP DISPLACEMENT

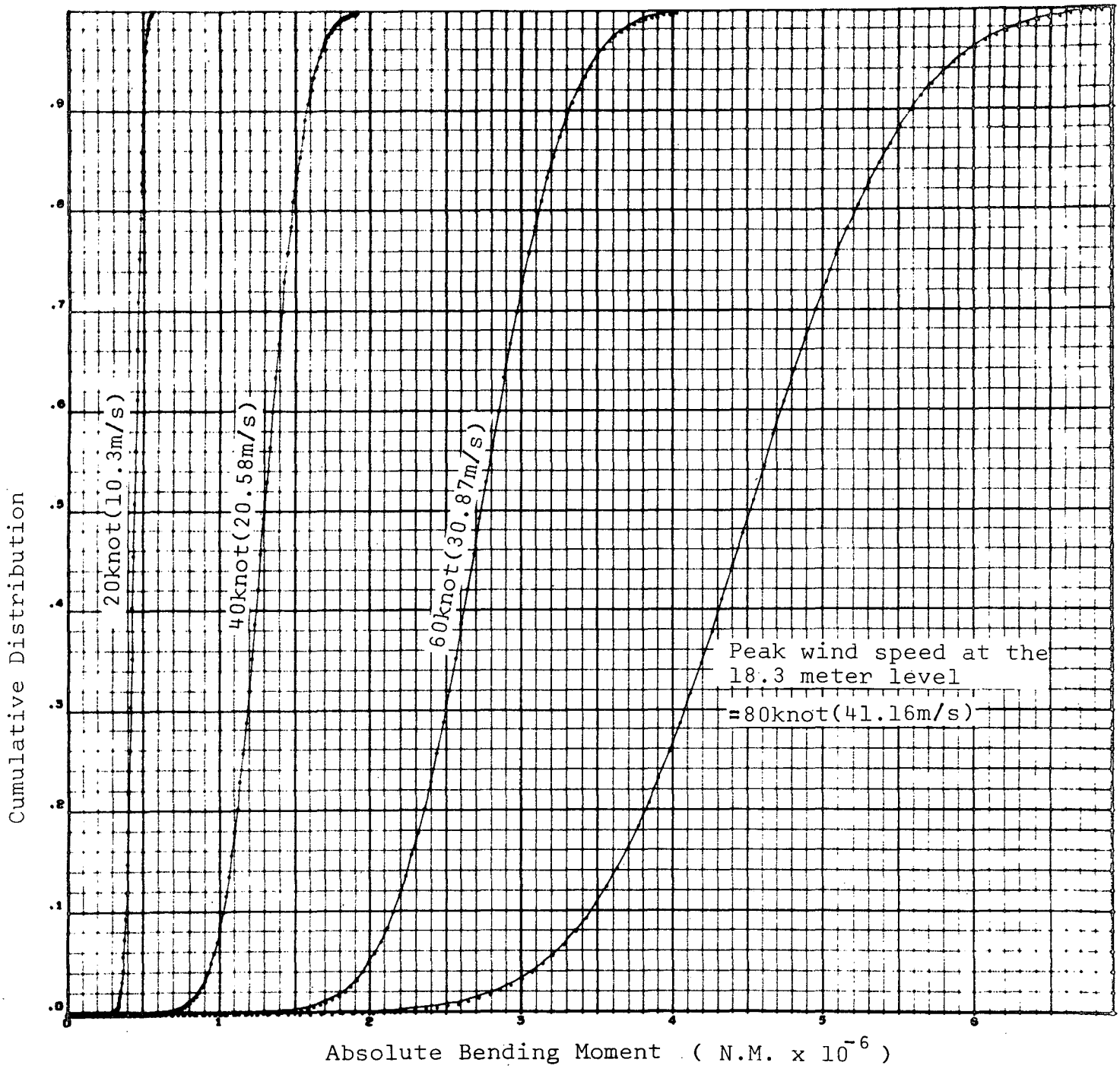

FIG. 5.1.11 CUMULATIVE DISTRIBUTION VERSUS BASE BENDING MOMENT

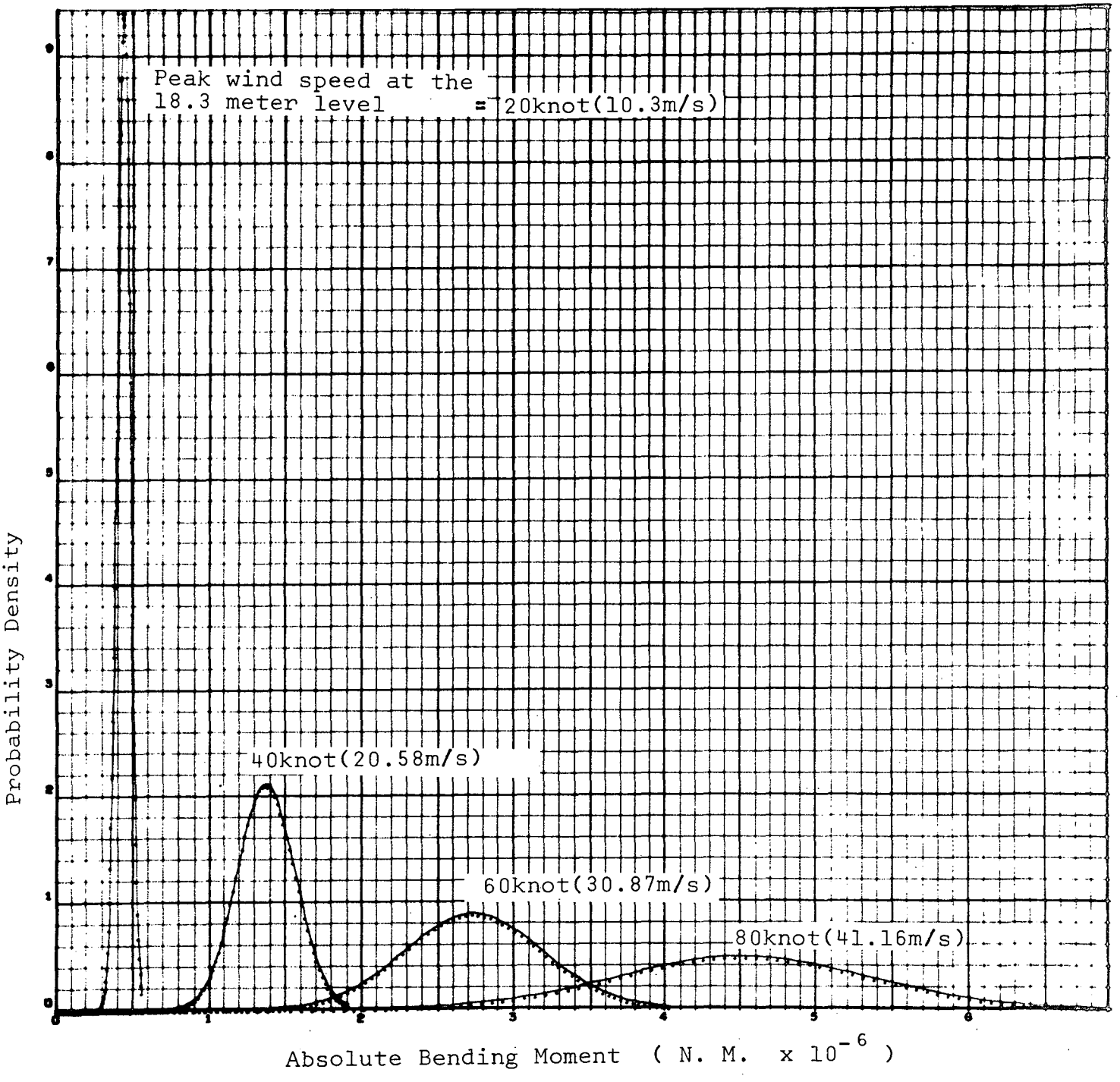

FIG. 5.1.12 PROBABILITY DENSITY VERSUS BASE BENDING MOMENT

5.2 SUMMARY OF PROPELLANT LOAD CONDITIONS AND STRUCTURAL DYNAMIC CHARACTERISTICS FOR CASE 2

Propellant Loading Configuration

Service Module	S-IB RP-1	S-IB LOX	S-IVB LOX	S-IVB LH_2
full	empty	empty	empty	empty

Structural Dynamic Characteristics

Mode No.	Natural Frequency Hz	Generalized Mass kg.(lb.sec.^{2}/in)	Structural Damping Ratio
1	0.489192	11985.08(68.4385)	0.015
2	1.73683	2868.43(16.3813)	0.015
3	2.66273	7180.72(41.005)	0.015

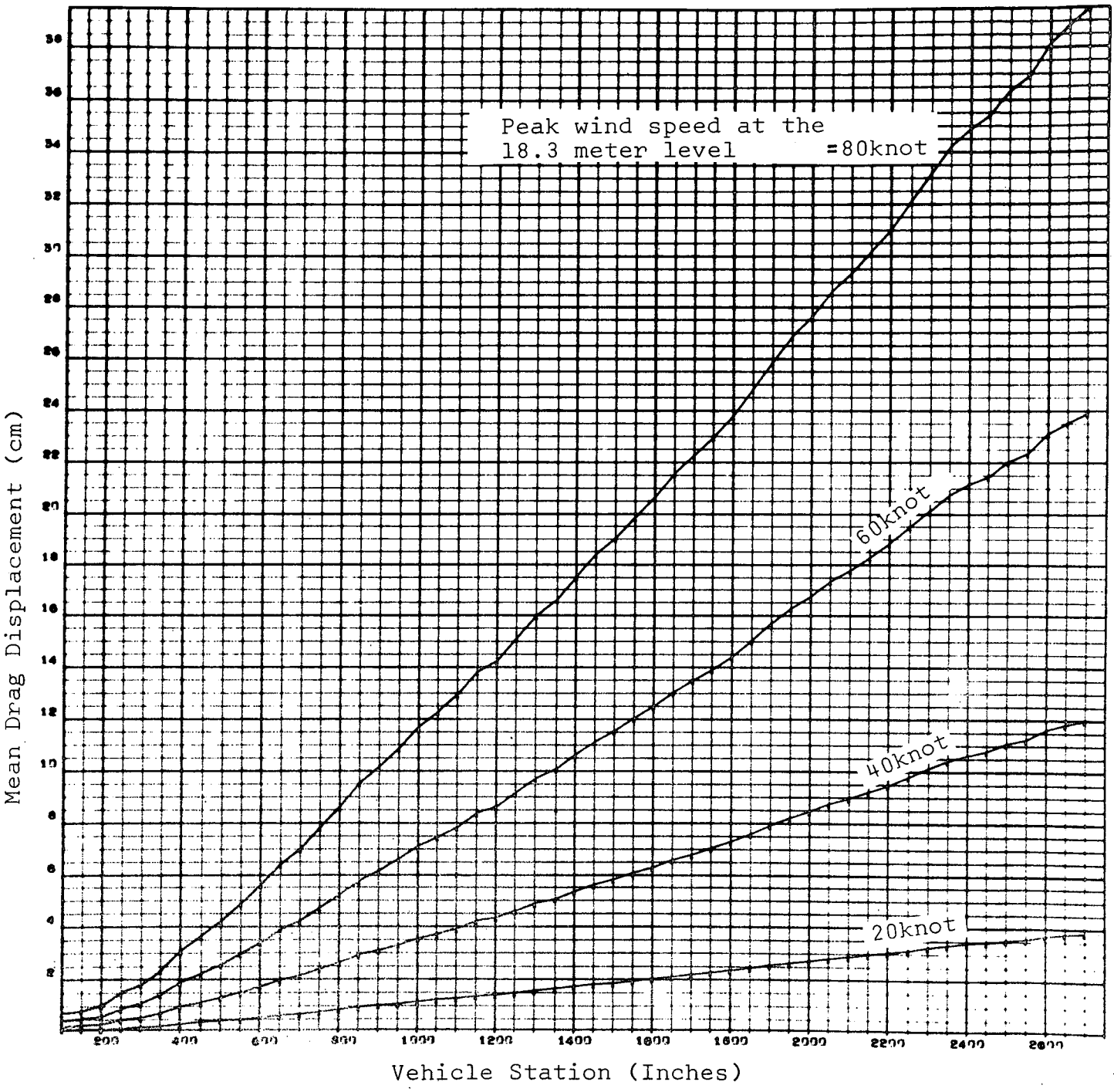

FIG. 5.2.1 MEAN DRAG DISPLACEMENT VERSUS VEHICLE STATION

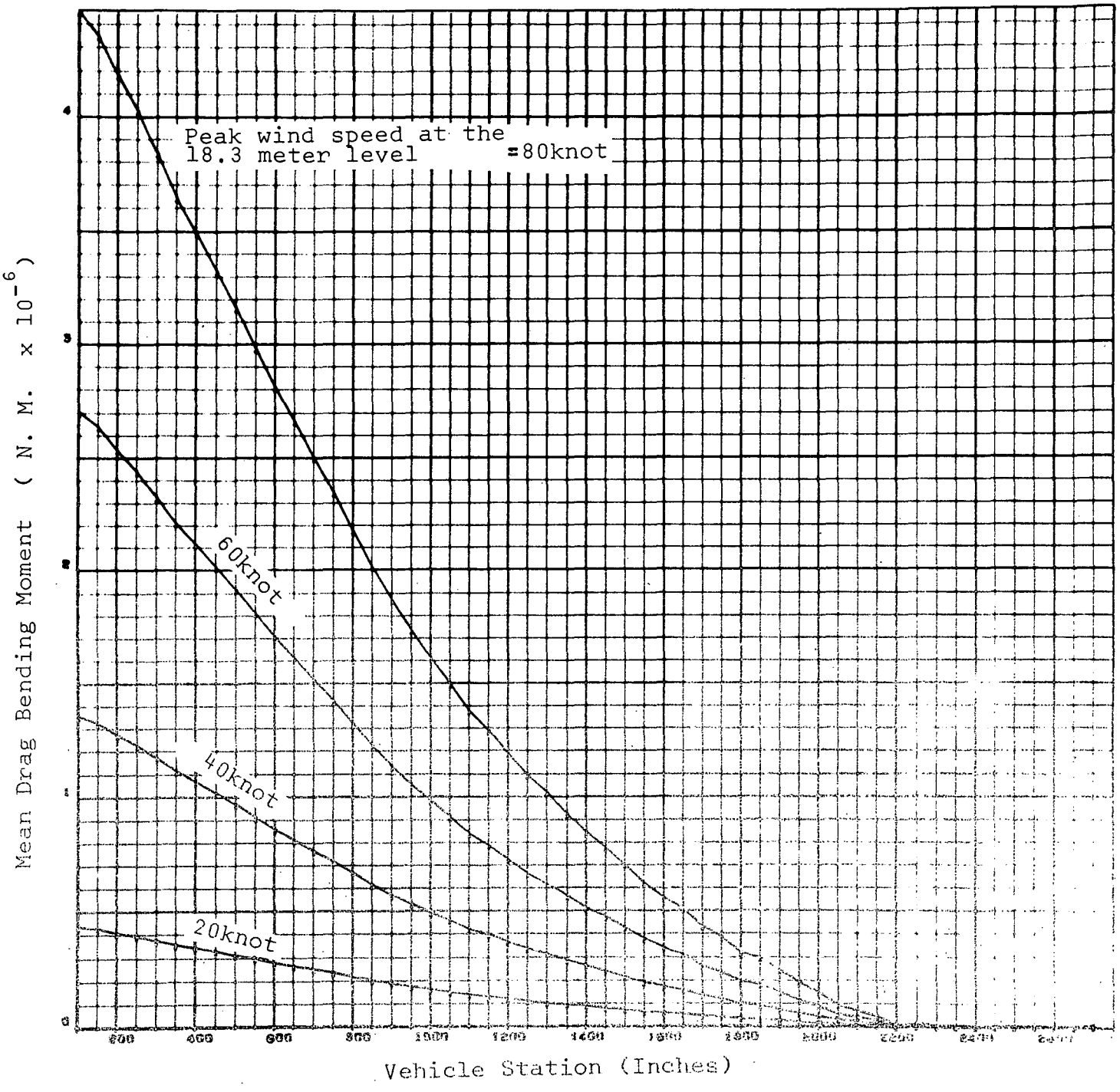

FIG. 5.2.2 MEAN DRAG BENDING MOMENT VERSUS VEHICLE STATION

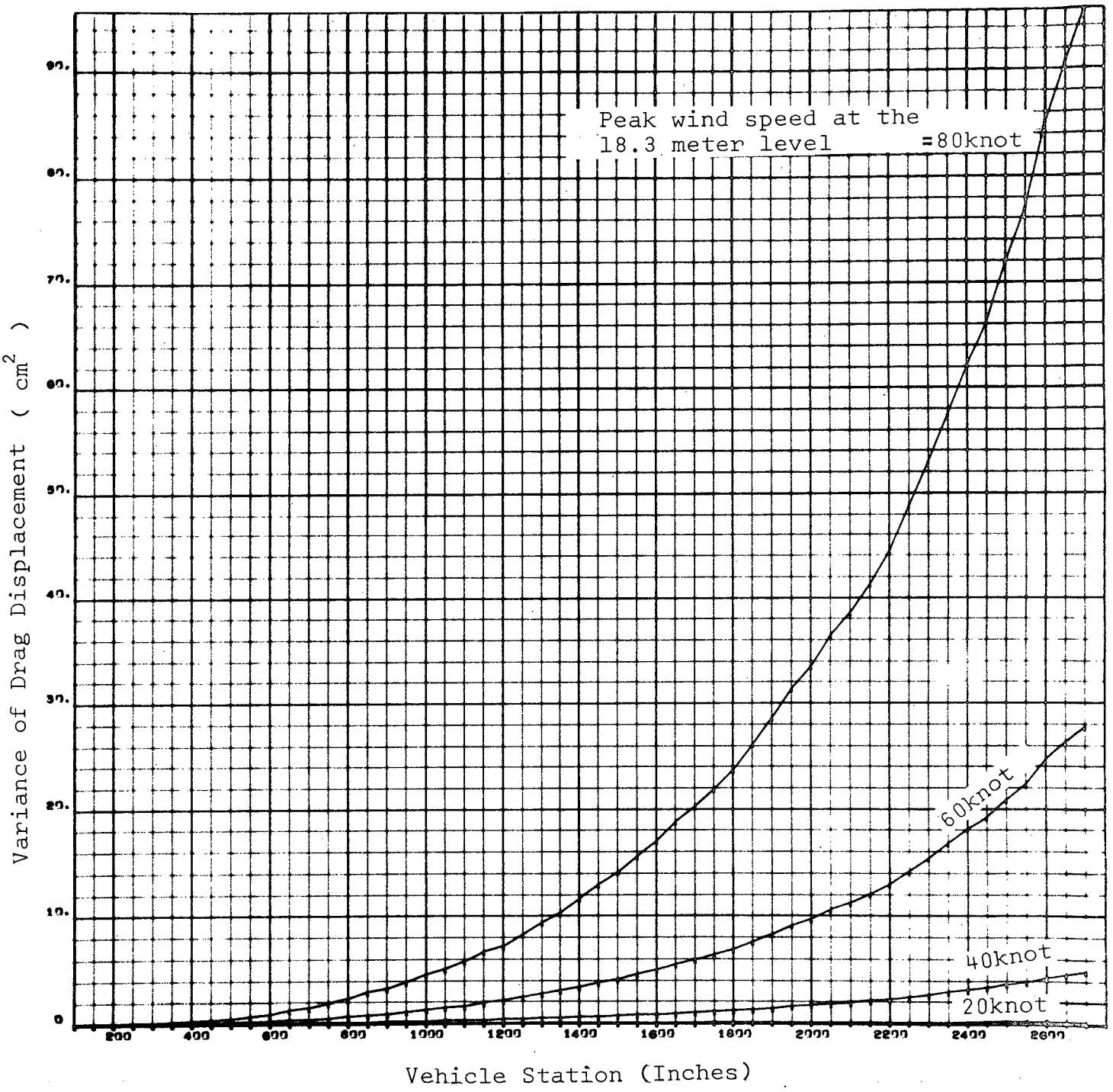

FIG. 5.2.3 VARIANCE OF DRAG DISPLACEMENT VERSUS VEHICLE STATION

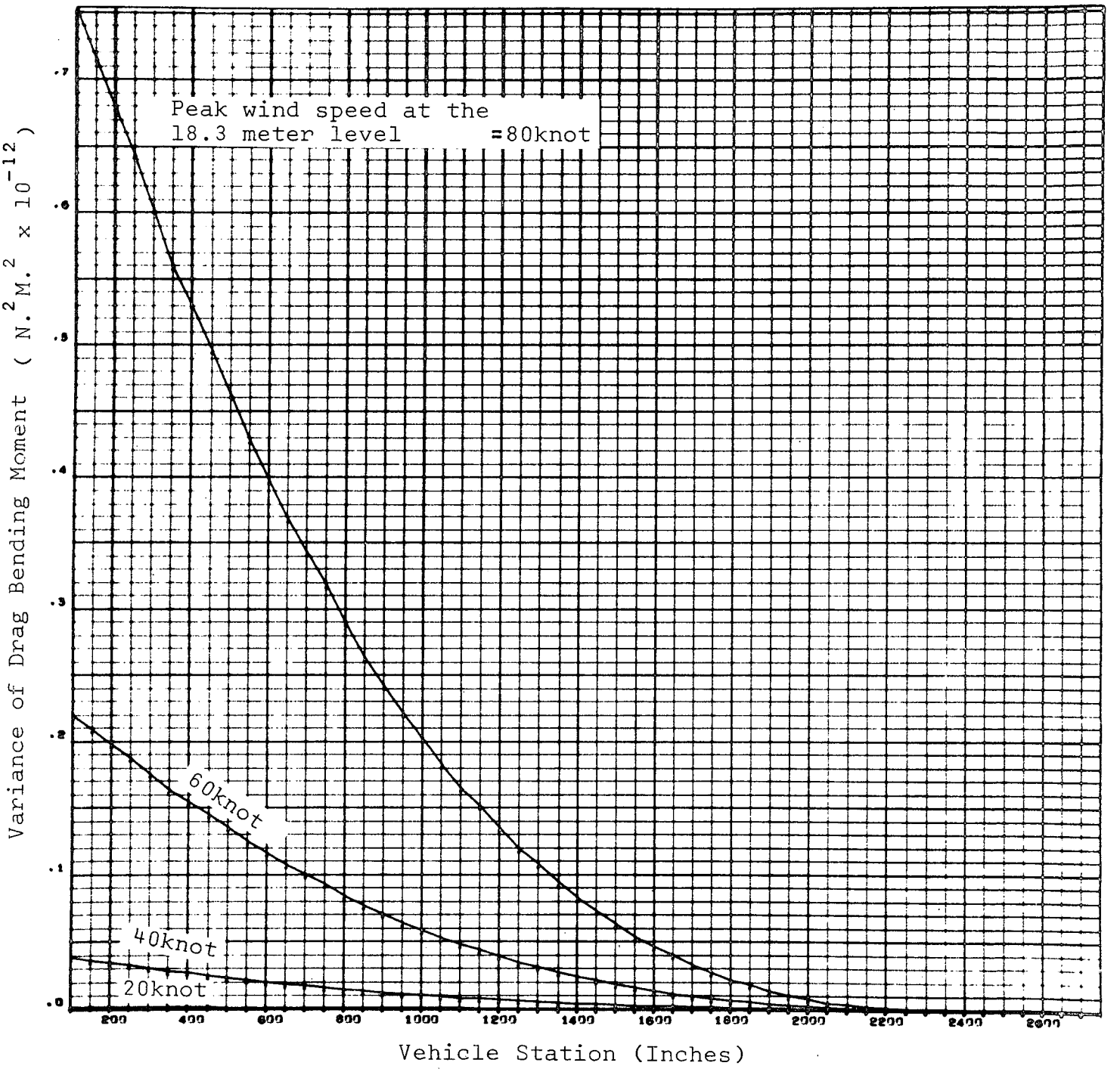

FIG. 5.2.4 VARIANCE OF DRAG BENDING MOMENT VERSUS VEHICLE STATION

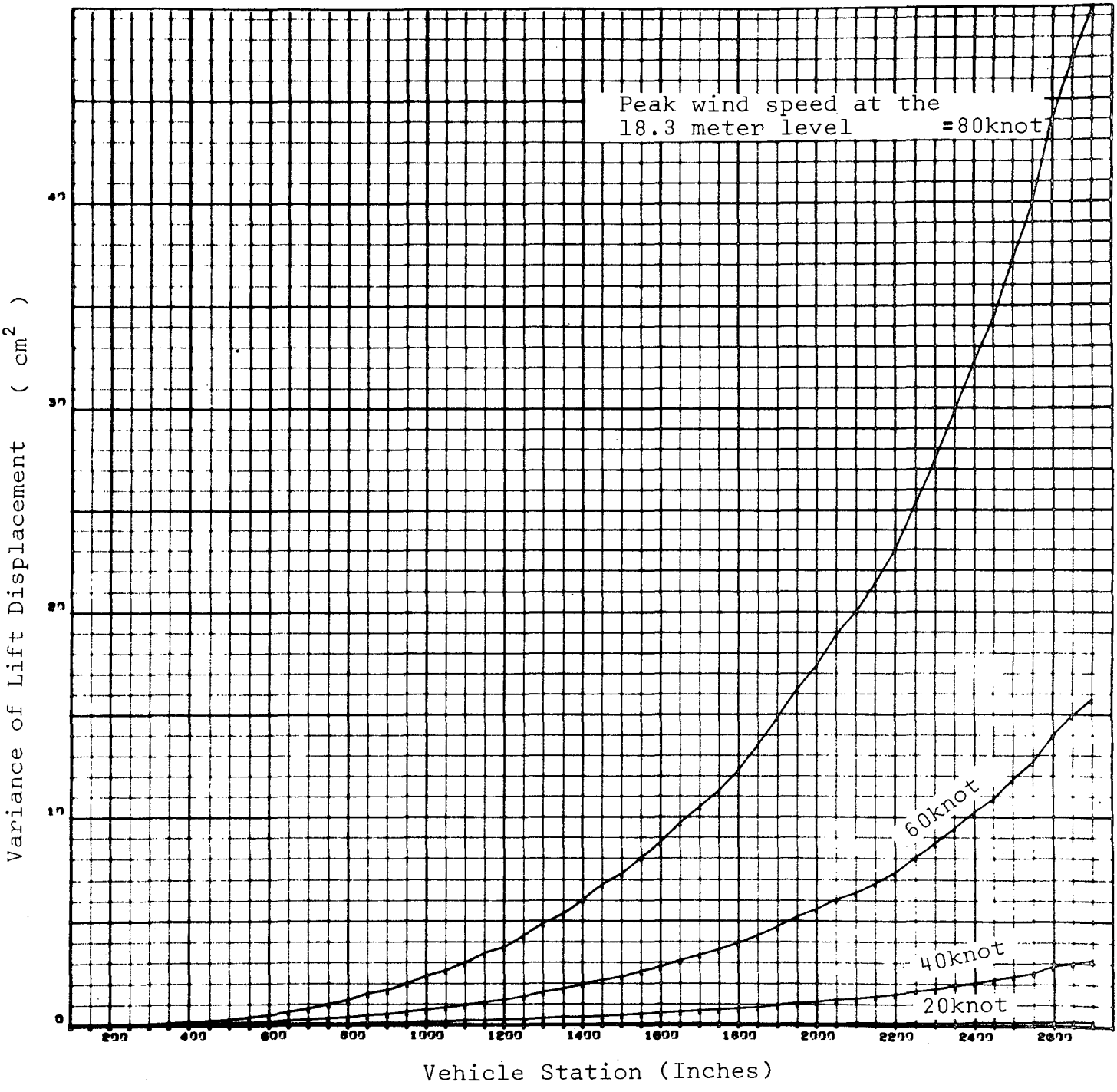

FIG. 5.2.5 VARIANCE OF LIFT DISPLACEMENT VERSUS VEHICLE STATION

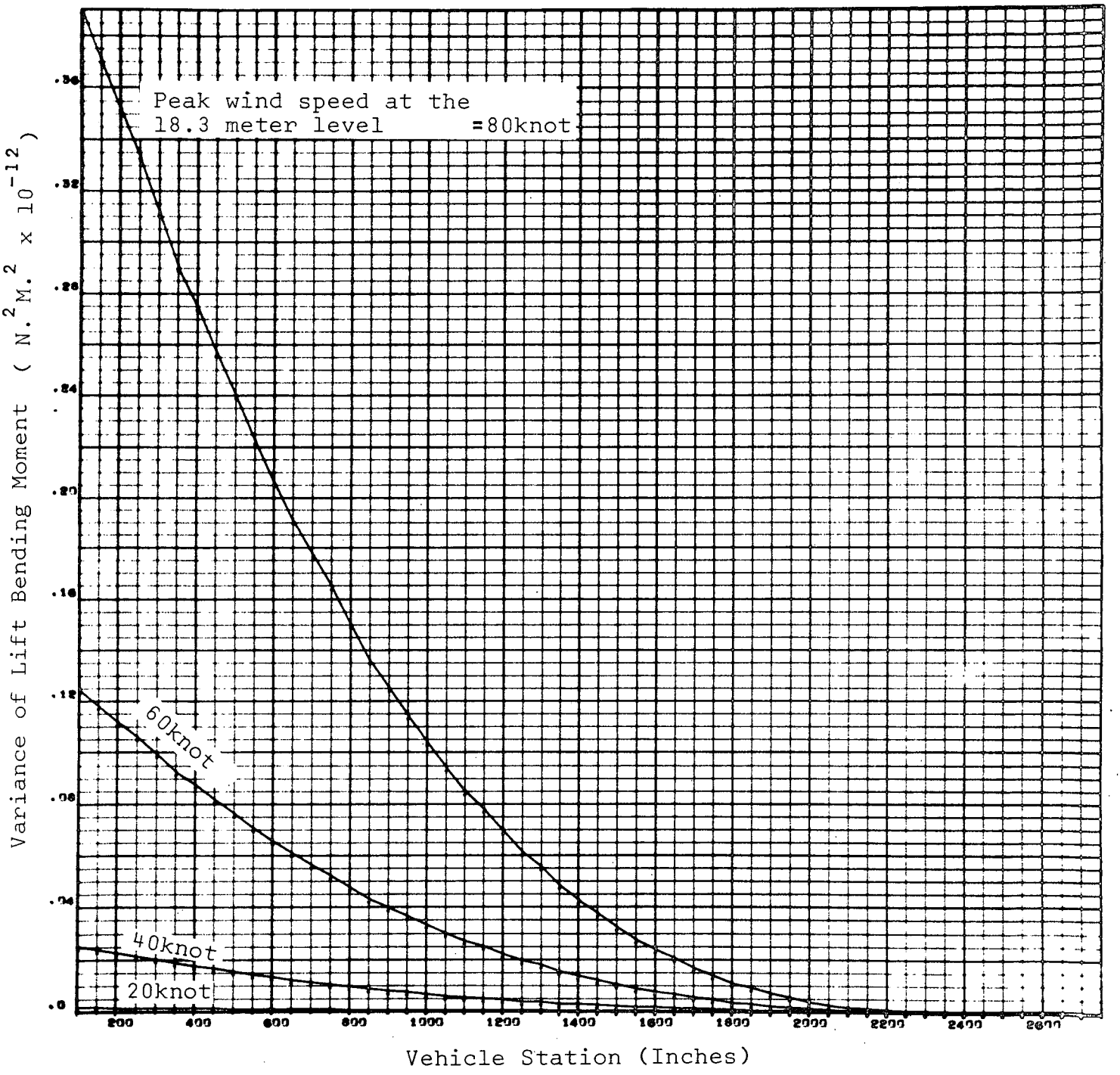

FIG. 5.2.6 VARIANCE OF LIFT BENDING MOMENT VERSUS VEHICLE STATION

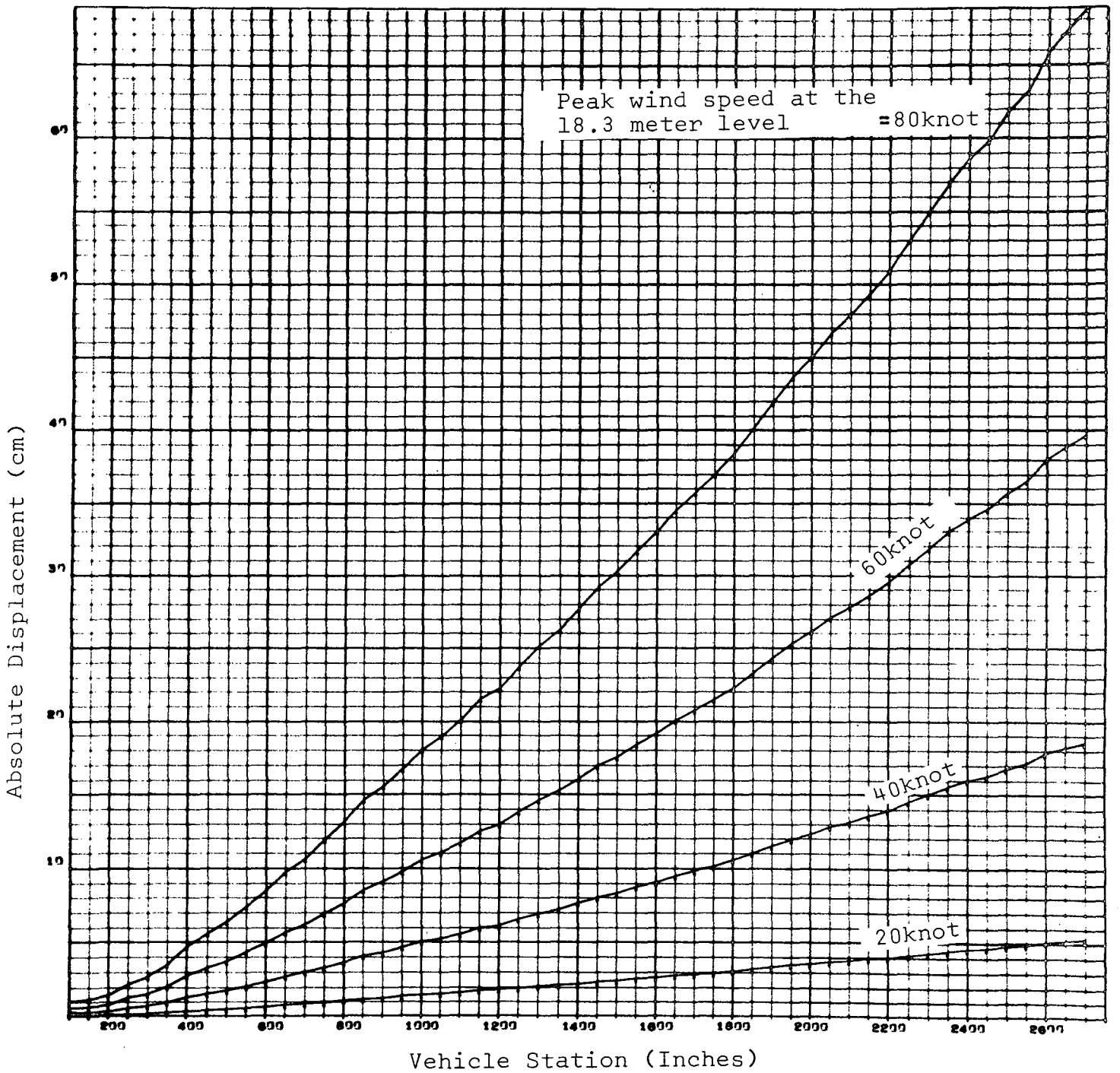

FIG. 5.2.7 ABSOLUTE DISPLACEMENT VERSUS VEHICLE STATION FOR CONCURRENT 3 SIGMA LIFT AND DRAG RESPONSE

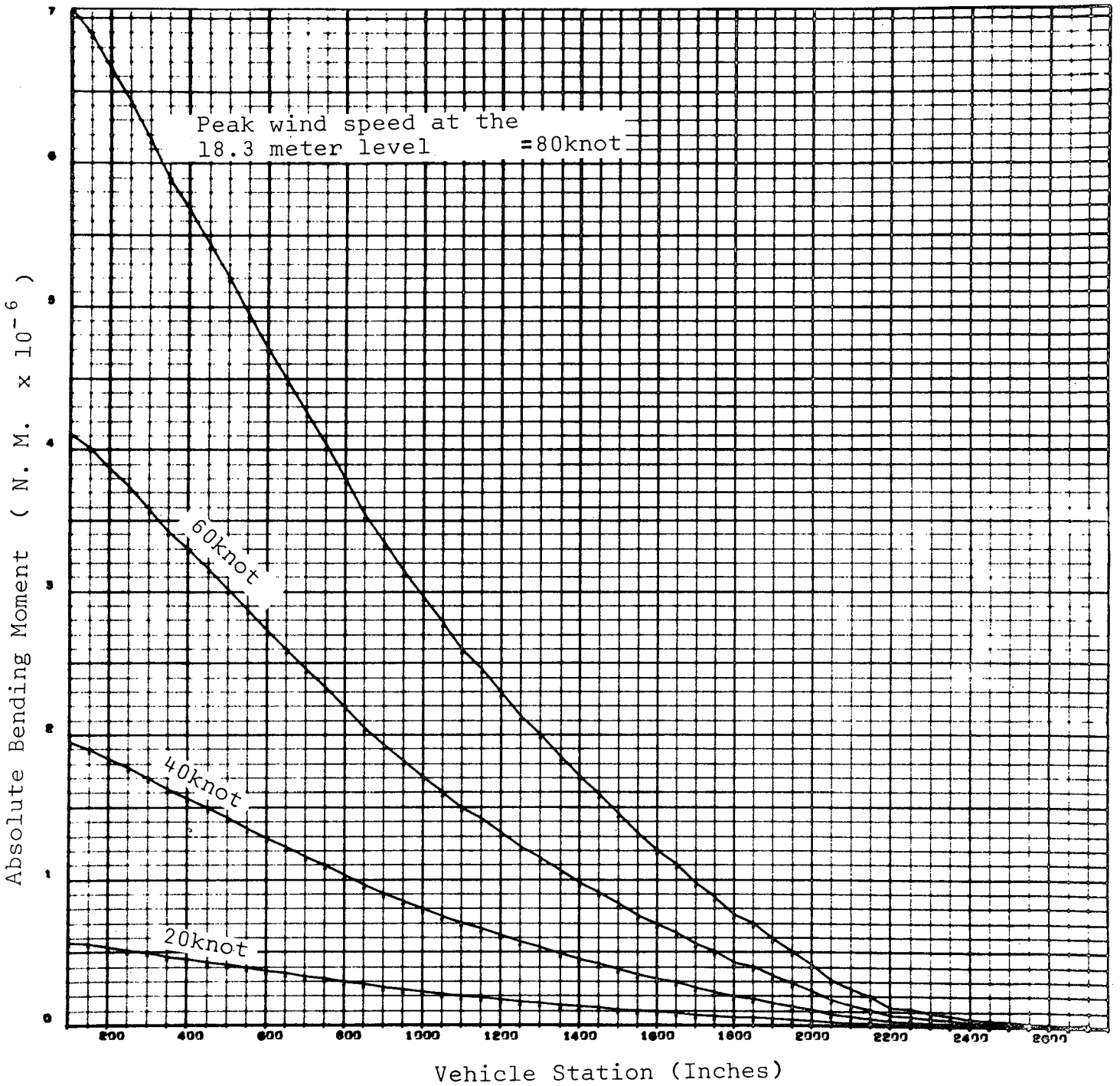

FIG. 5.2.8 ABSOLUTE BENDING MOMENT VERSUS VEHICLE STATION FOR CONCURRENT 3 SIGMA LIFT AND DRAG RESPONSE

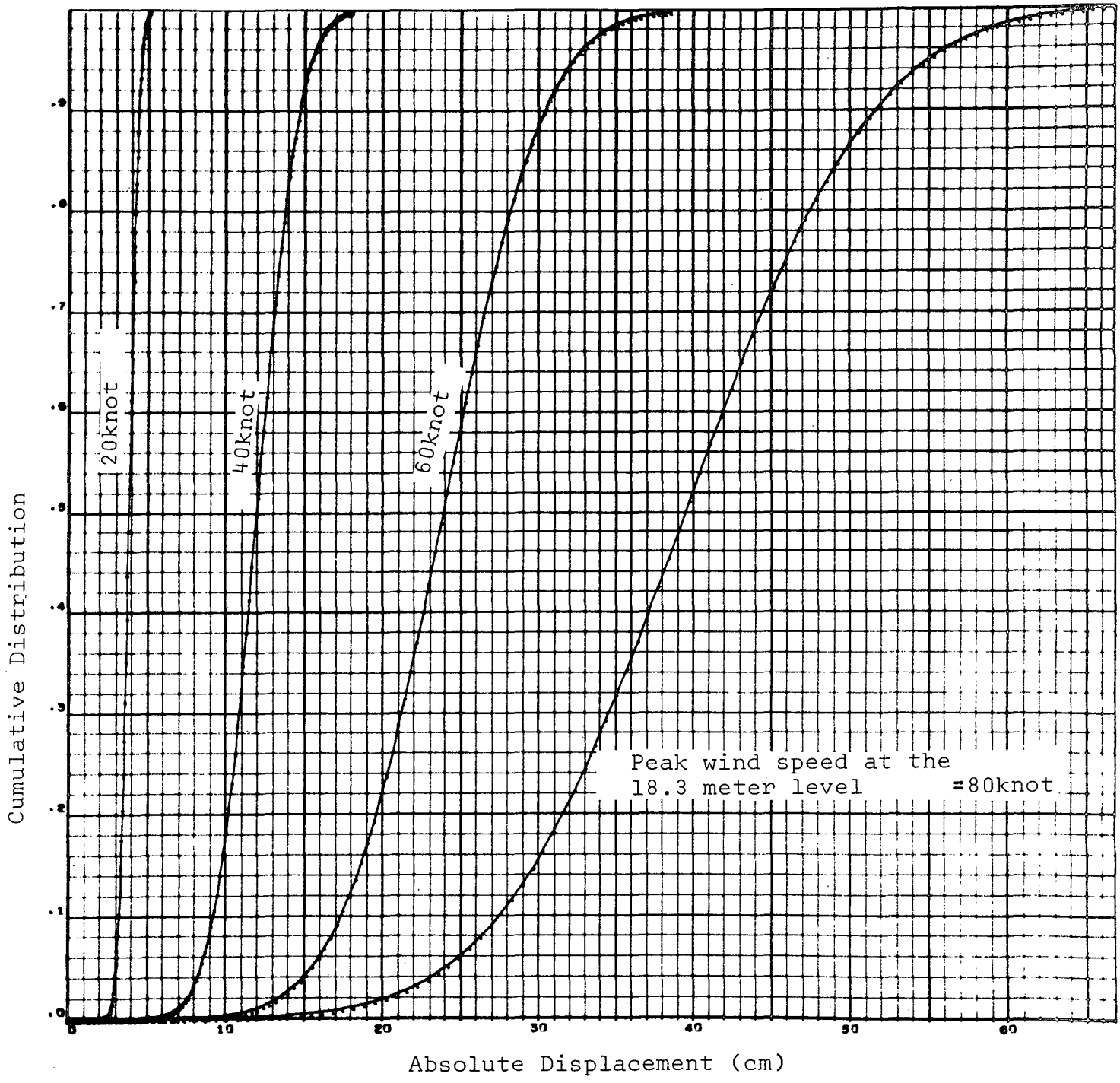

FIG. 5.2.9 CUMULATIVE DISTRIBUTION VERSUS TIP DISPLACEMENT

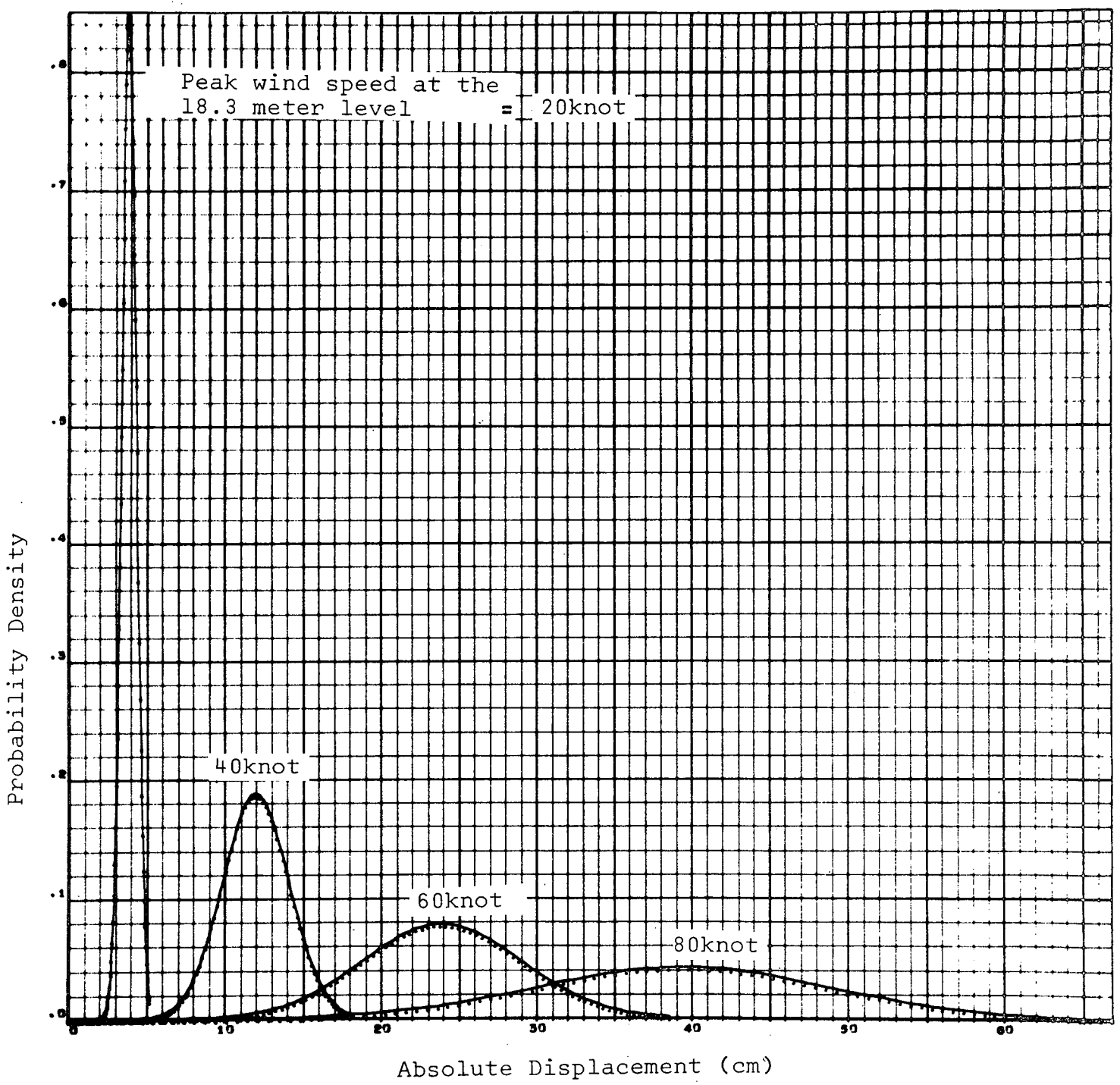

FIG. 5.2.10 PROBABILITY DENSITY VERSUS TIP DISPLACEMENT

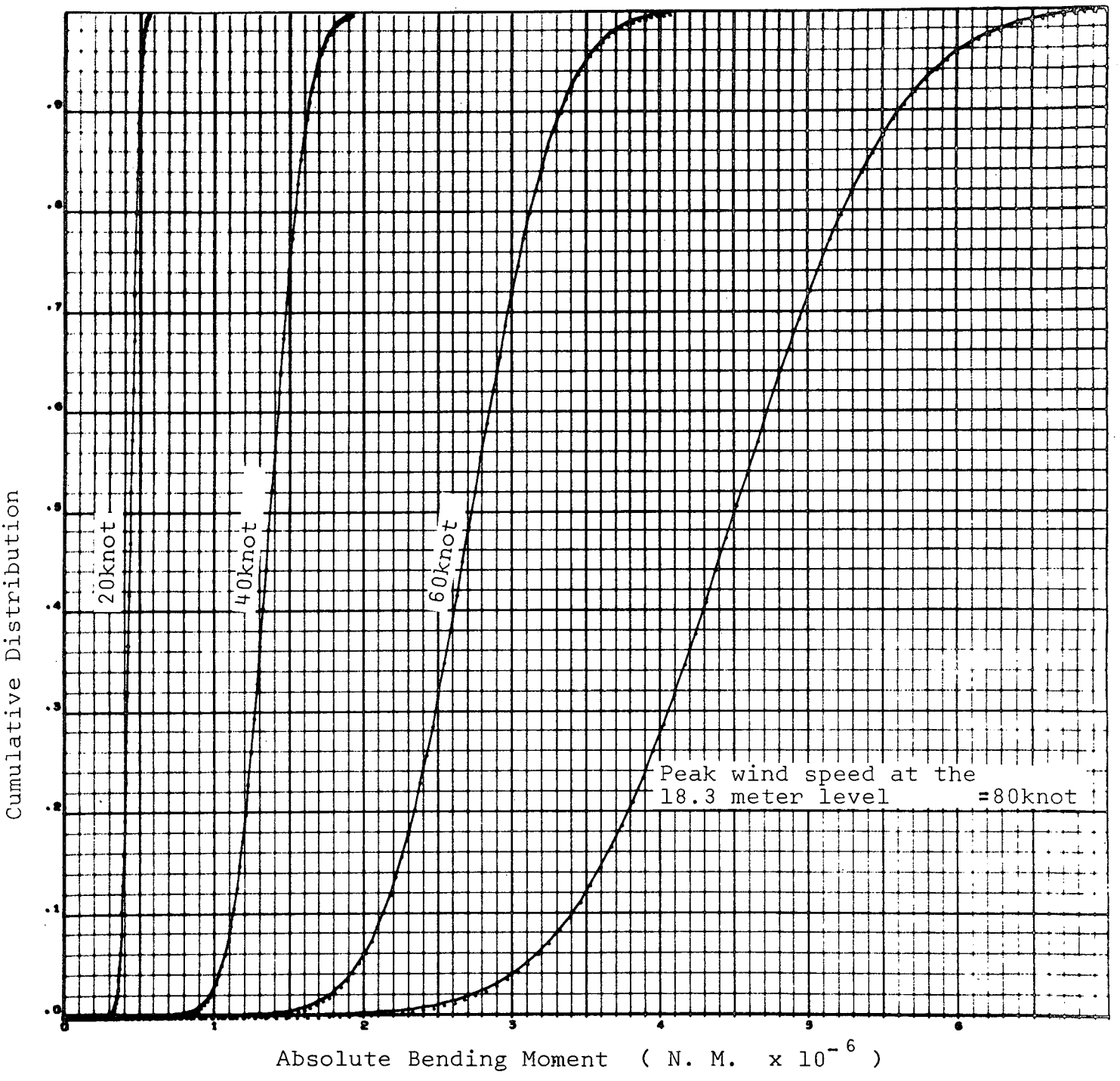

FIG. 5.2.11 CUMULATIVE DISTRIBUTION VERSUS BASE BENDING MOMENT

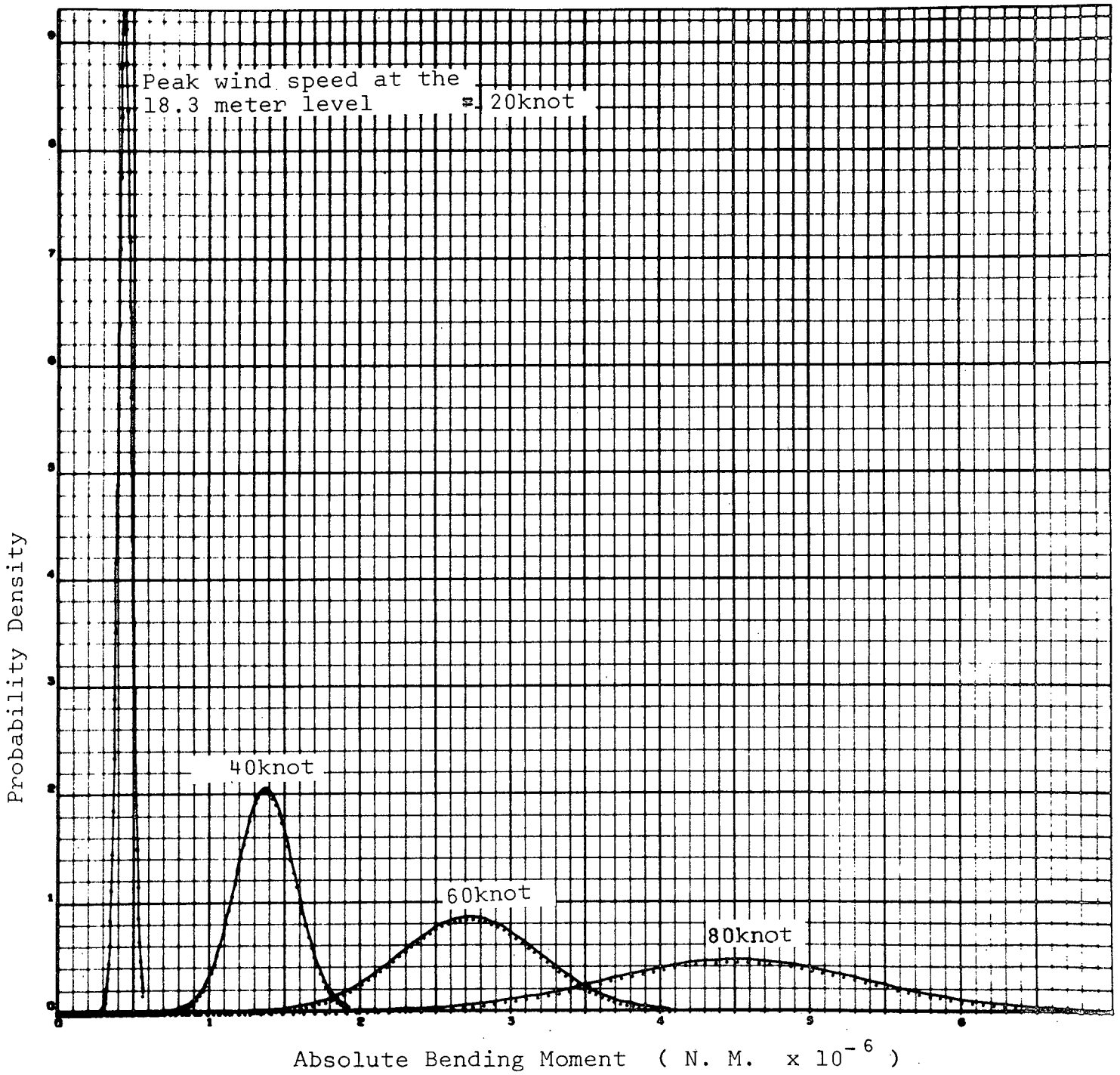

FIG. 5.2.12 PROBABILITY DENSITY VERSUS BASE BENDING MOMENT

5.3 SUMMARY OF PROPELLANT LOAD CONDITIONS AND STRUCTURAL DYNAMIC CHARACTERISTICS FOR CASE 3

Propellant Loading Configuration

Service Module	S-IB RP-1	S-IB LOX	S-IVB LOX	S-IVB LH_2
full	full	empty	empty	empty

Structural Dynamic Characteristics

Mode No.	Natural Frequency Hz	Generalized Mass kg.(lb.sec.^{2}/in)	Structural Damping Ratio
1	0.457132	14555.64(83.1191)	0.015
2	1.17657	11059.41(63.1538)	0.015
3	1.89755	7444.8(42.5126)	0.015

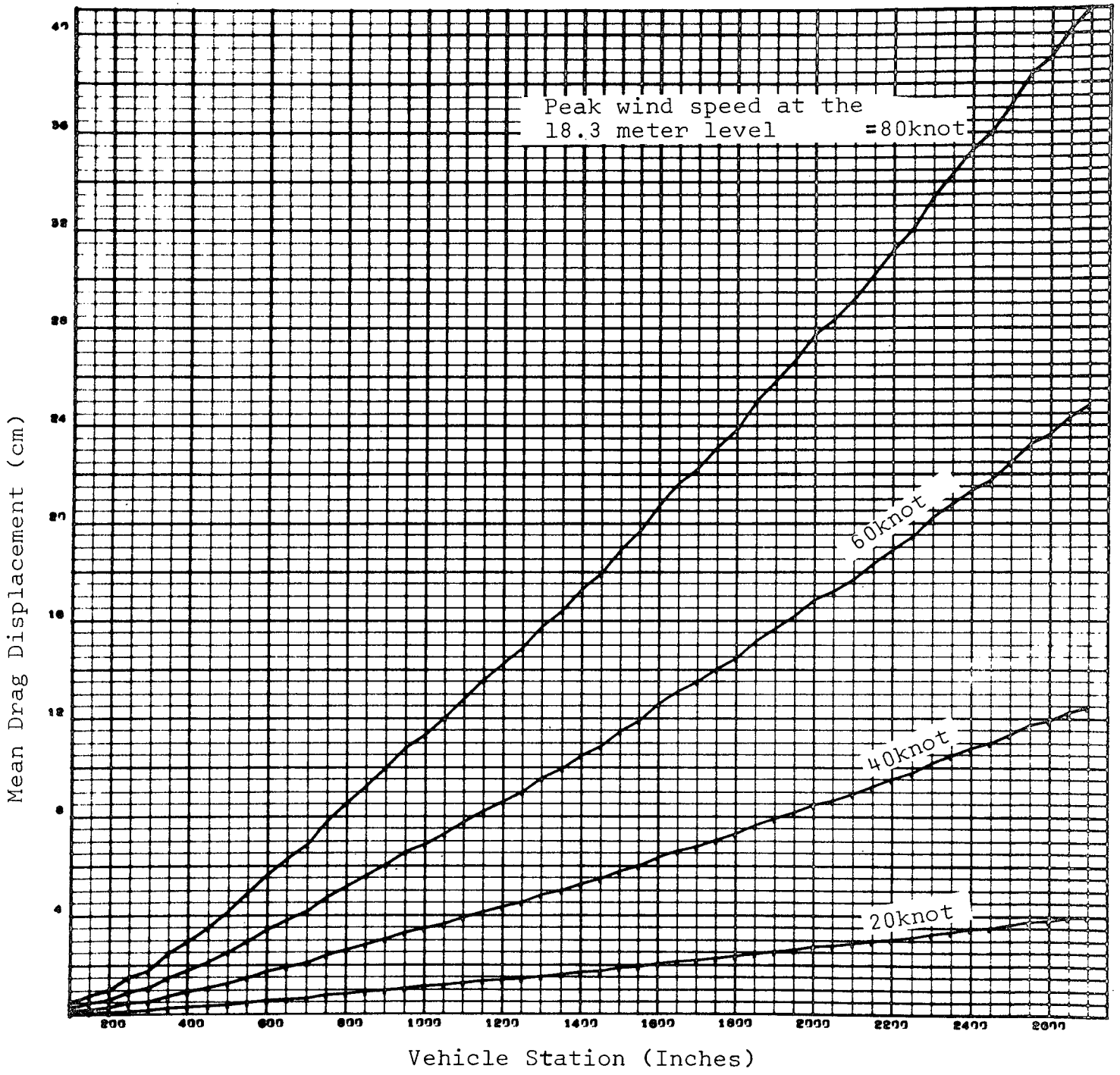

FIG. 5.3.1 MEAN DRAG DISPLACEMENT VERSUS VEHICLE STATION

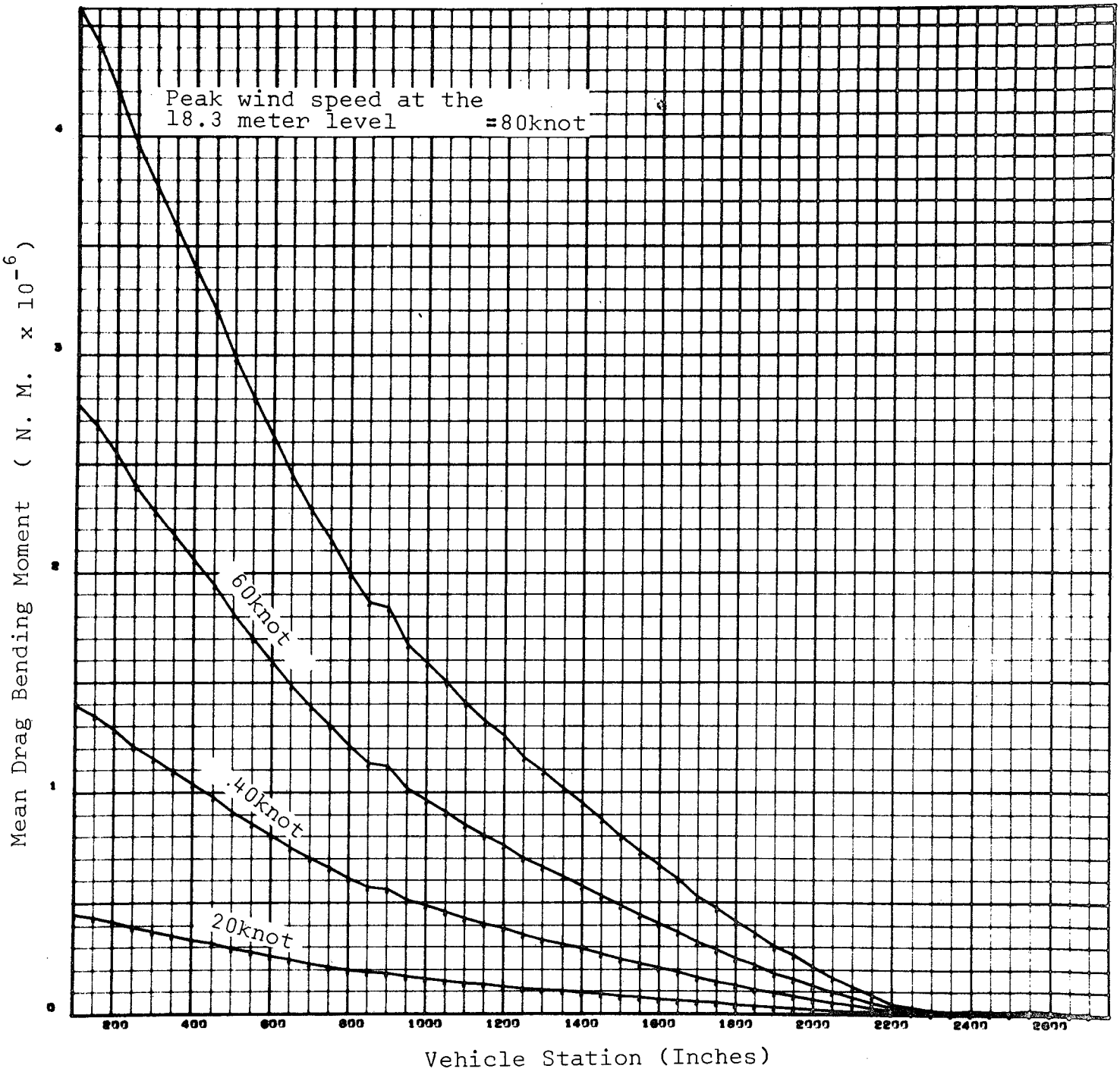

FIG. 5.3.2 MEAN DRAG BENDING MOMENT VERSUS VEHICLE STATION

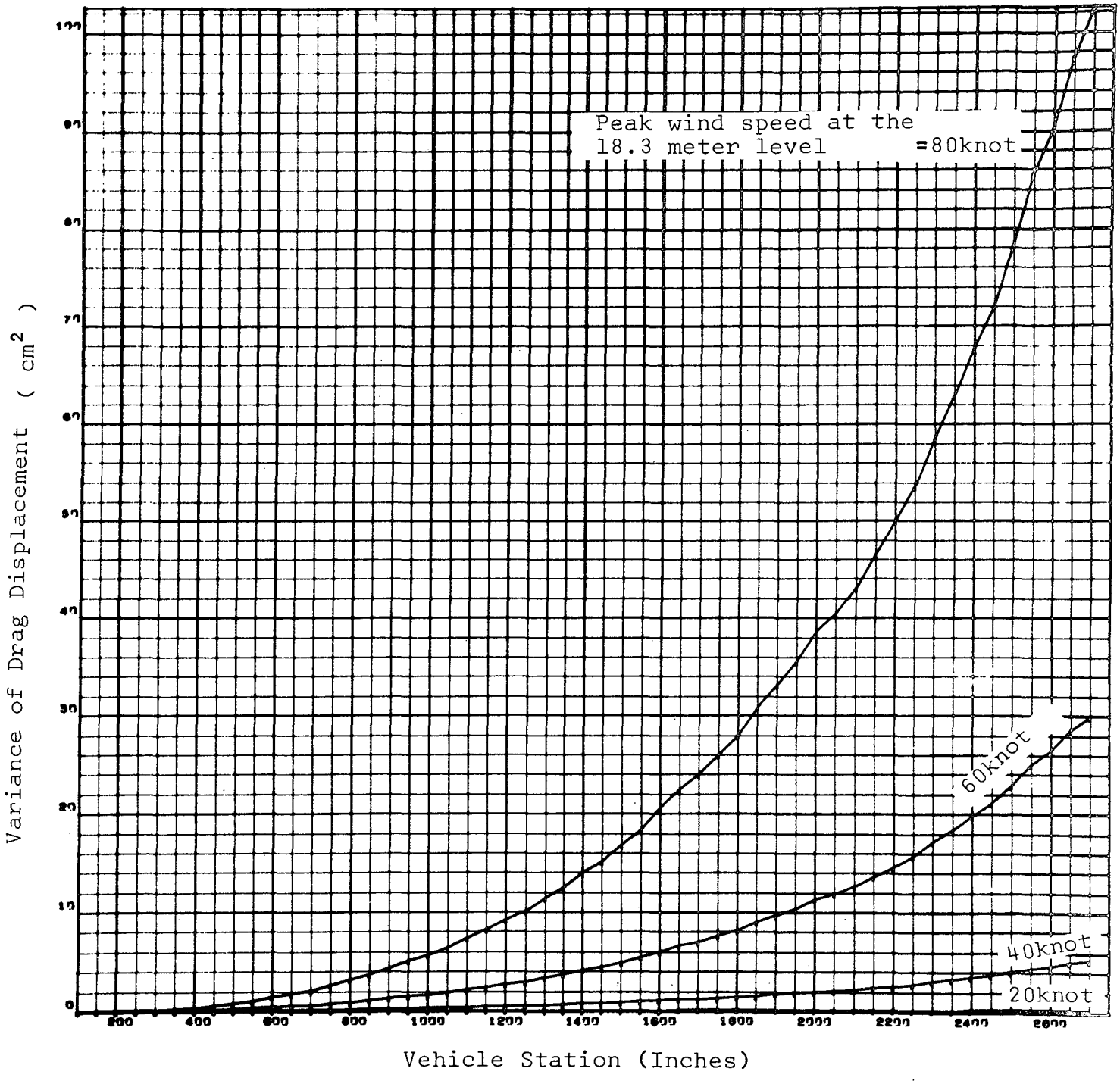

FIG. 5.3.3 VARIANCE OF DRAG DISPLACEMENT VERSUS VEHICLE STATION

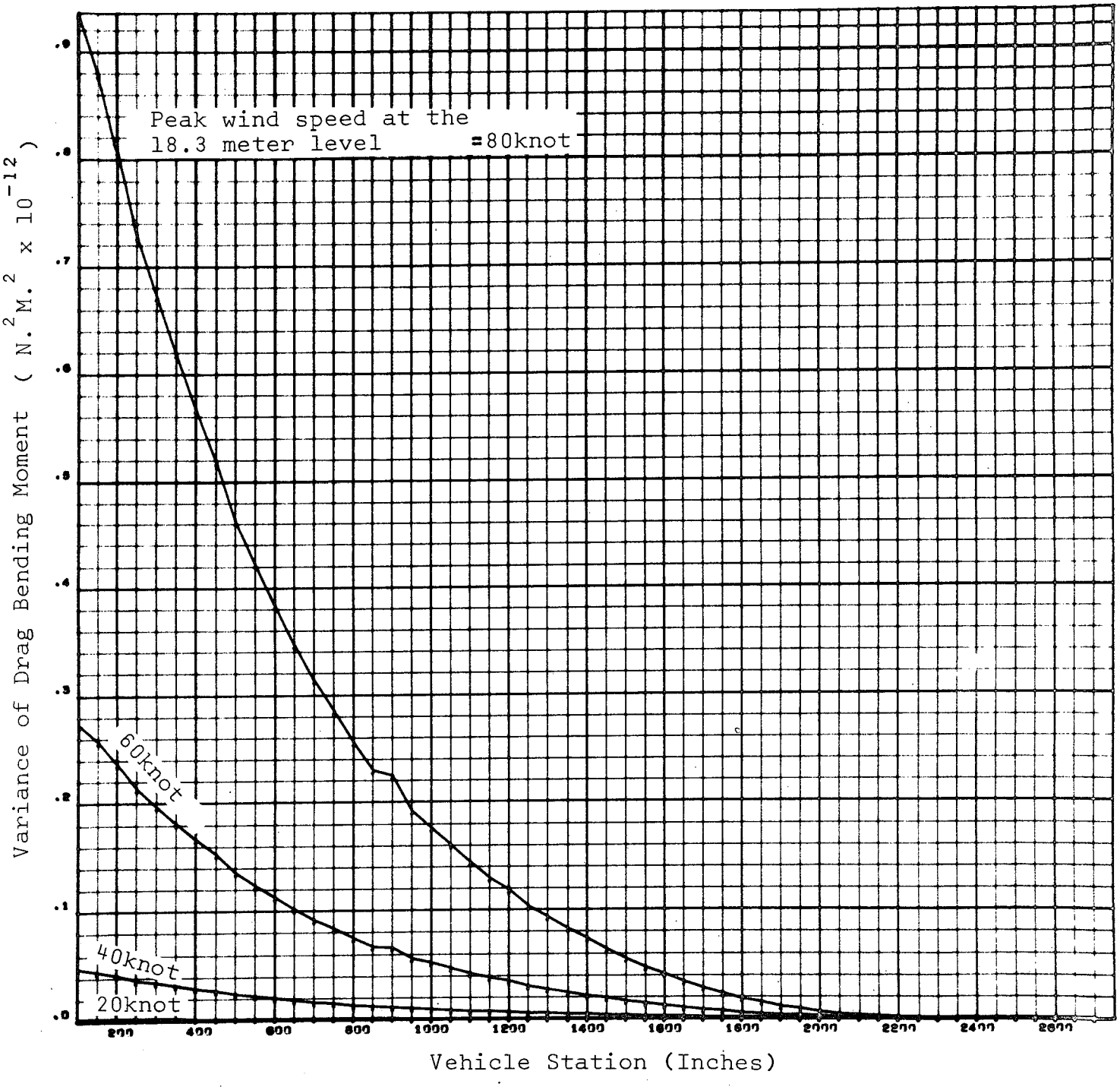

FIG. 5.3.4 VARIANCE OF DRAG BENDING MOMENT VERSUS VEHICLE STATION

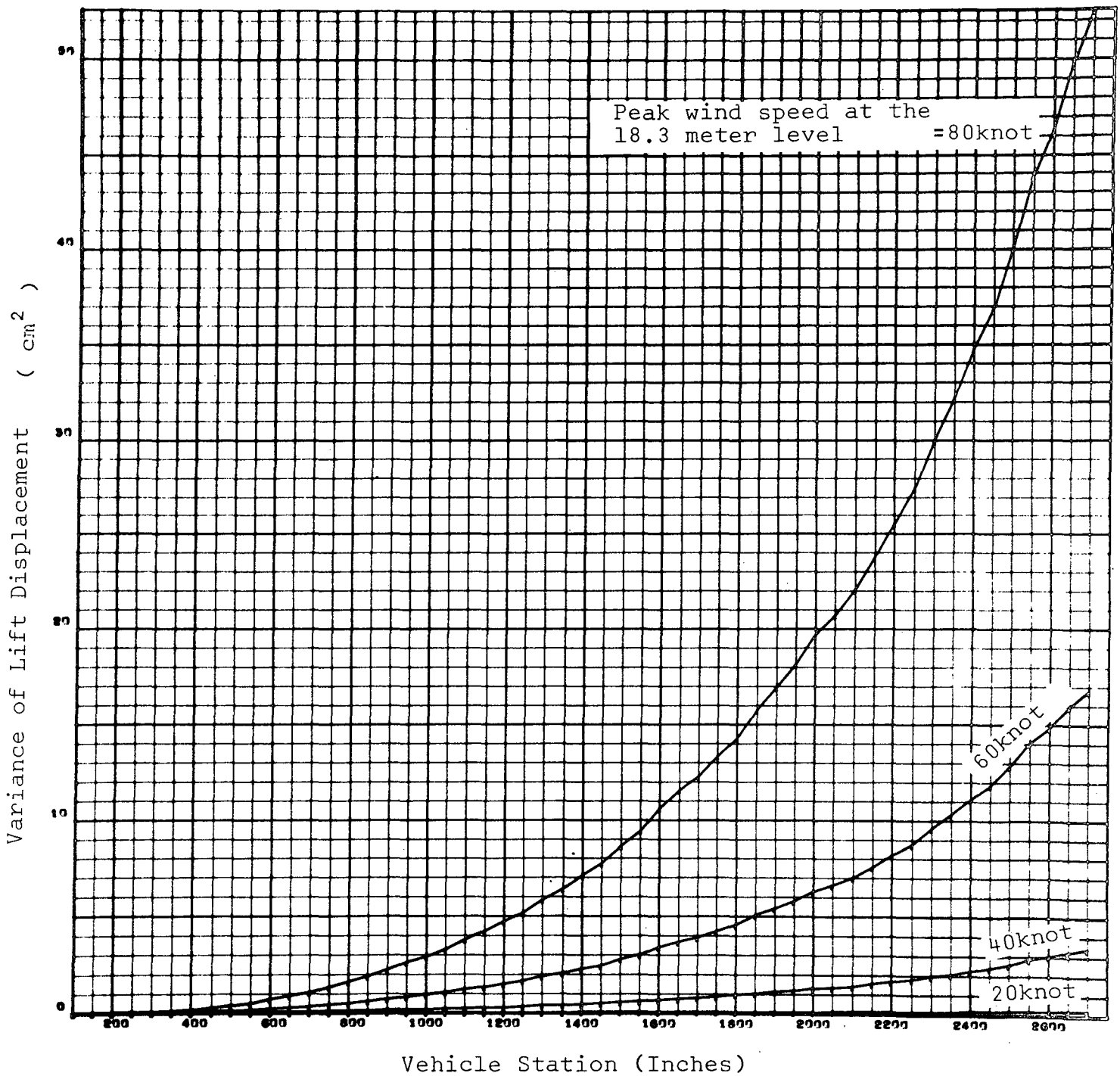

FIG. 5.3.5 VARIANCE OF LIFT DISPLACEMENT VERSUS VEHICLE STATION

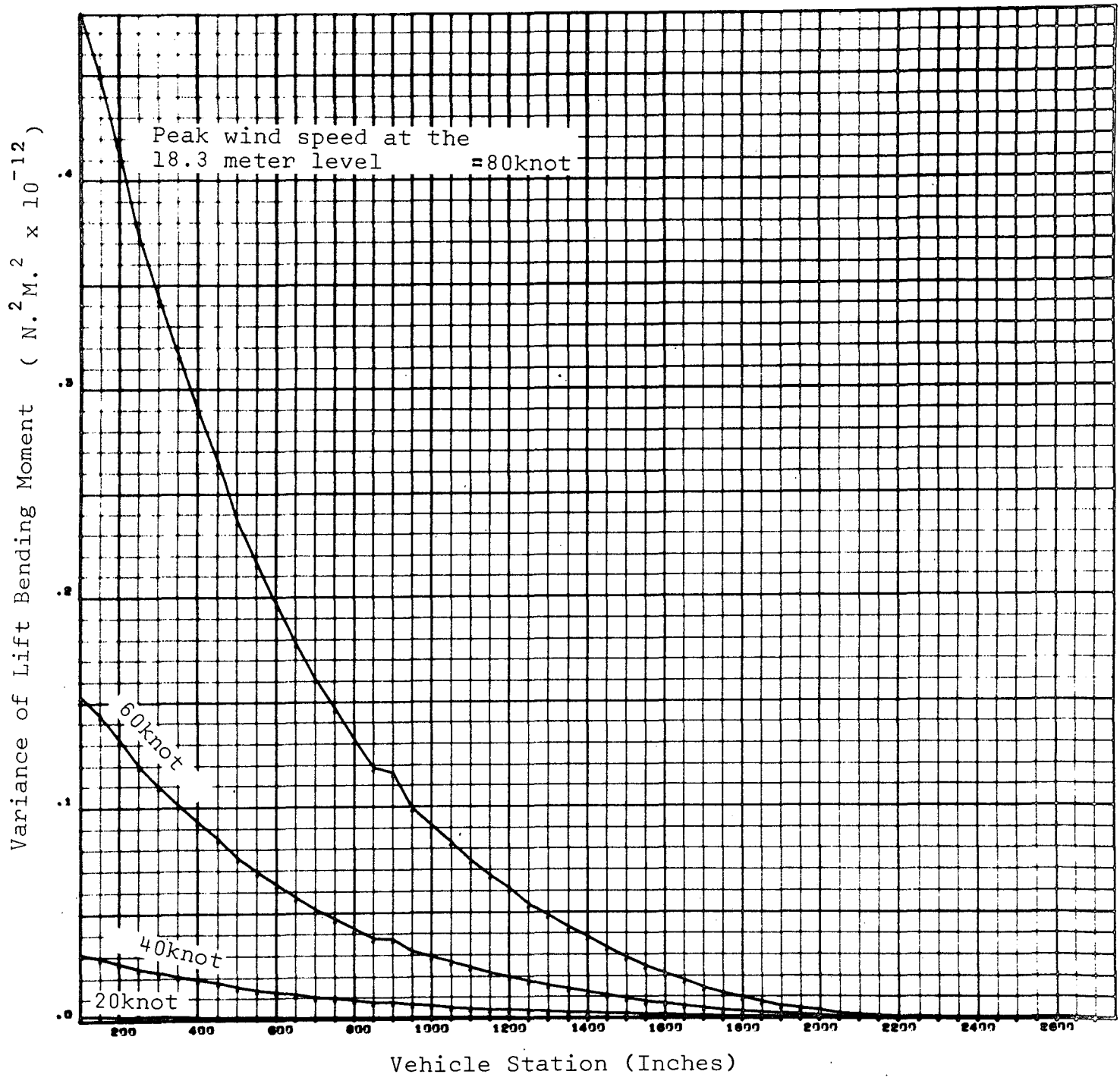

FIG. 5.3.6 VARIANCE OF LIFT BENDING MOMENT VERSUS VEHICLE STATION

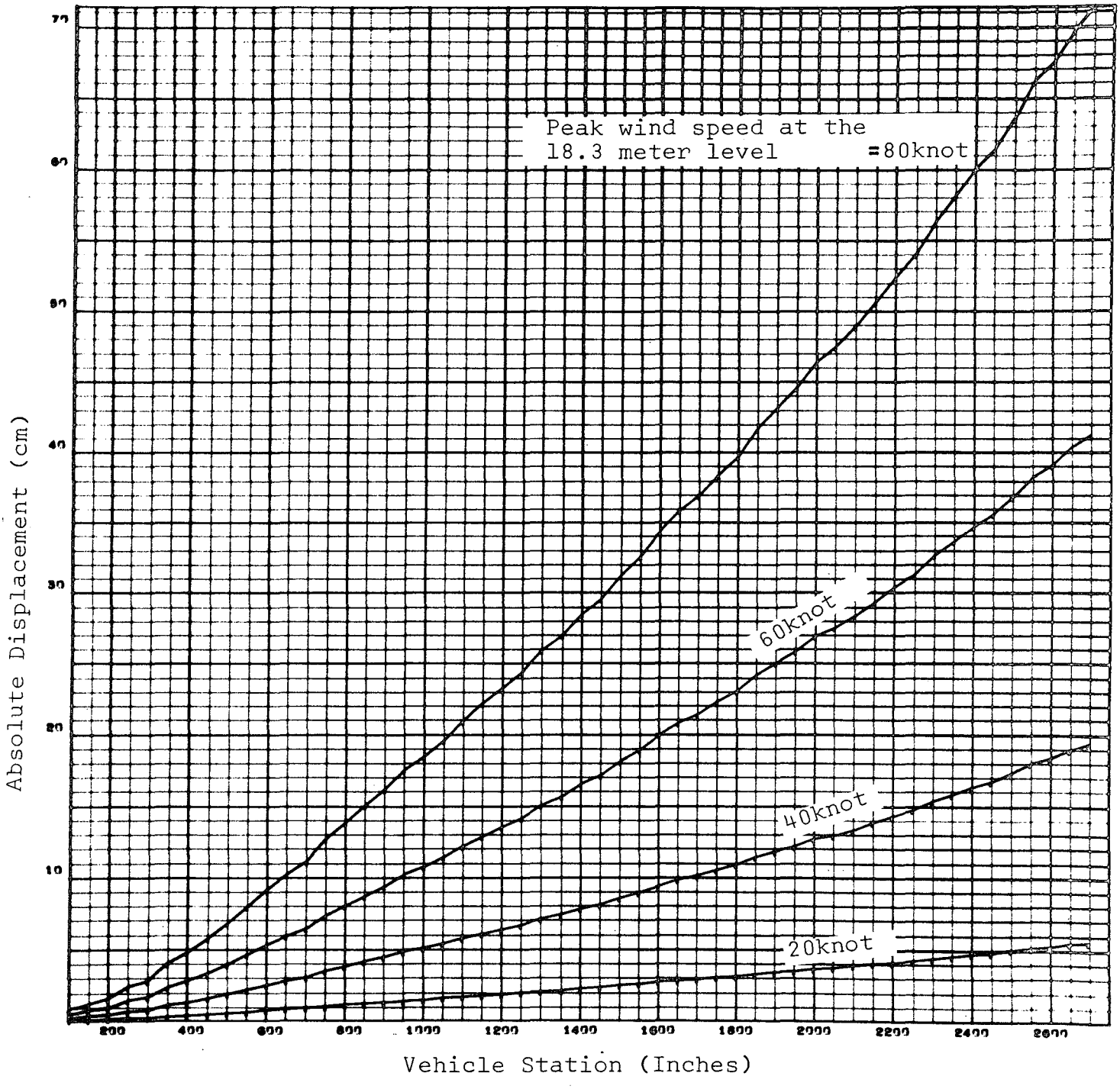

FIG. 5.3.7 ABSOLUTE DISPLACEMENT VERSUS VEHICLE STATION FOR CONCURRENT 3 SIGMA LIFT AND DRAG RESPONSE

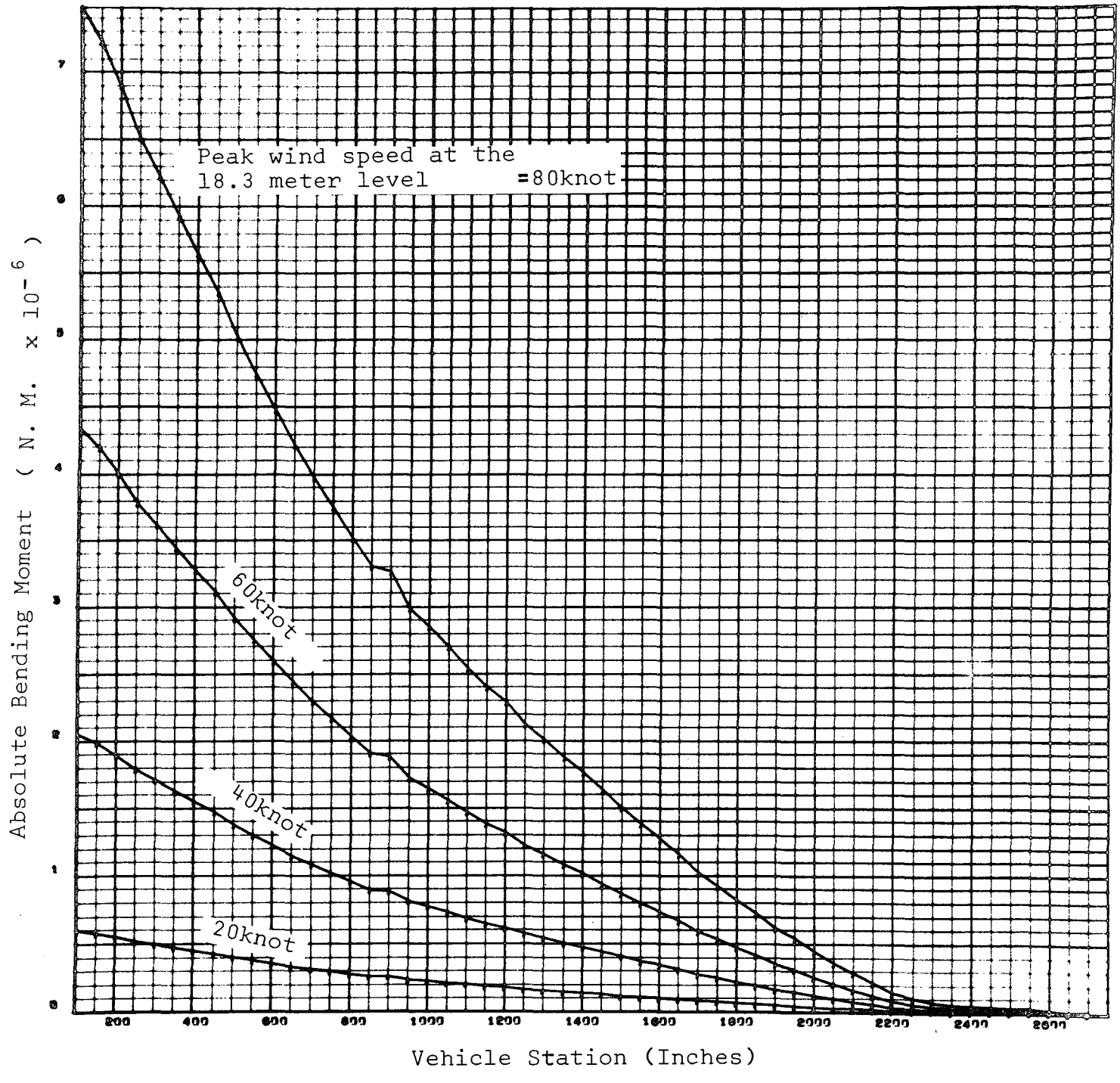

FIG. 5.3.8 ABSOLUTE BENDING MOMENT VERSUS VEHICLE STATION FOR CONCURRENT 3 SIGMA LIFT AND DRAG RESPONSE

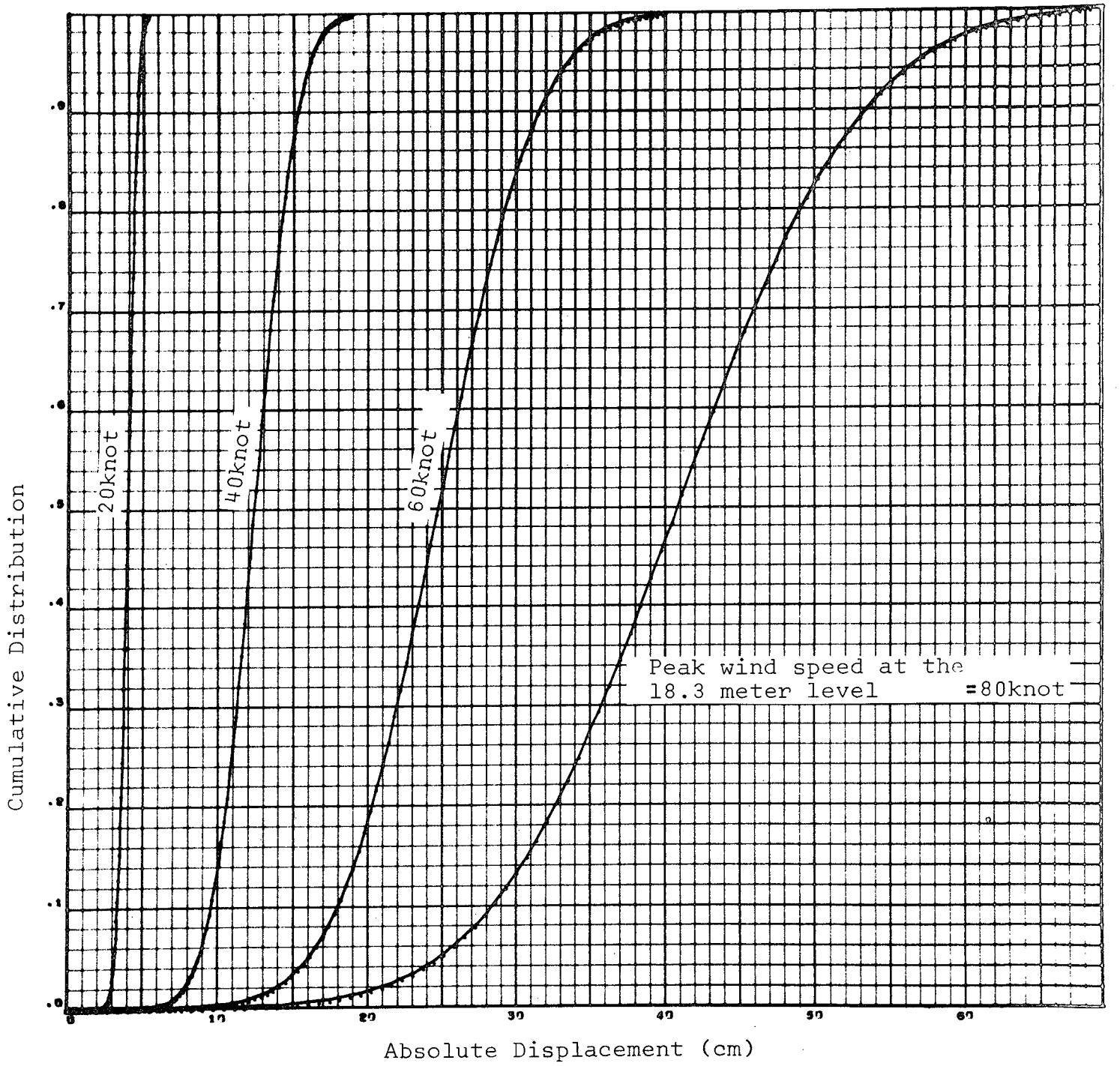

FIG. 5.3.9 CUMULATIVE DISTRIBUTION VERSUS TIP DISPLACEMENT

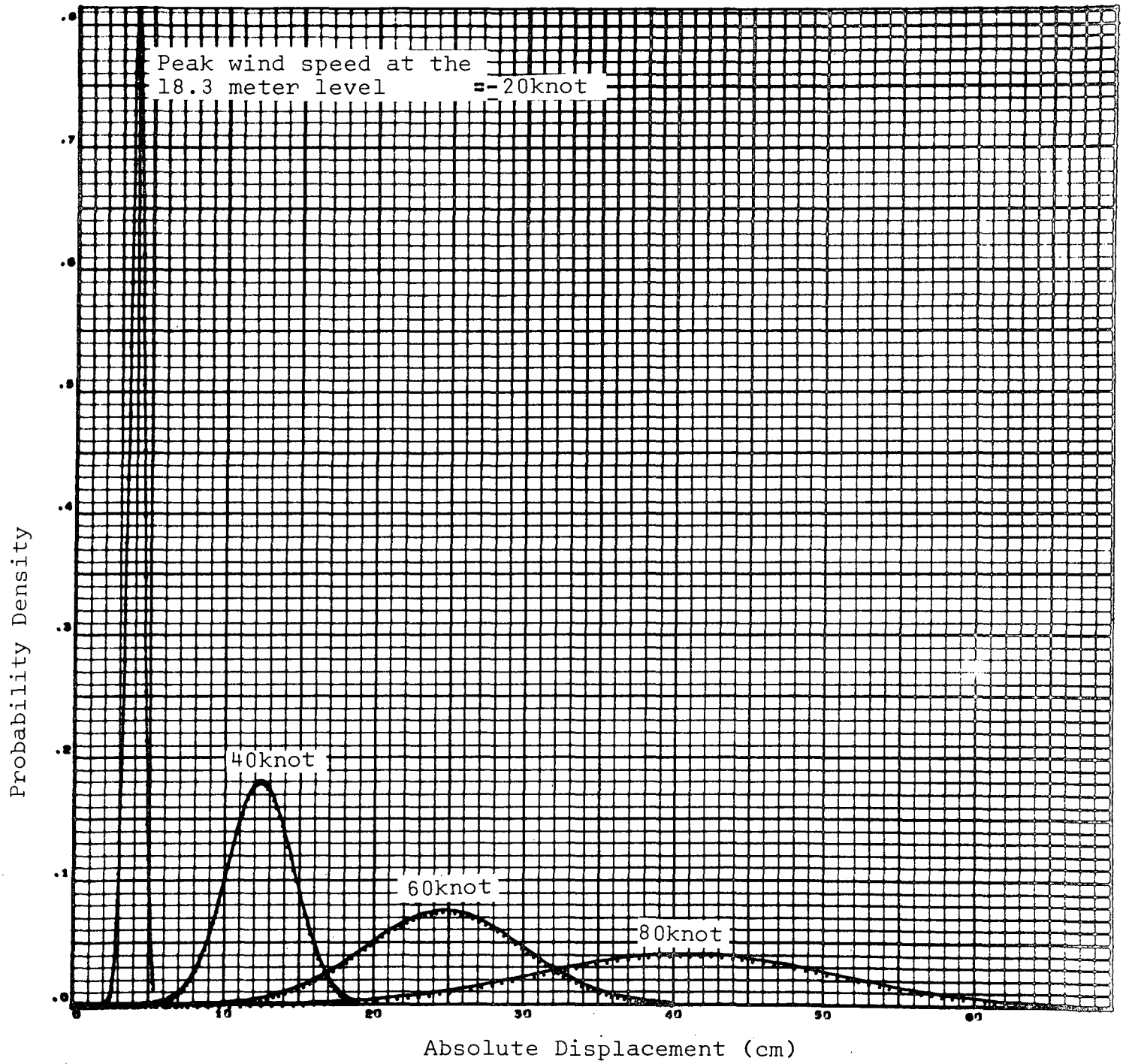

FIG. 5.3.10 PROBABILITY DENSITY VERSUS TIP DISPLACEMENT

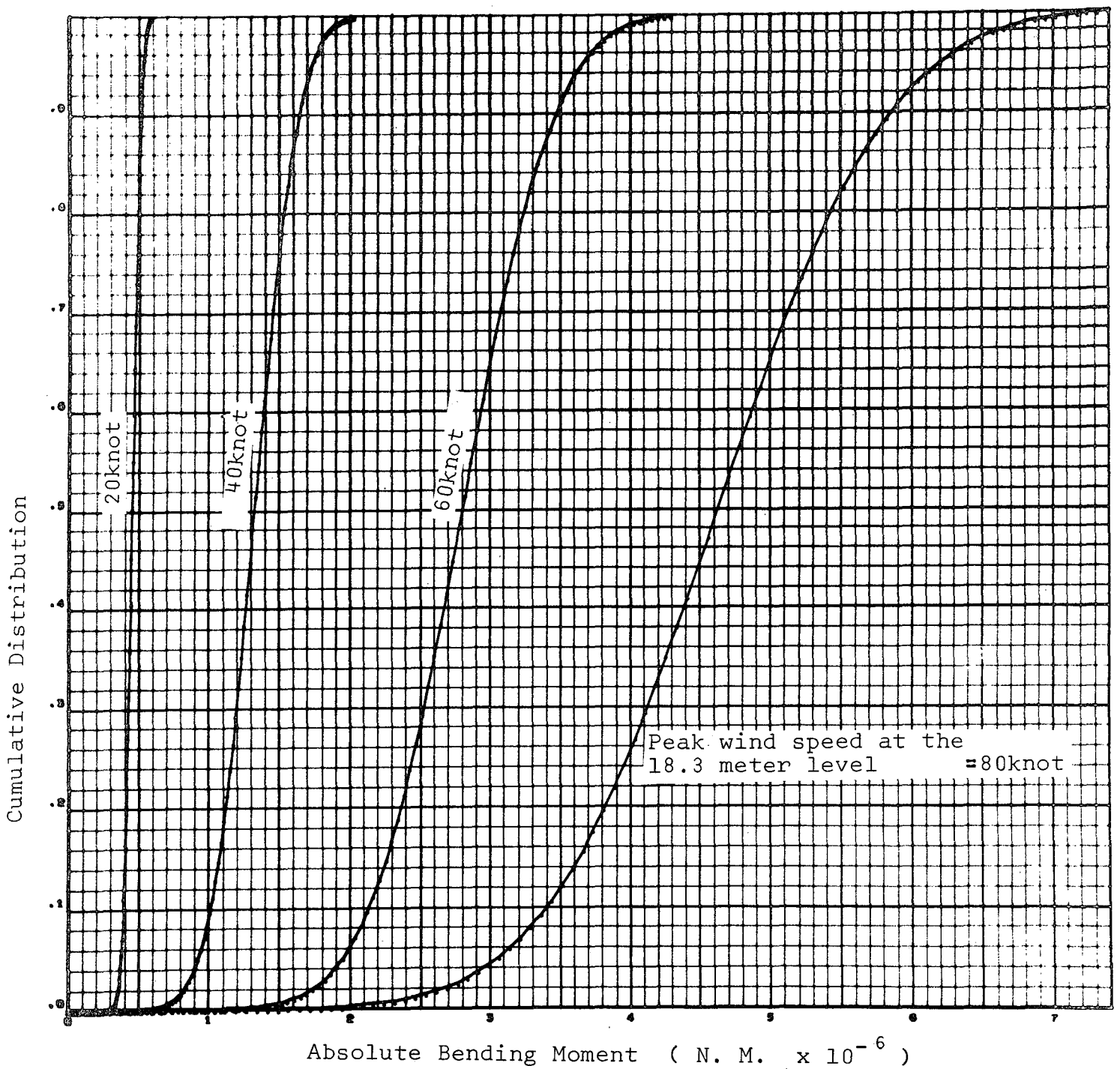

FIG. 5.3.11 CUMULATIVE DISTRIBUTION VERSUS BASE BENDING MOMENT

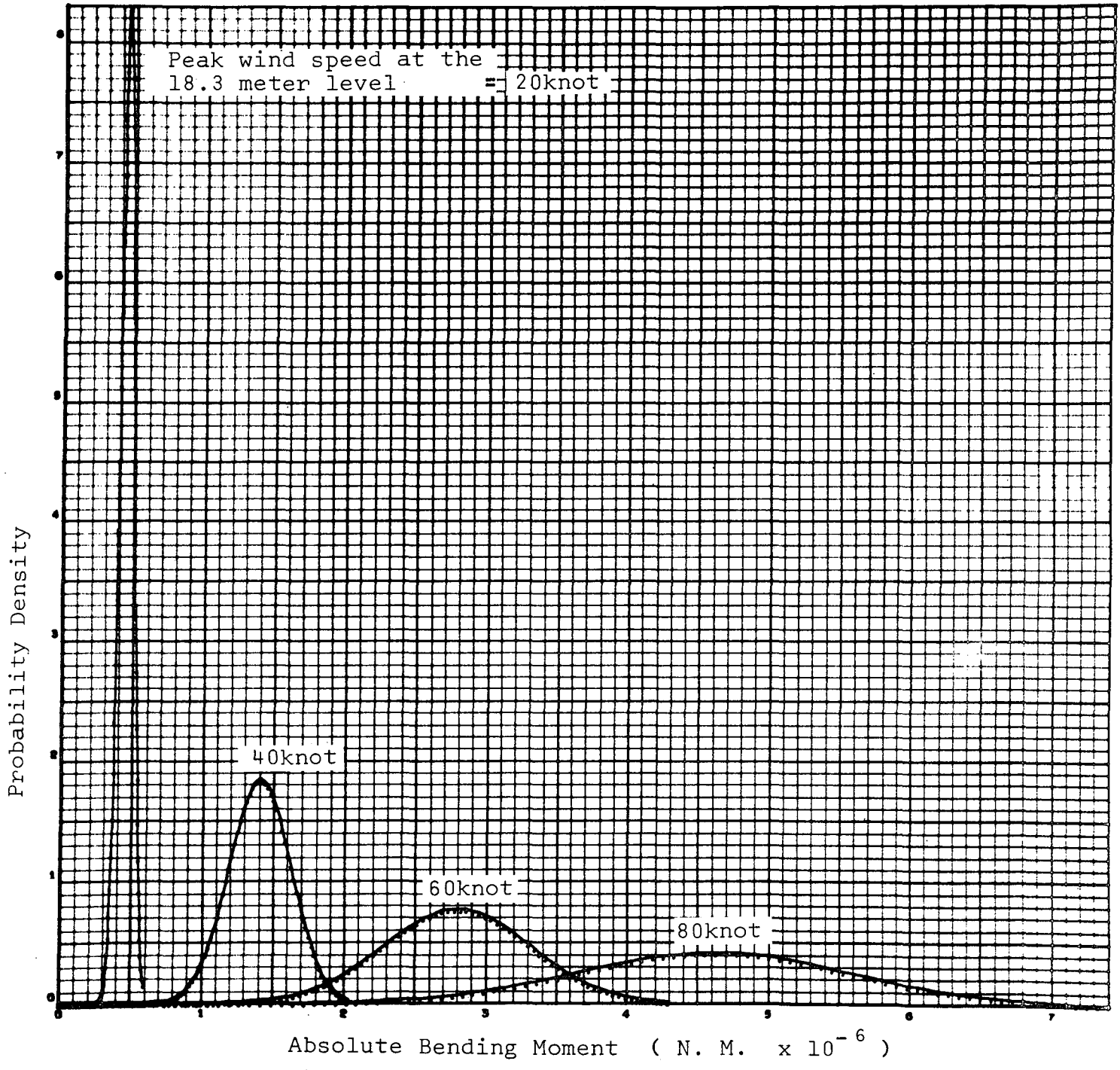

FIG. 5.3.12 PROBABILITY DENSITY VERSUS BASE BENDING MOMENT

5.4 SUMMARY OF PROPELLANT LOAD CONDITIONS AND STRUCTURAL DYNAMIC CHARACTERISTICS FOR CASE 4

Propellant Loading Configuration

Service Module	S-IB RP-1	S-IB LOX	S-IVB LOX	S-IVB LH_2
full	full	full	empty	empty

Structural Dynamic Characteristics

Mode No.	Natural Frequency Hz	Generalized Mass kg.(lb.sec.^{2}/in)	Structural Damping Ratio
1	0.397529	23749.34(135.619)	0.015
2	0.920018	9802.76(55.978)	0.015
3	1.73651	165651.93(945.944)	0.015

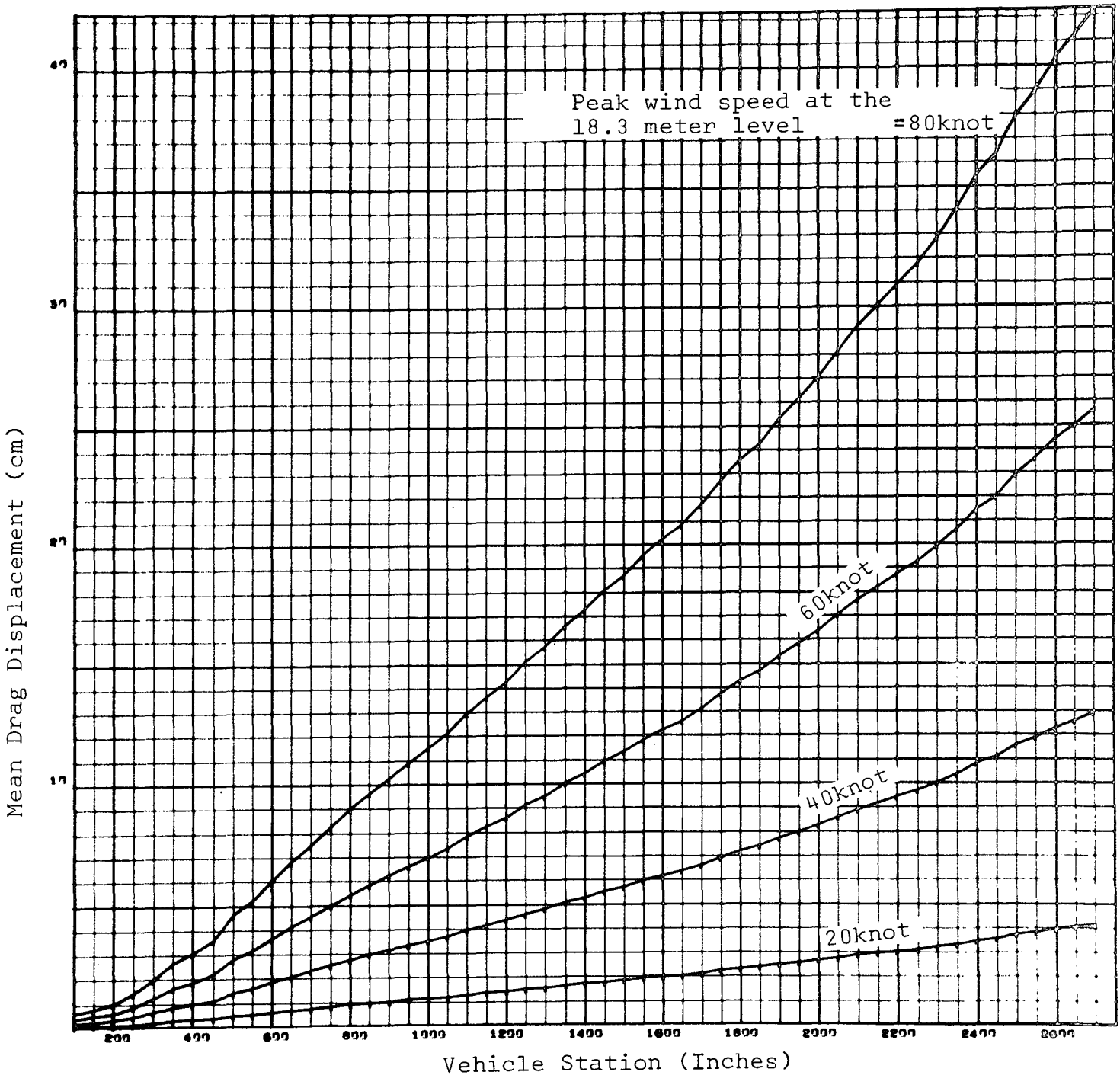

FIG. 5.4.1 MEAN DRAG DISPLACEMENT VERSUS VEHICLE STATION

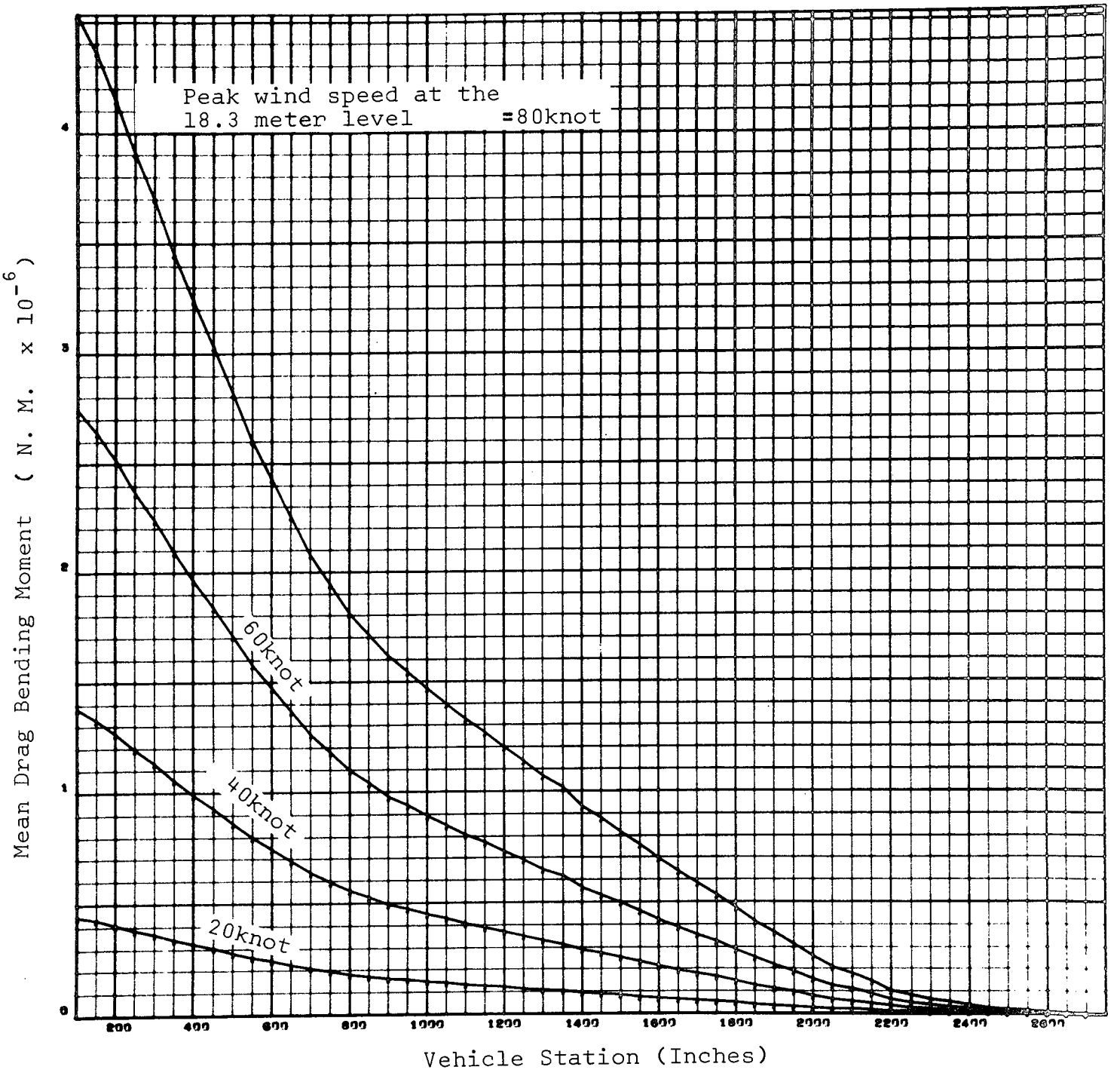

FIG. 5.4.2 MEAN DRAG BENDING MOMENT VERSUS VEHICLE STATION

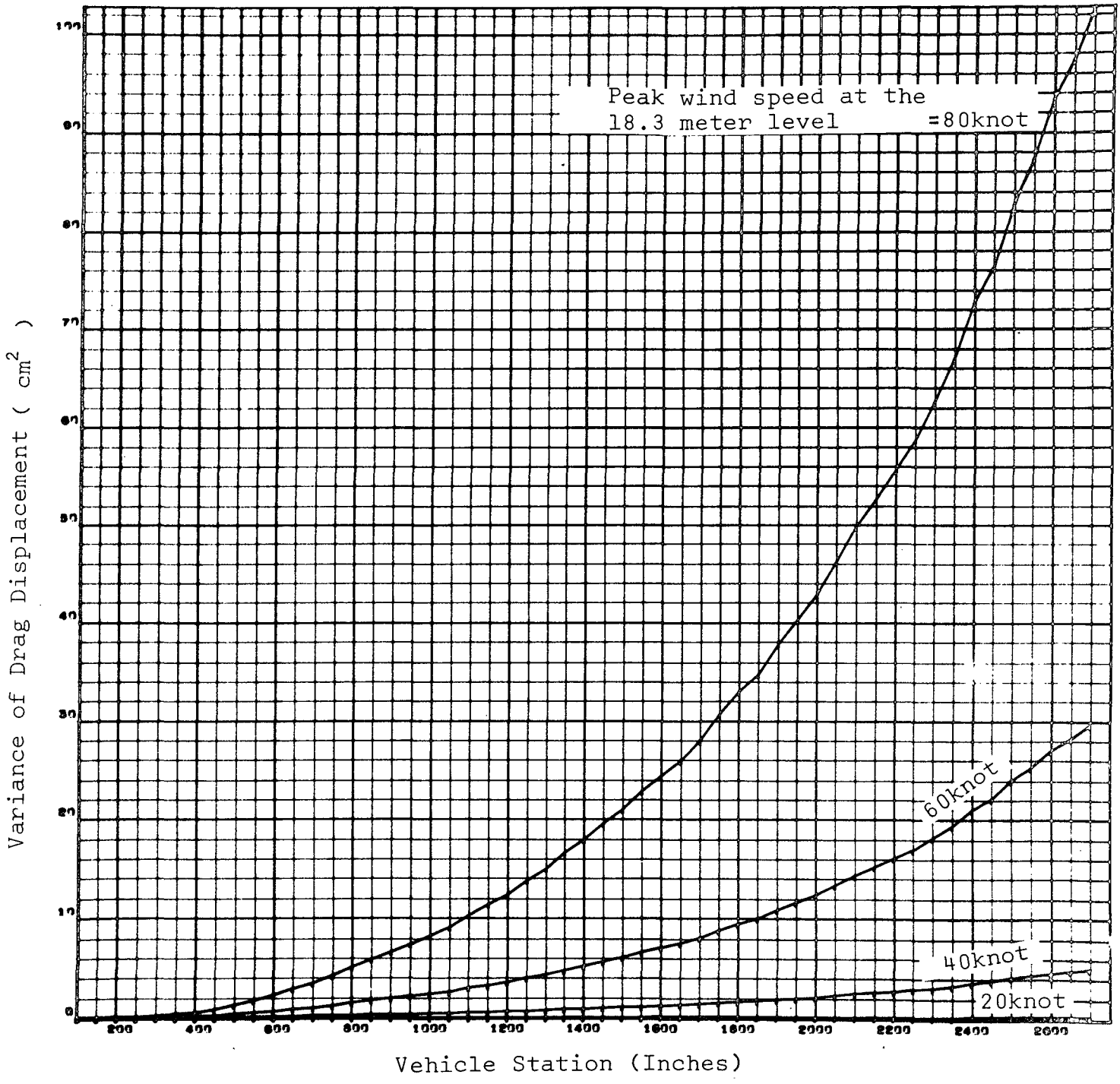

FIG. 5.4.3 VARIANCE OF DRAG DISPLACEMENT VERSUS VEHICLE STATION

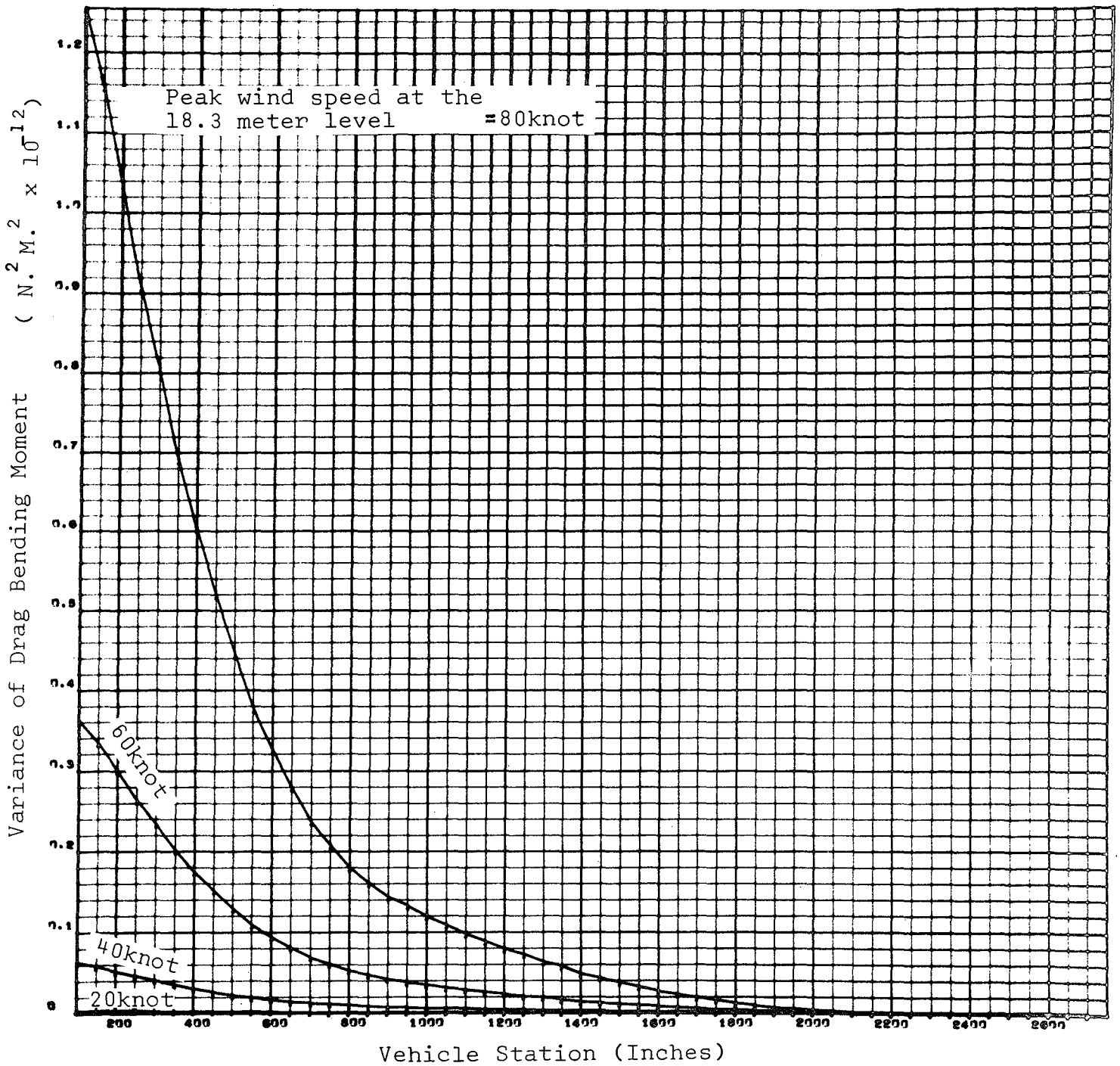

FIG. 5.4.4 VARIANCE OF DRAG BENDING MOMENT VERSUS VEHICLE STATION

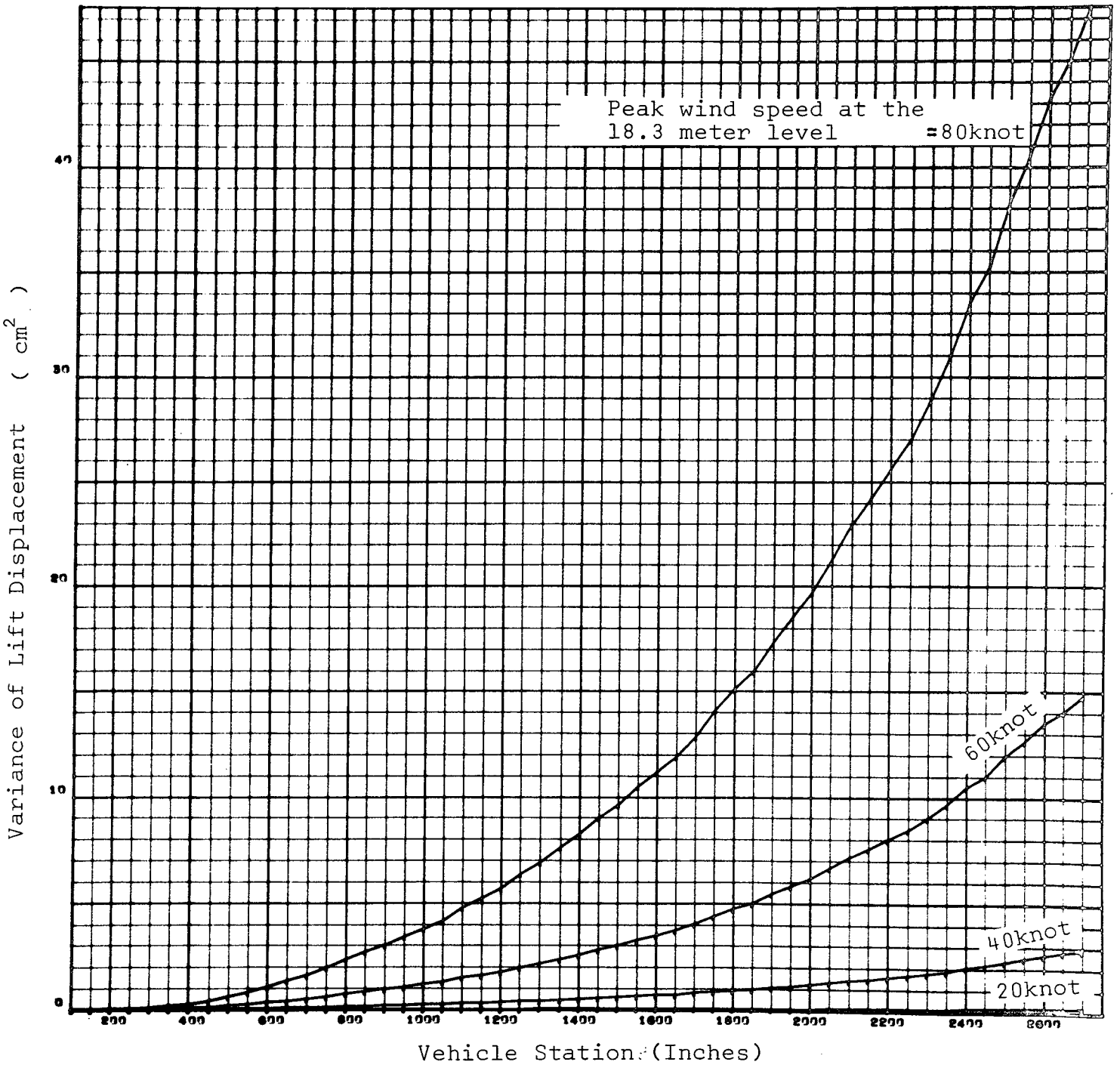

FIG. 5.4.5 VARIANCE OF LIFT DISPLACEMENT VERSUS VEHICLE STATION

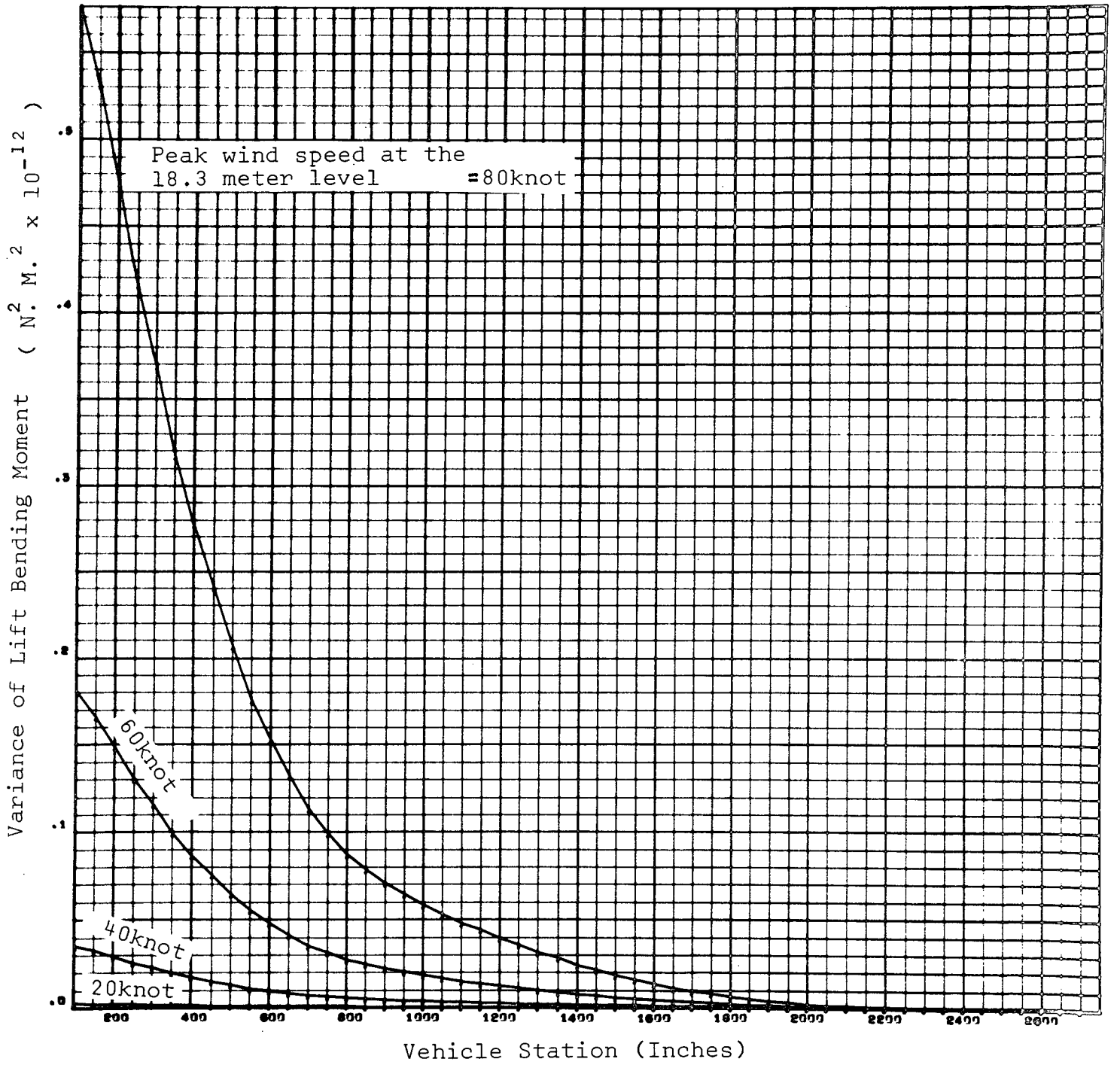

FIG. 5.4.6 VARIANCE OF LIFT BENDING MOMENT VERSUS VEHICLE STATION

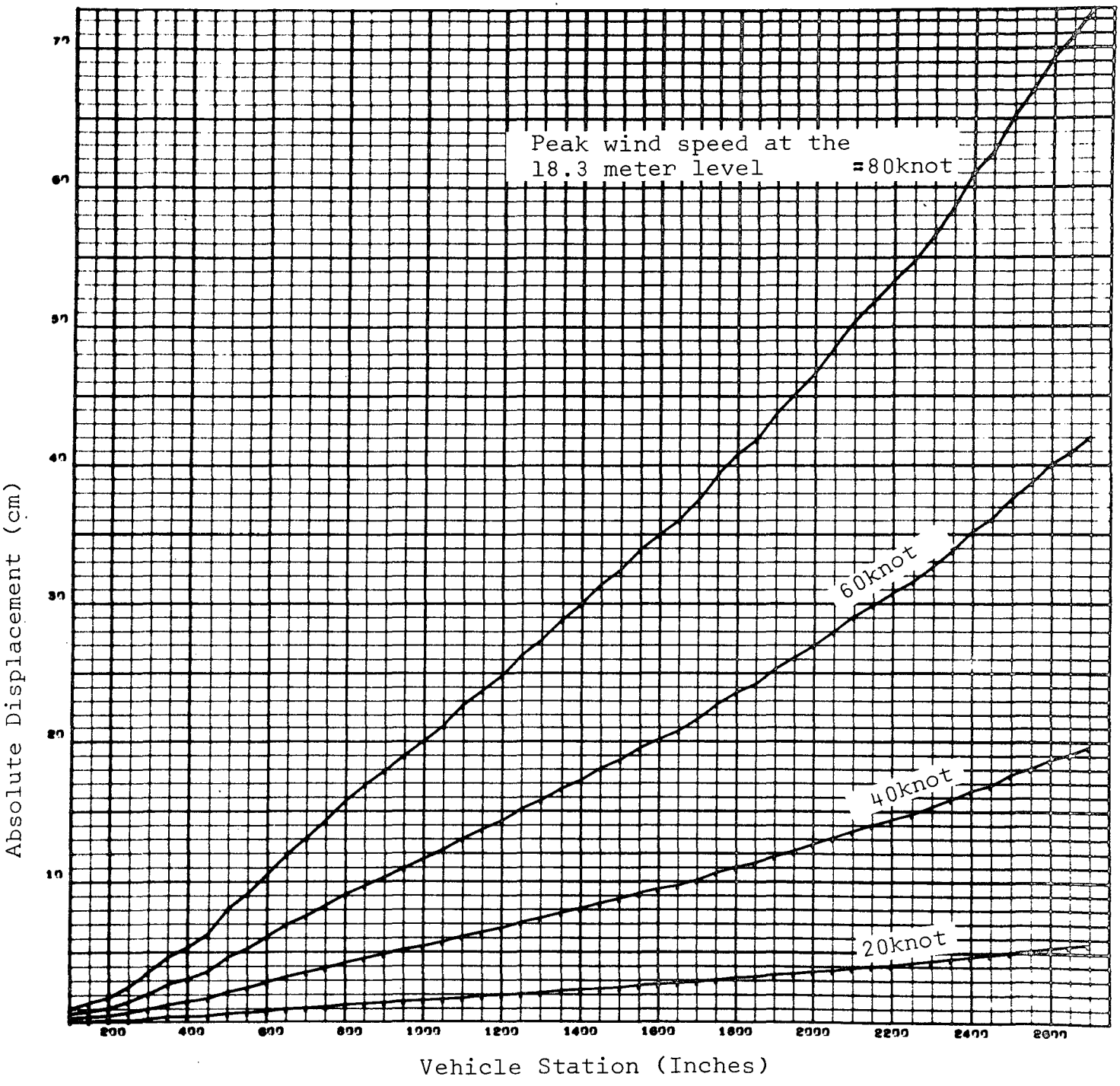

FIG. 5.4.7 ABSOLUTE DISPLACEMENT VERSUS VEHICLE STATION

FOR CONCURRENT 3 SIGMA LIFT AND DRAG RESPONSE

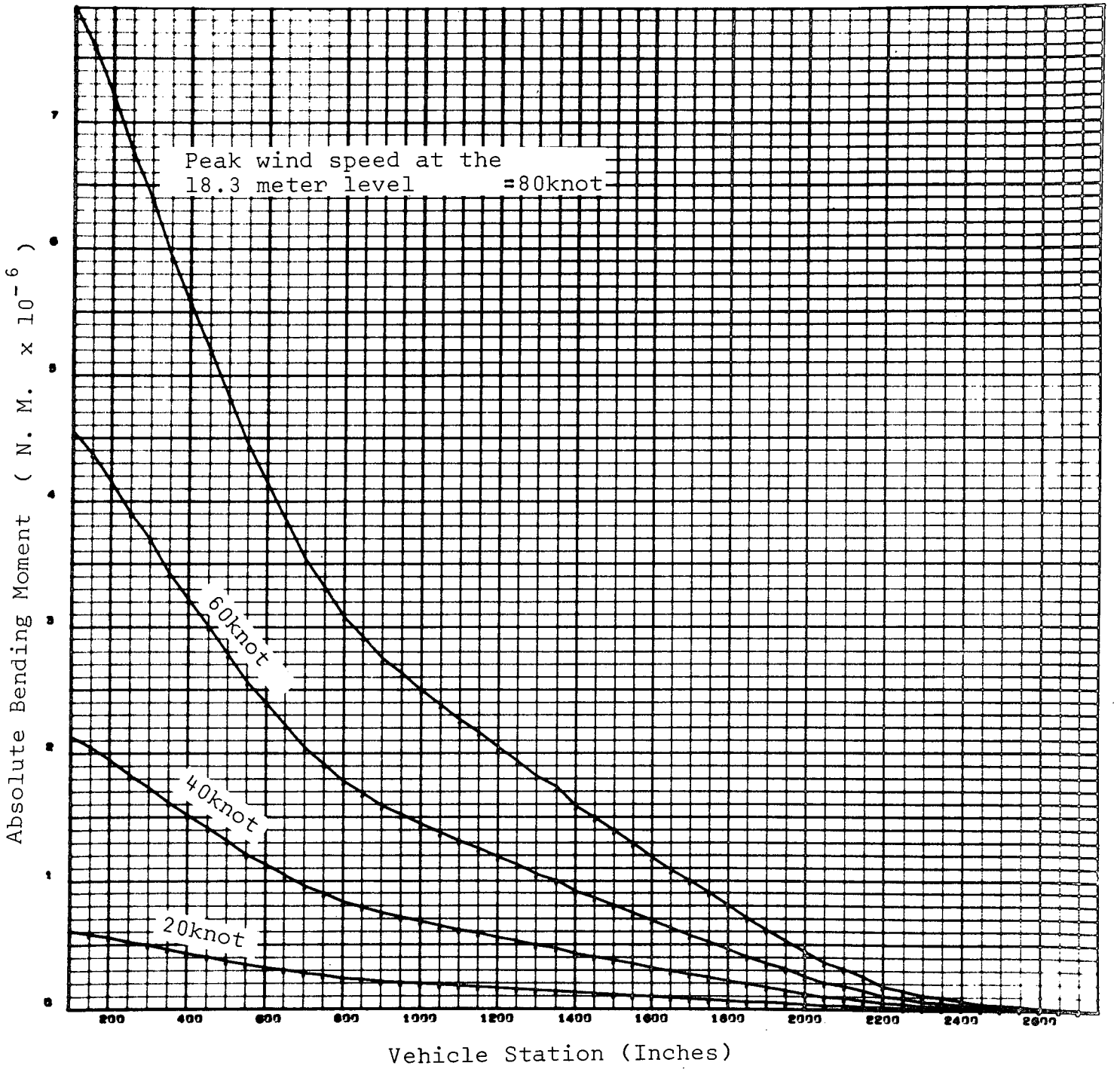

FIG. 5.4.8 ABSOLUTE BENDING MOMEMT VERSUS VEHICLE STATION FOR CONCURRENT 3 SIGMA LIFT AND DRAG RESPONSE

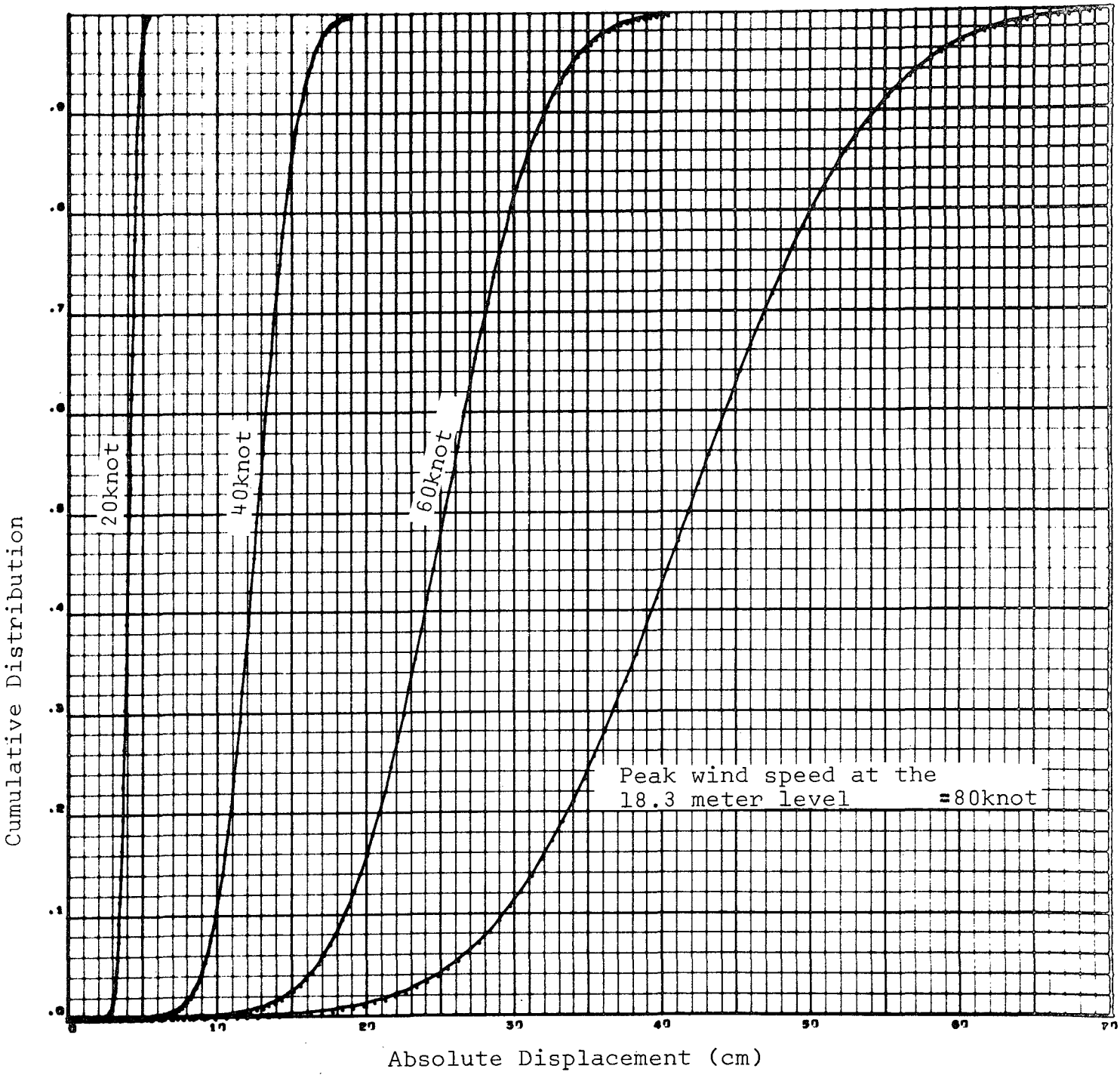

FIG. 5.4.9 CUMULATIVE DISTRIBUTION VERSUS TIP DISPLACEMENT

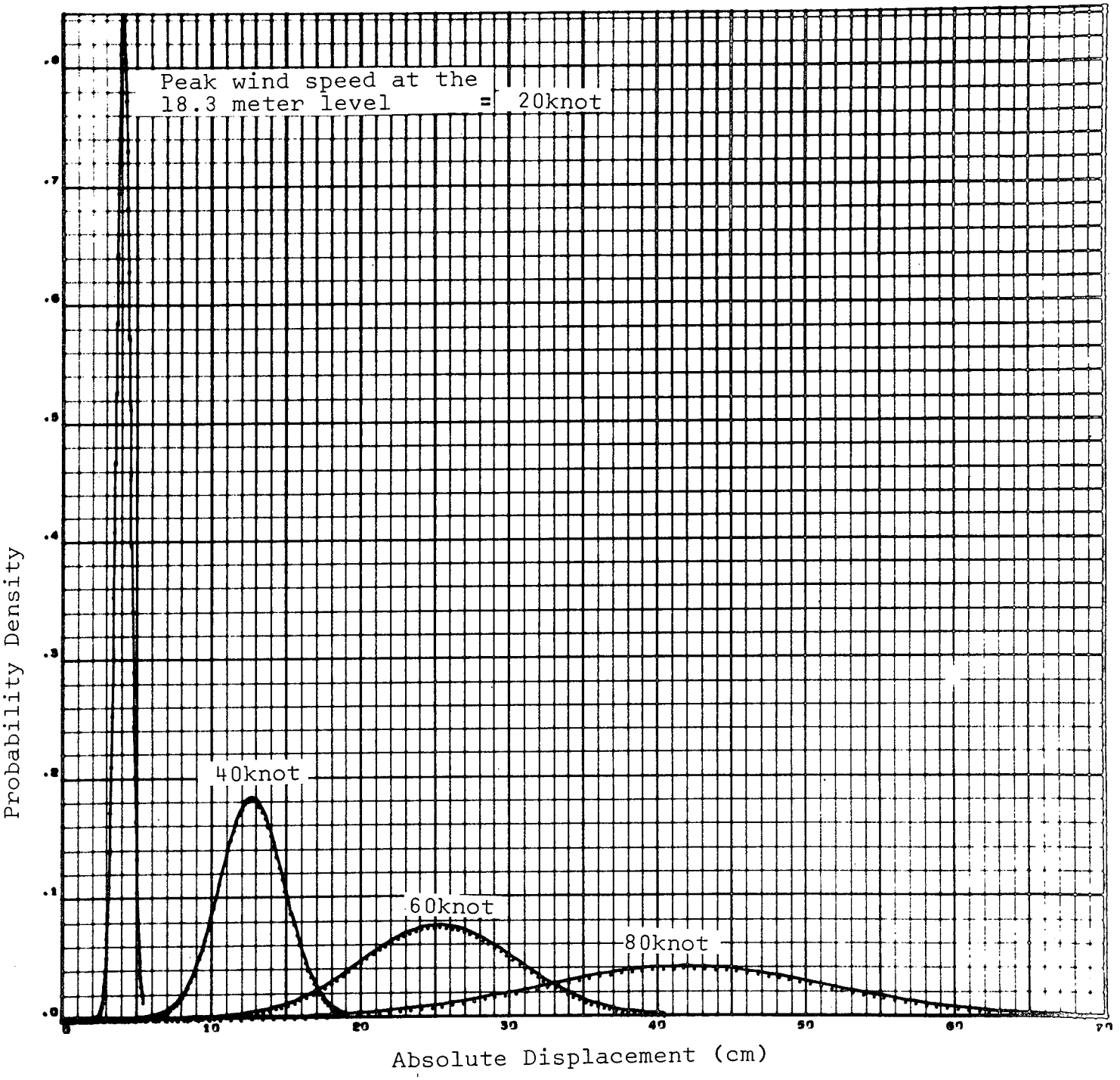

FIG. 5.4.10 PROBABILITY DENSITY VERSUS TIP DISPLACEMENT

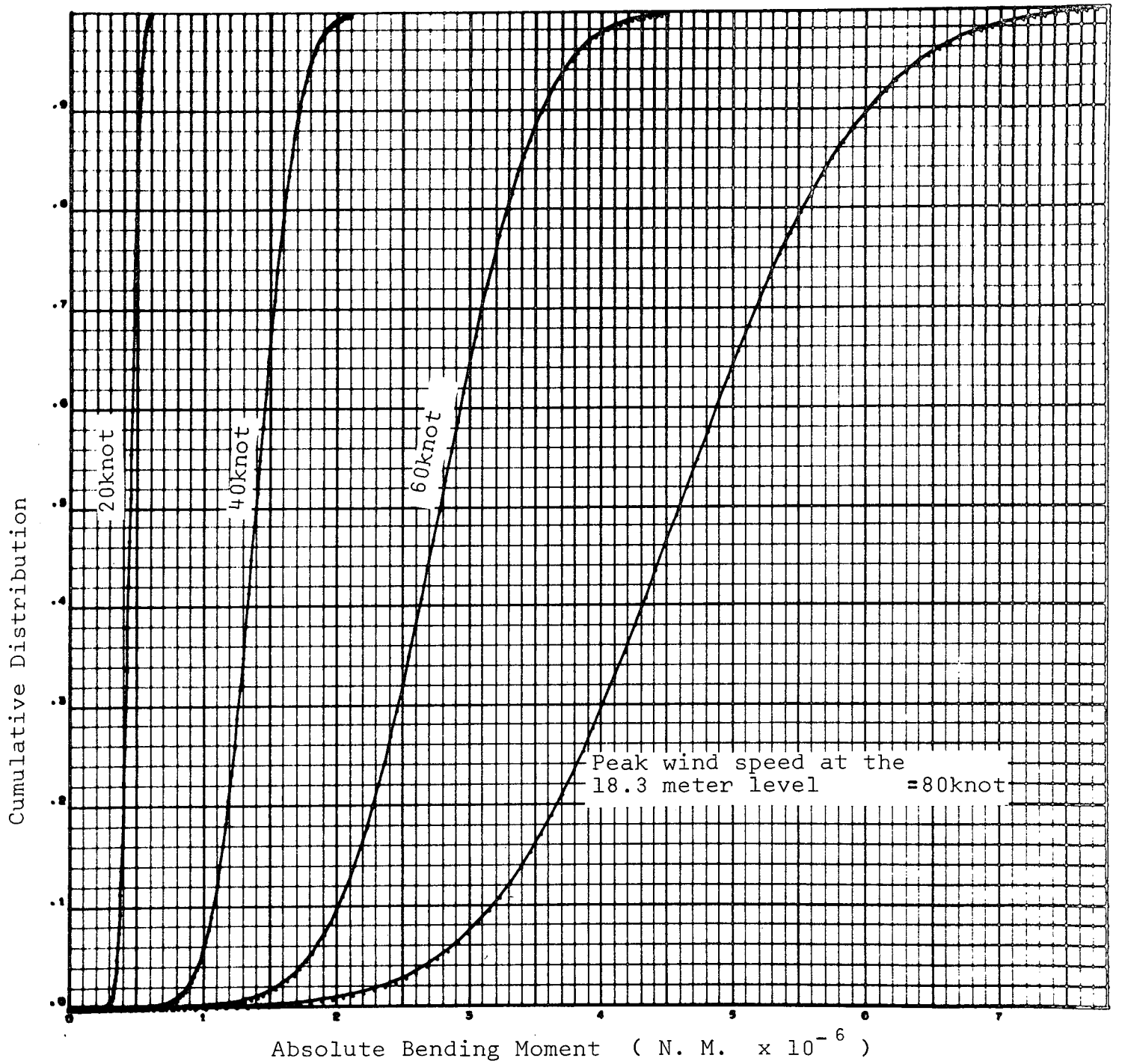

FIG. 5.4.11 CUMULATIVE DISTRIBUTION VERSUS BASE BENDING MOMENT

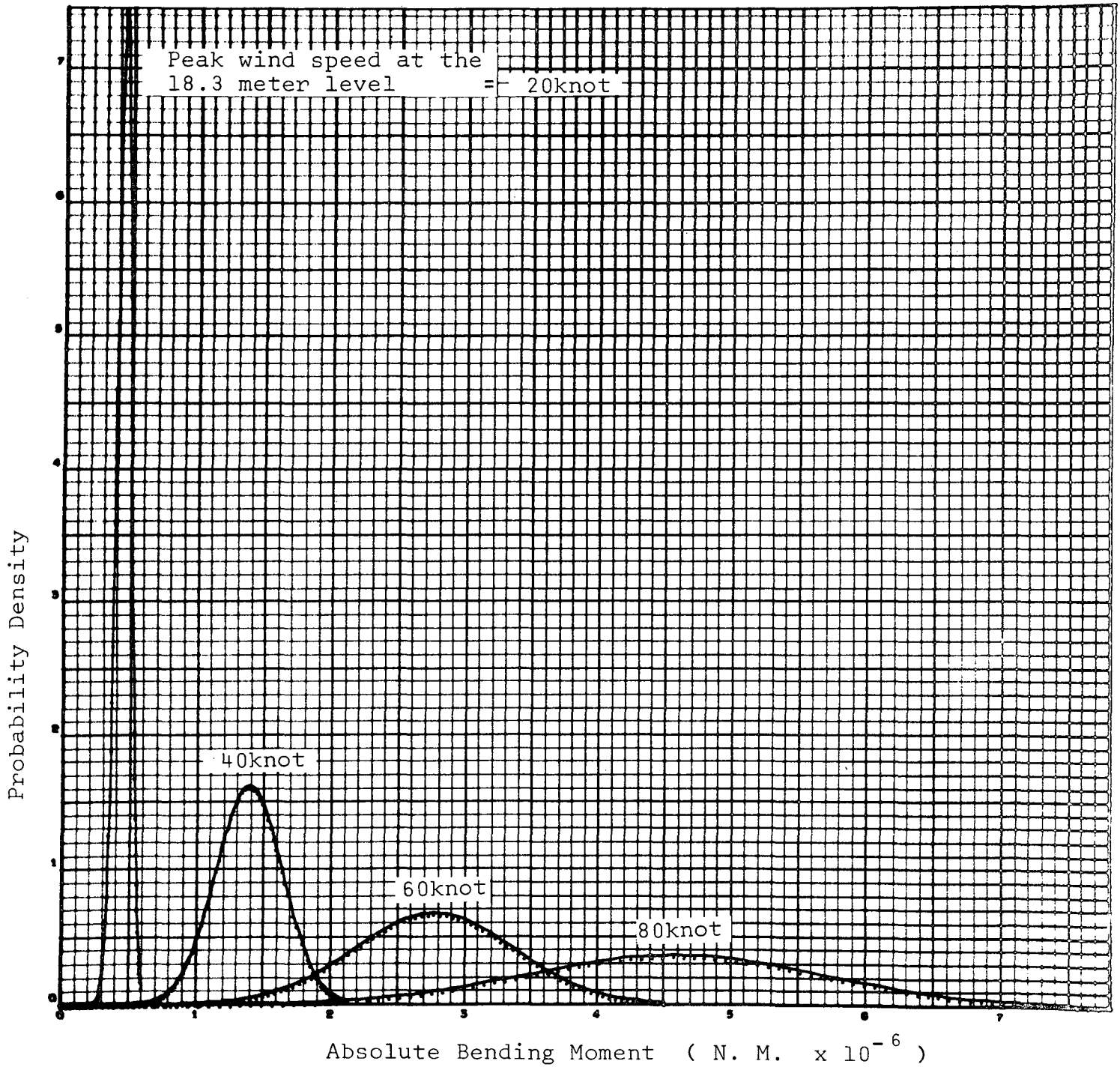

FIG. 5.4.12 PROBABILITY DENSITY VERSUS BASE BENDING MOMENT

5.5 SUMMARY OF PROPELLANT LOAD CONDITIONS AND STRUCTURAL DYNAMIC CHARACTERISTICS FOR CASE 5

Propellant Loading Configuration

Service Module	S-IB RP-1	S-IB LOX	S-IVB LOX	S-IVB LH_2
full	full	full	full	empty

Structural Dynamic Characteristics

Mode No.	Natural Frequency Hz	Generalized Mass kg.(lb.sec.^{2}/in)	Structural Damping Ratio
1	0.32144	39648.49(226.41)	0.015
2	0.911911	8469.76(48.366)	0.015
3	1.69961	18366.91(104.883)	0.015

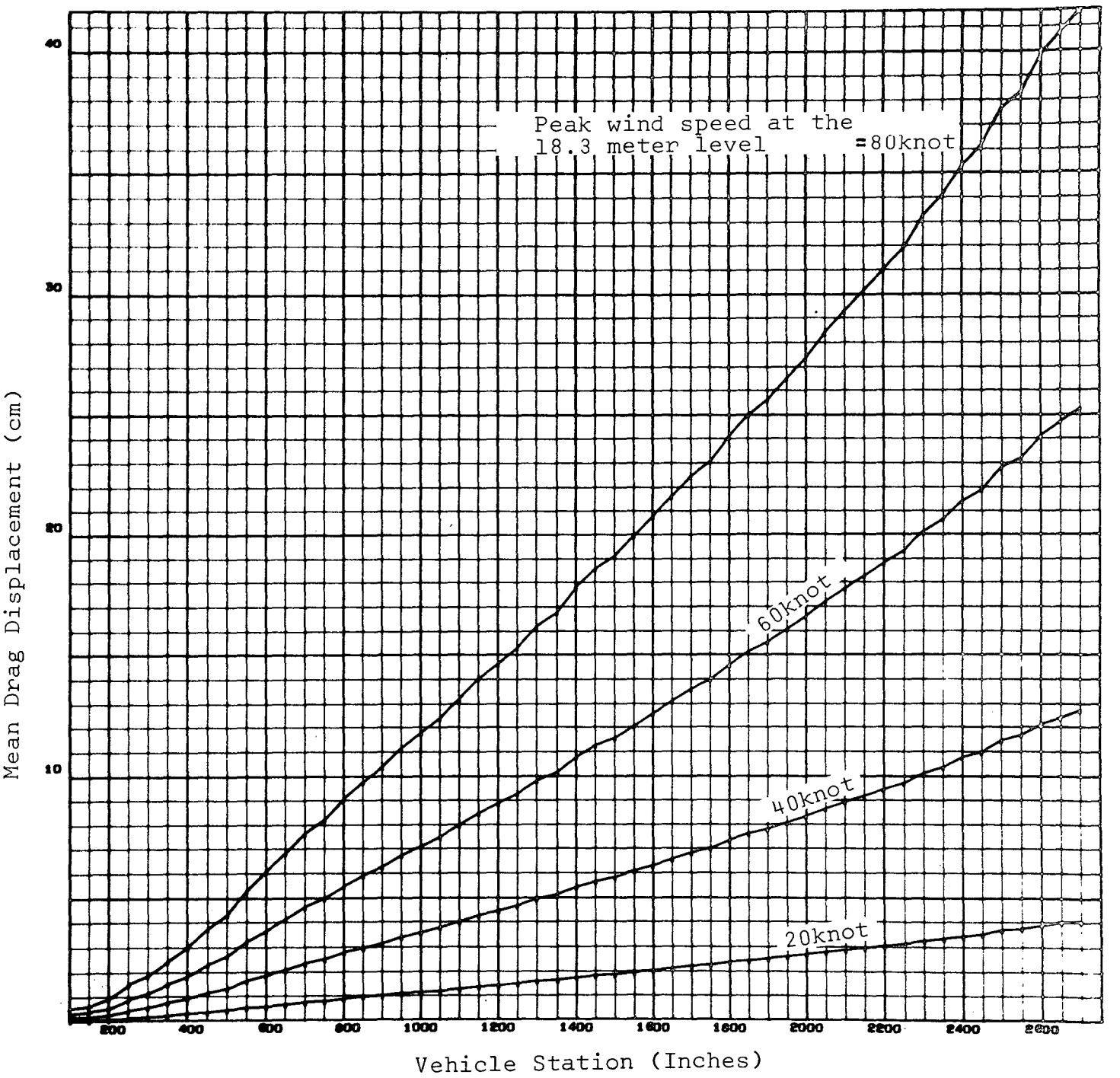

FIG. 5.5.1 MEAN DRAG DISPLACEMENT VERSUS VEHICLE STATION

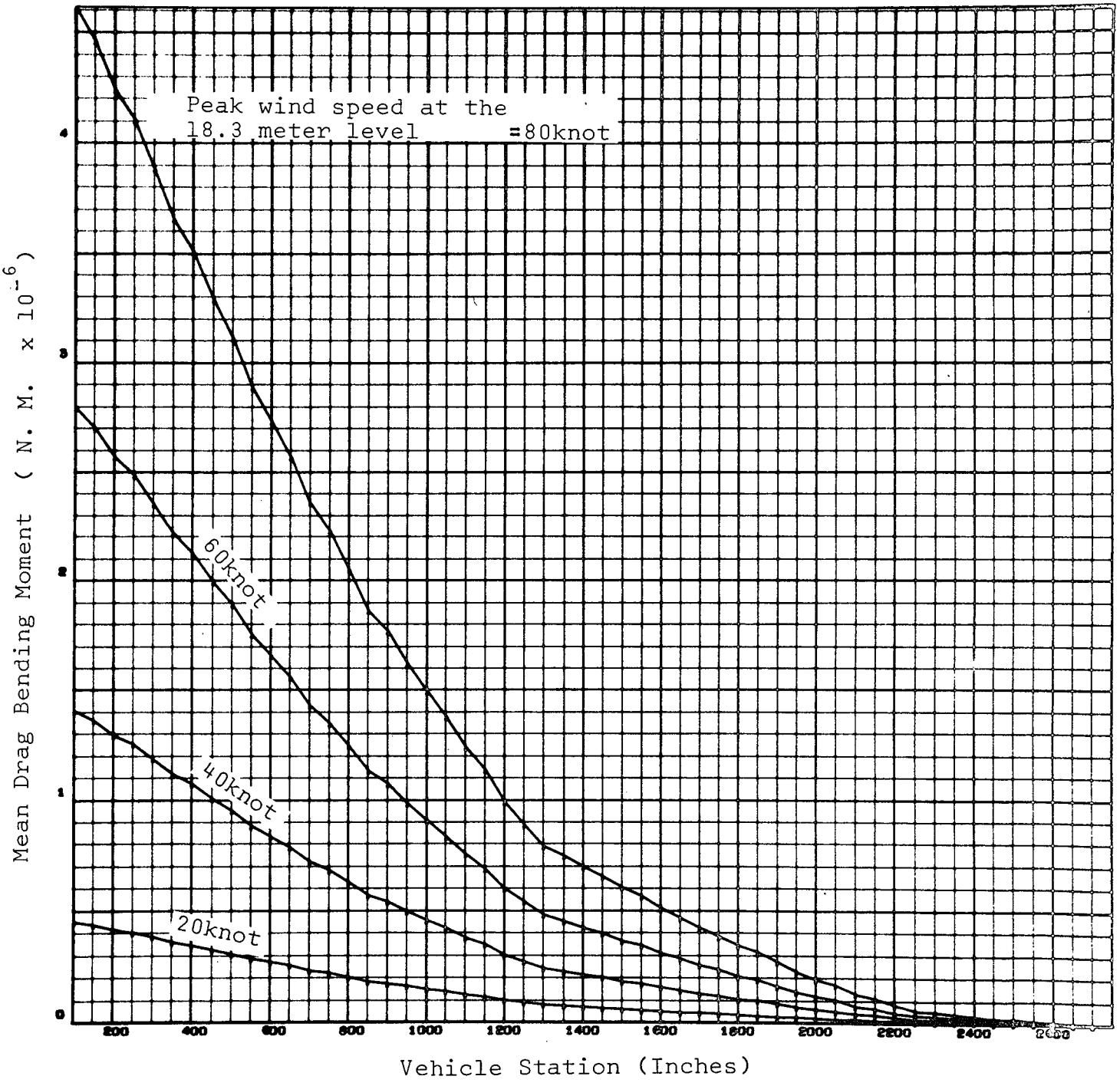

FIG. 5.5.2 MEAN DRAG BENDING MOMENT VERSUS VEHICLE STATION

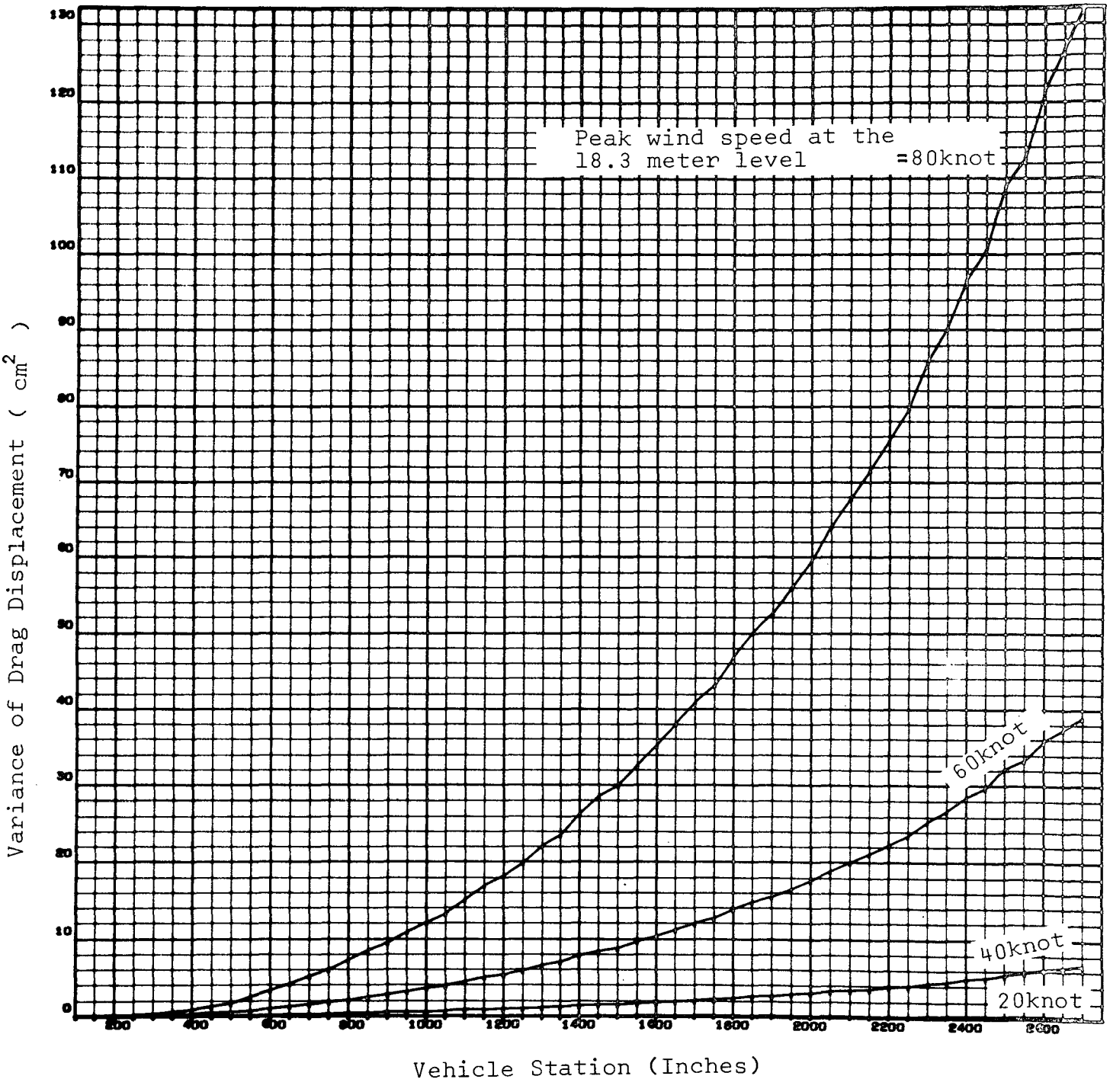

FIG. 5.5.3 VARIANCE OF DRAG DISPLACEMENT VERSUS VEHICLE STATION

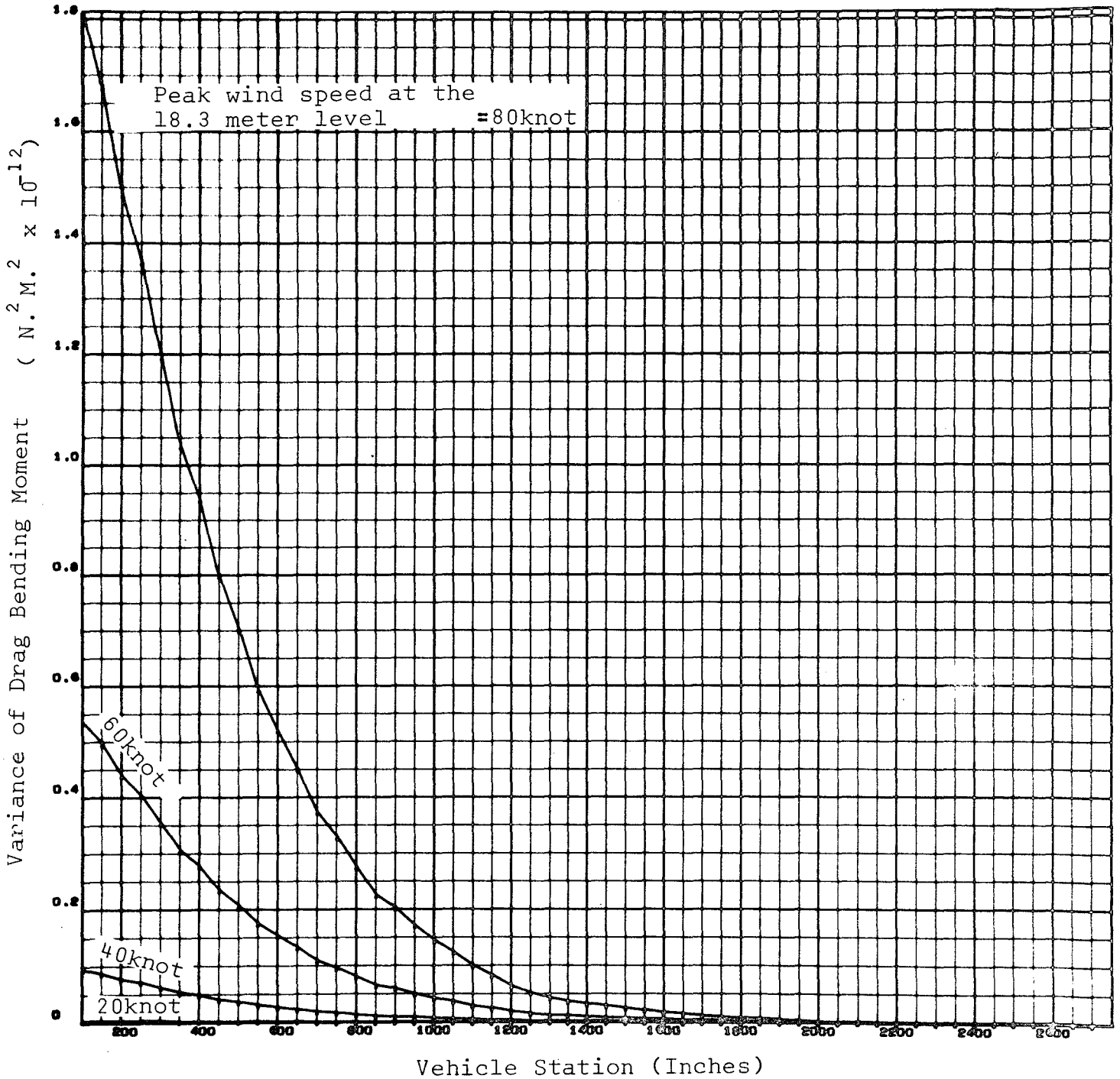

FIG. 5.5.4 VARIANCE OF DRAG BENDING MOMENT VERSUS VEHICLE STATION

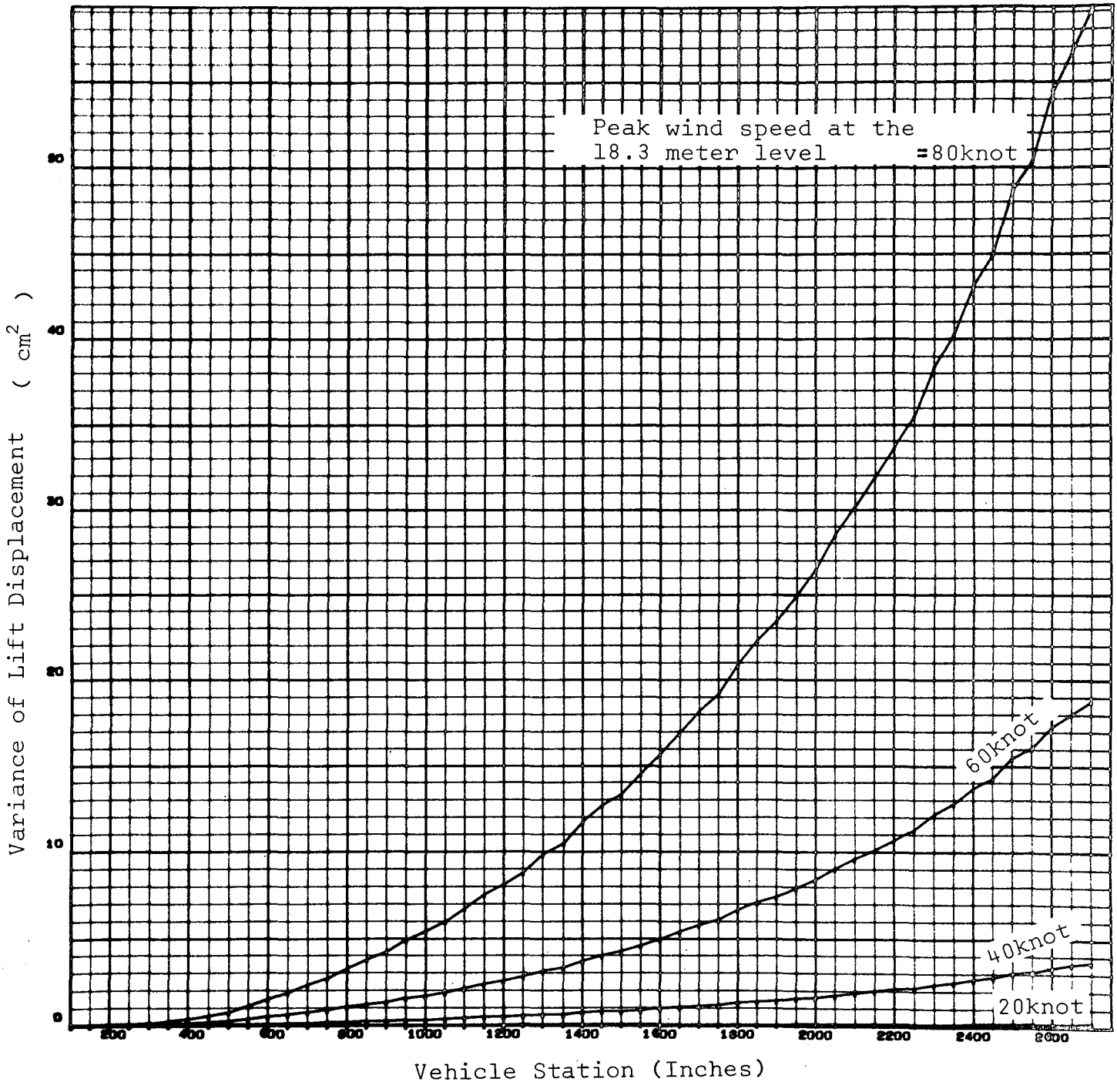

FIG. 5.5.5 VARIANCE OF LIFT DISPLACEMENT VERSUS VEHICLE STATION

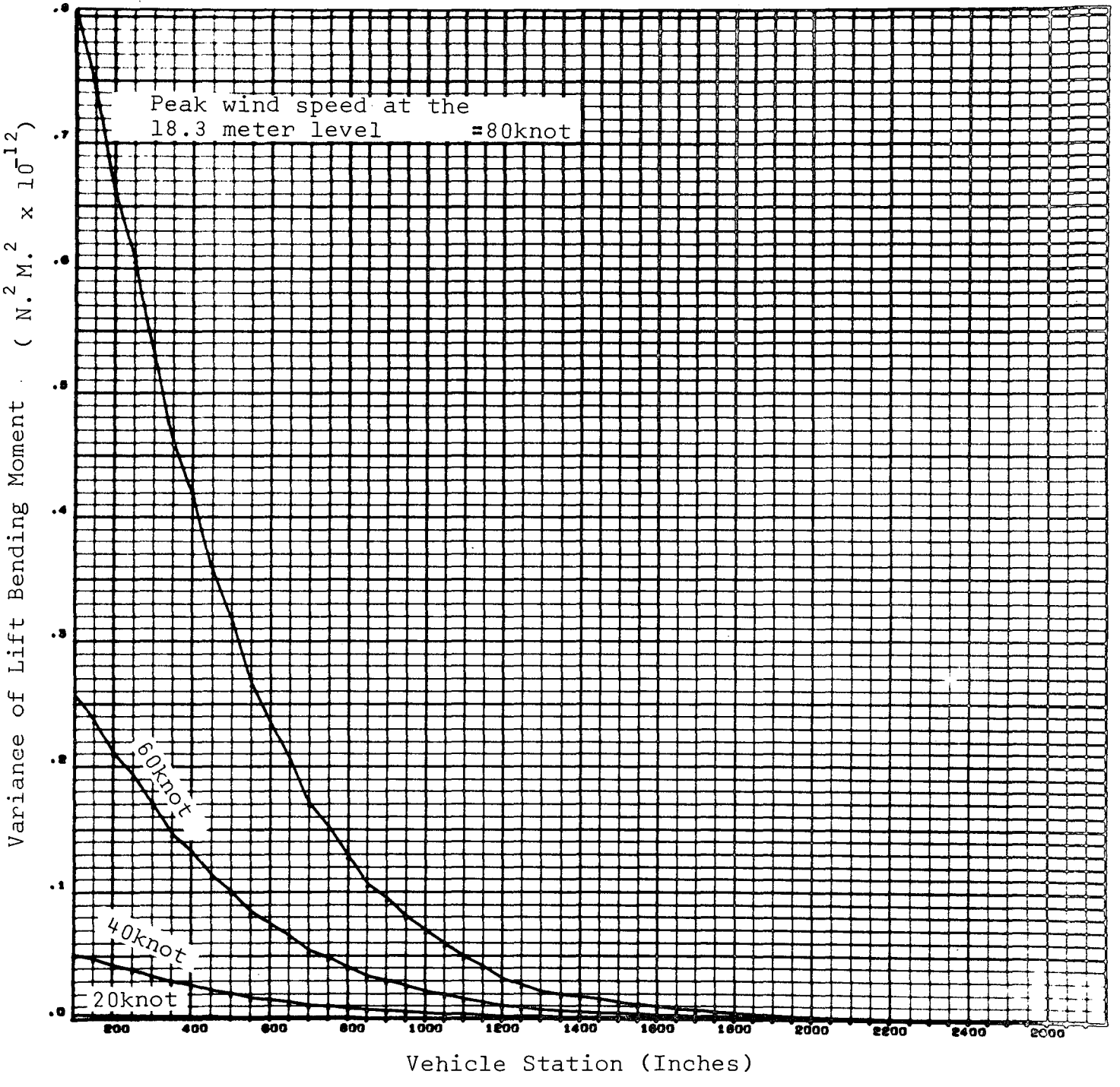

FIG. 5.5.6 VARIANCE OF LIFT BENDING MOMENT VERSUS VEHICLE STATION

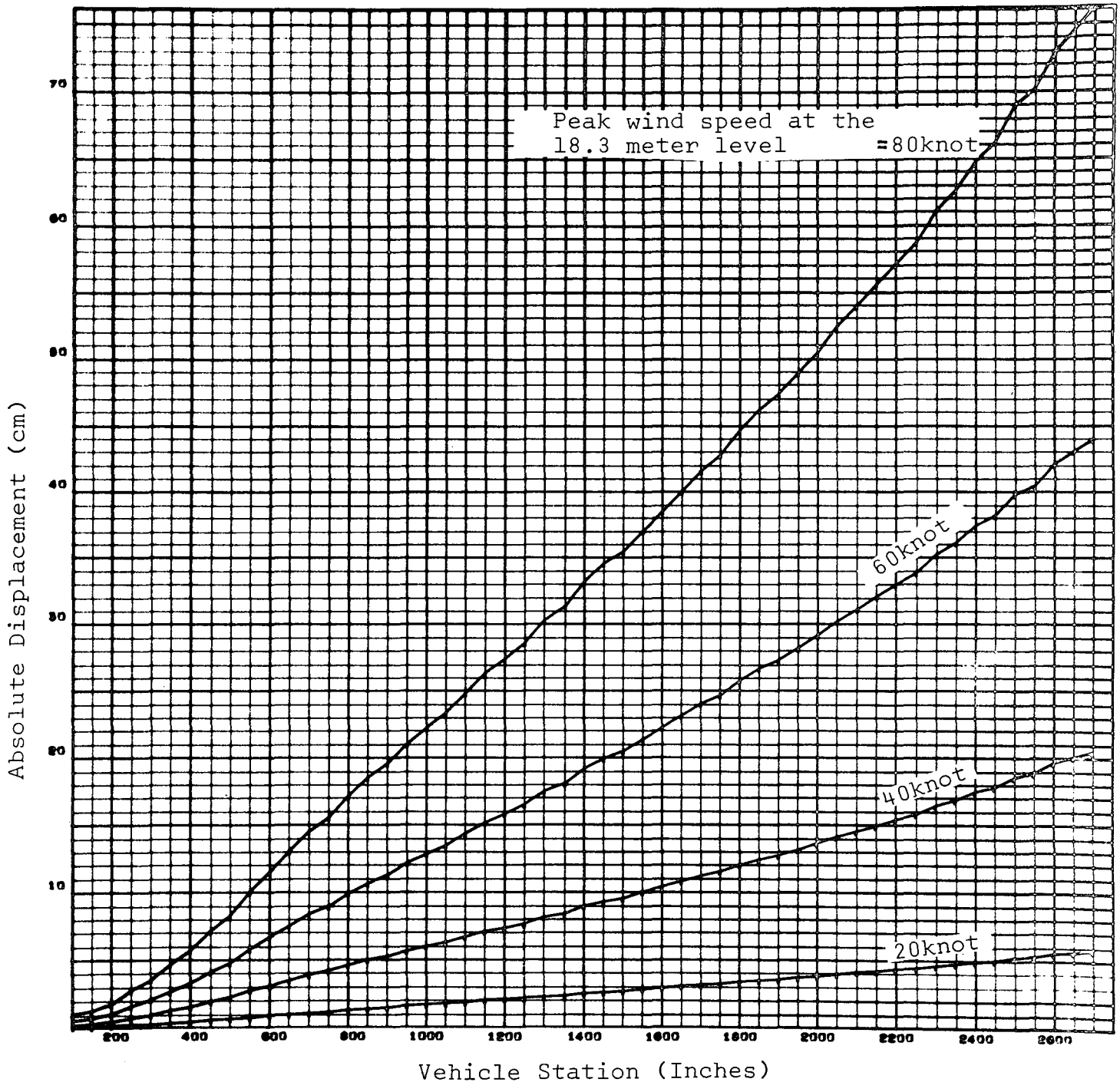

FIG. 5.5.7 ABSOLUTE DISPLACEMENT VERSUS VEHICLE STATION FOR CONCURRENT 3 SIGMA LIFT AND DRAG RESPONSE

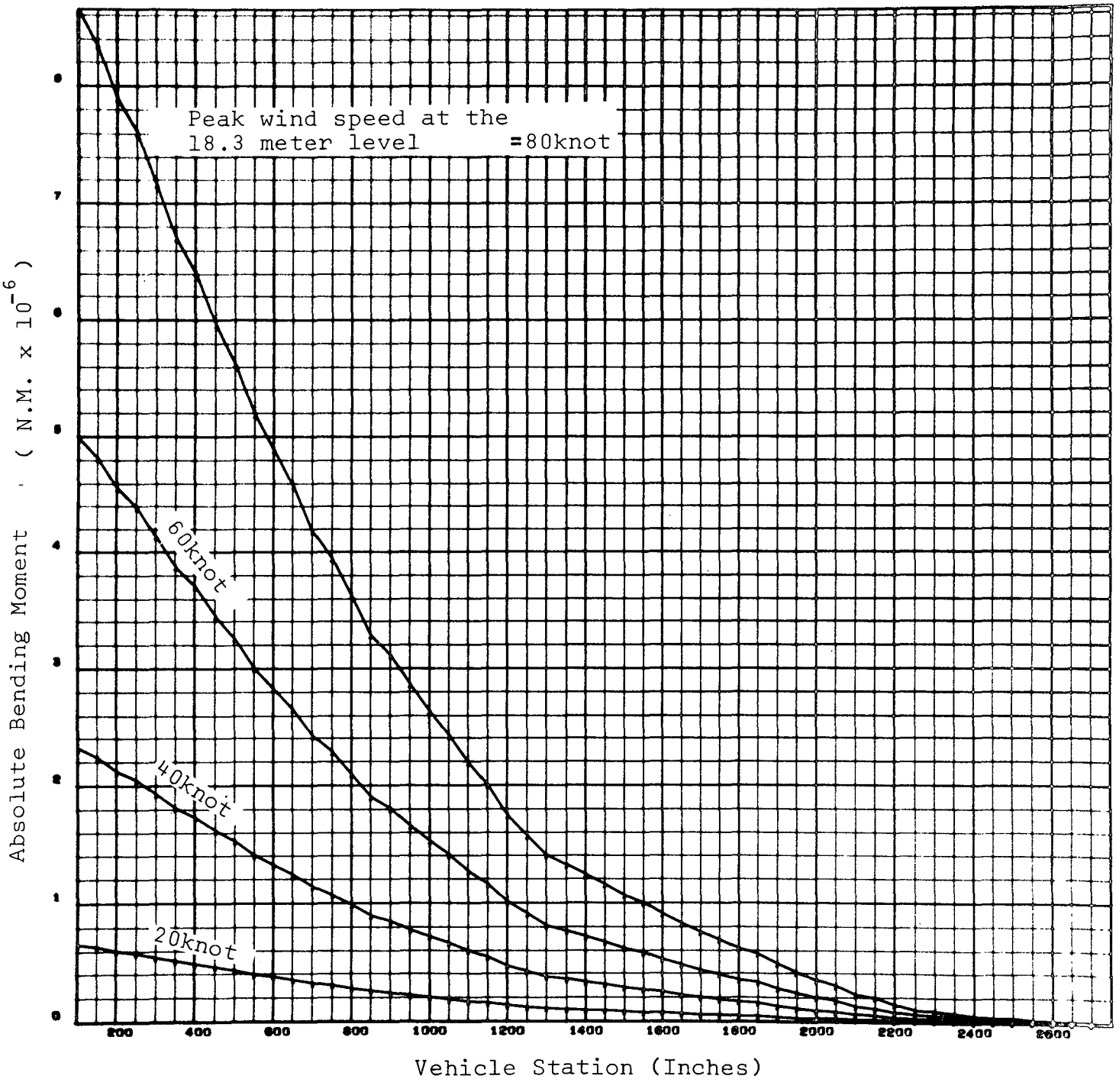

FIG. 5.5.8 ABSOLUTE BENDING MOMENT VERSUS VEHICLE STATION FOR CONCURRENT 3 SIGMA LIFT AND DRAG RESPONSE

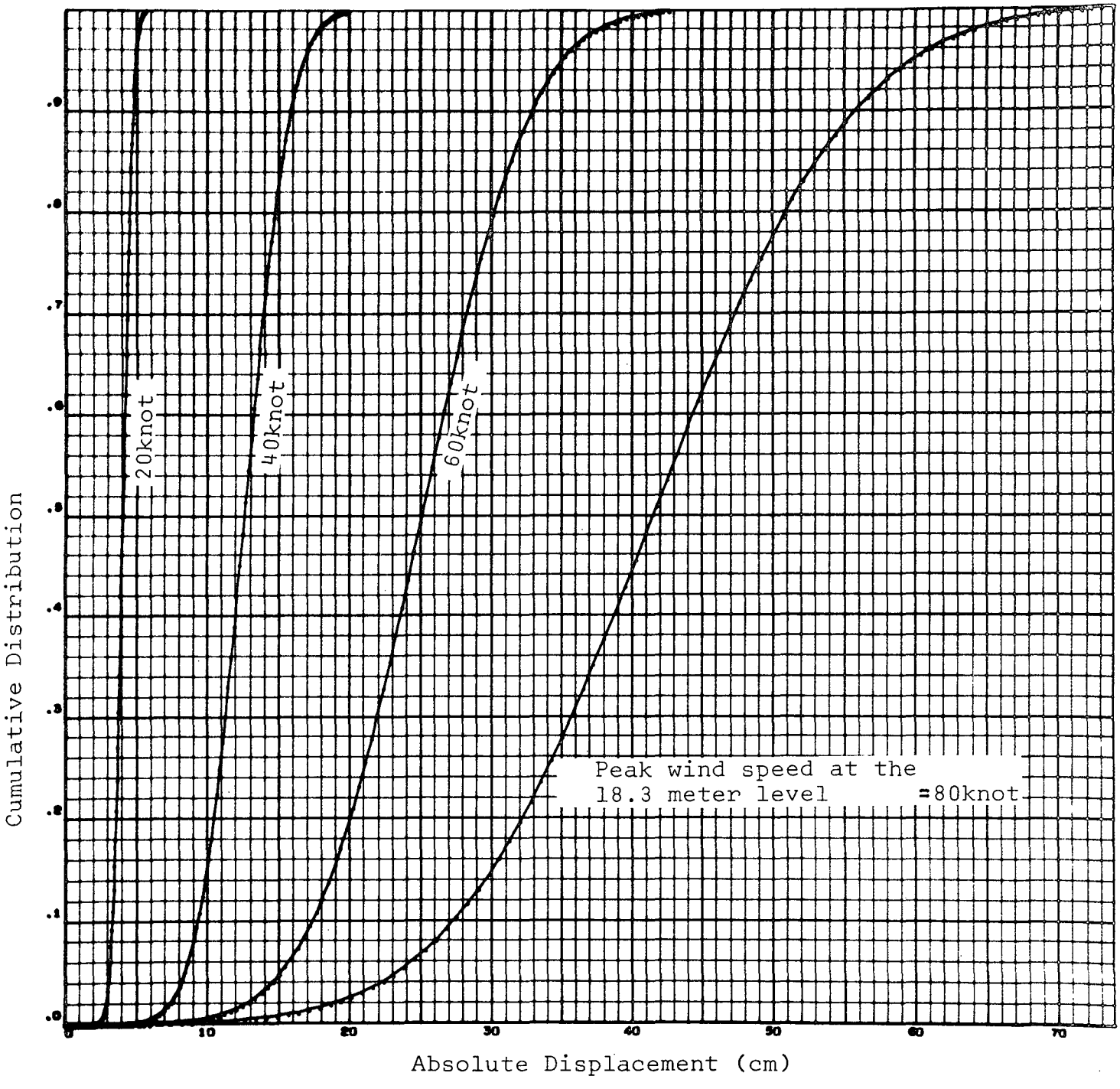

FIG. 5.5.9 CUMULATIVE DISTRIBUTION VERSUS TIP DISPLACEMENT

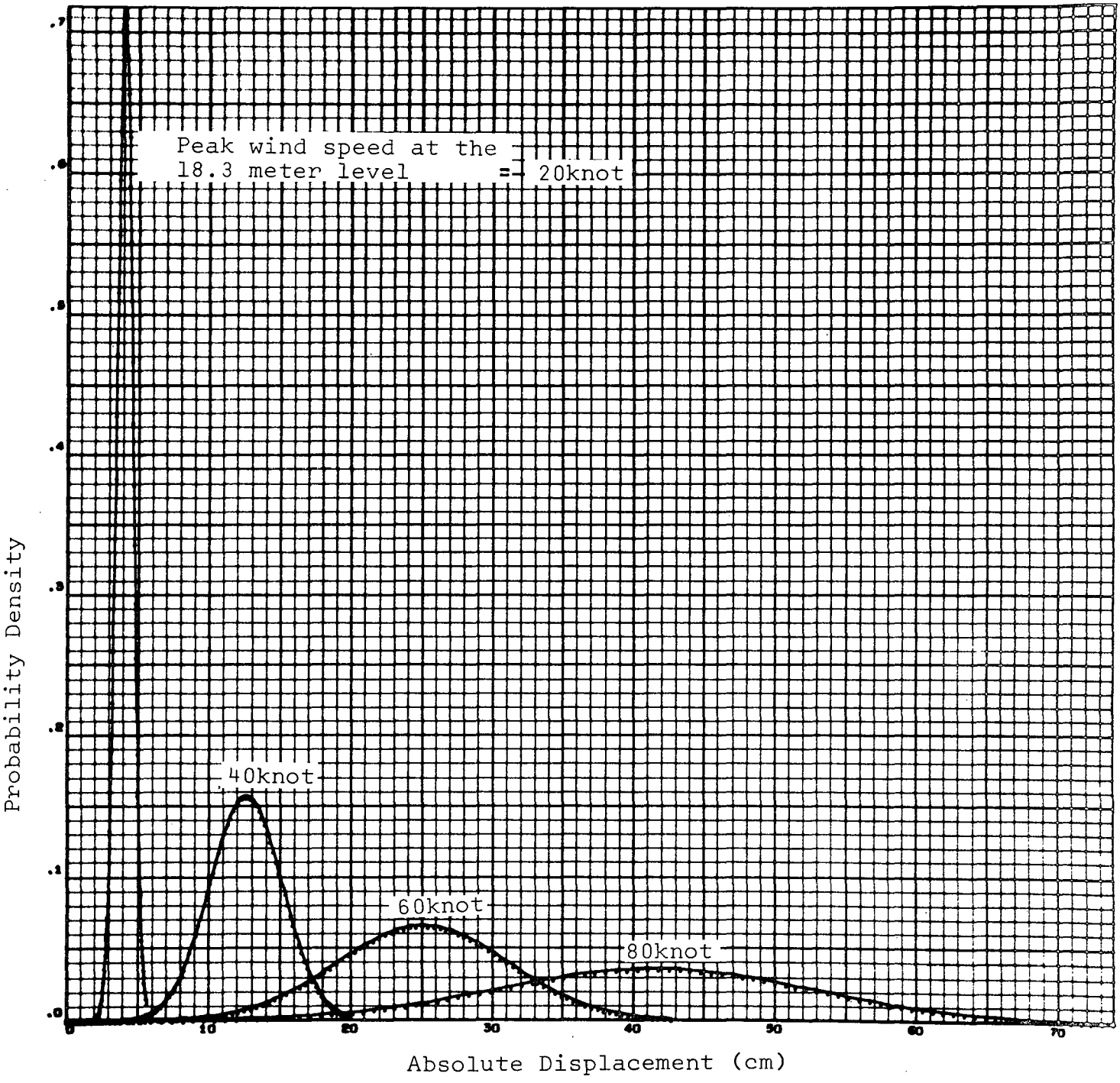

FIG. 5.5.10 PROBABILITY DENSITY VERSUS TIP DISPLACEMENT

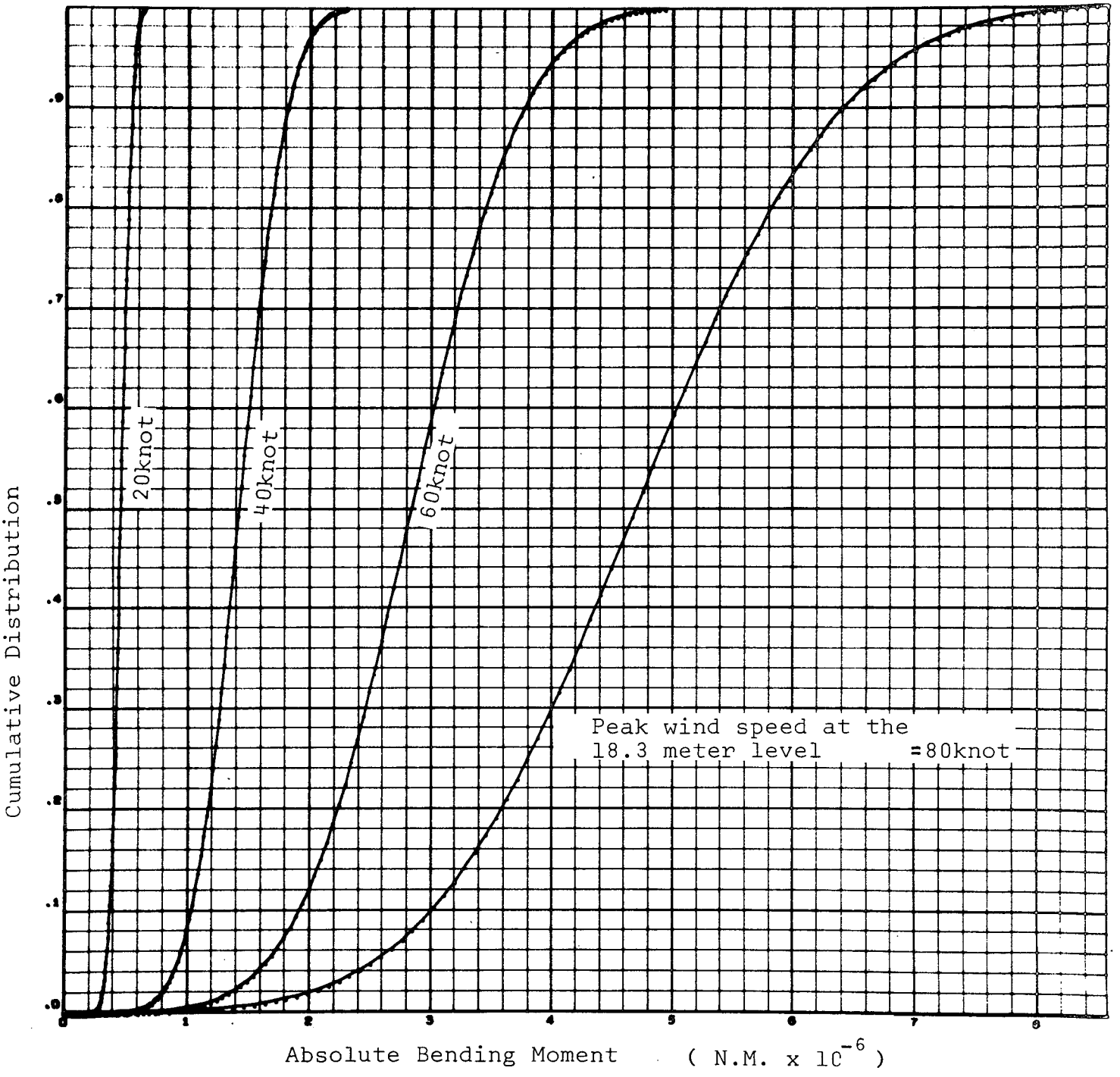

FIG. 5.5.11 CUMULATIVE DISTRIBUTION VERSUS BASE BENDING MOMENT

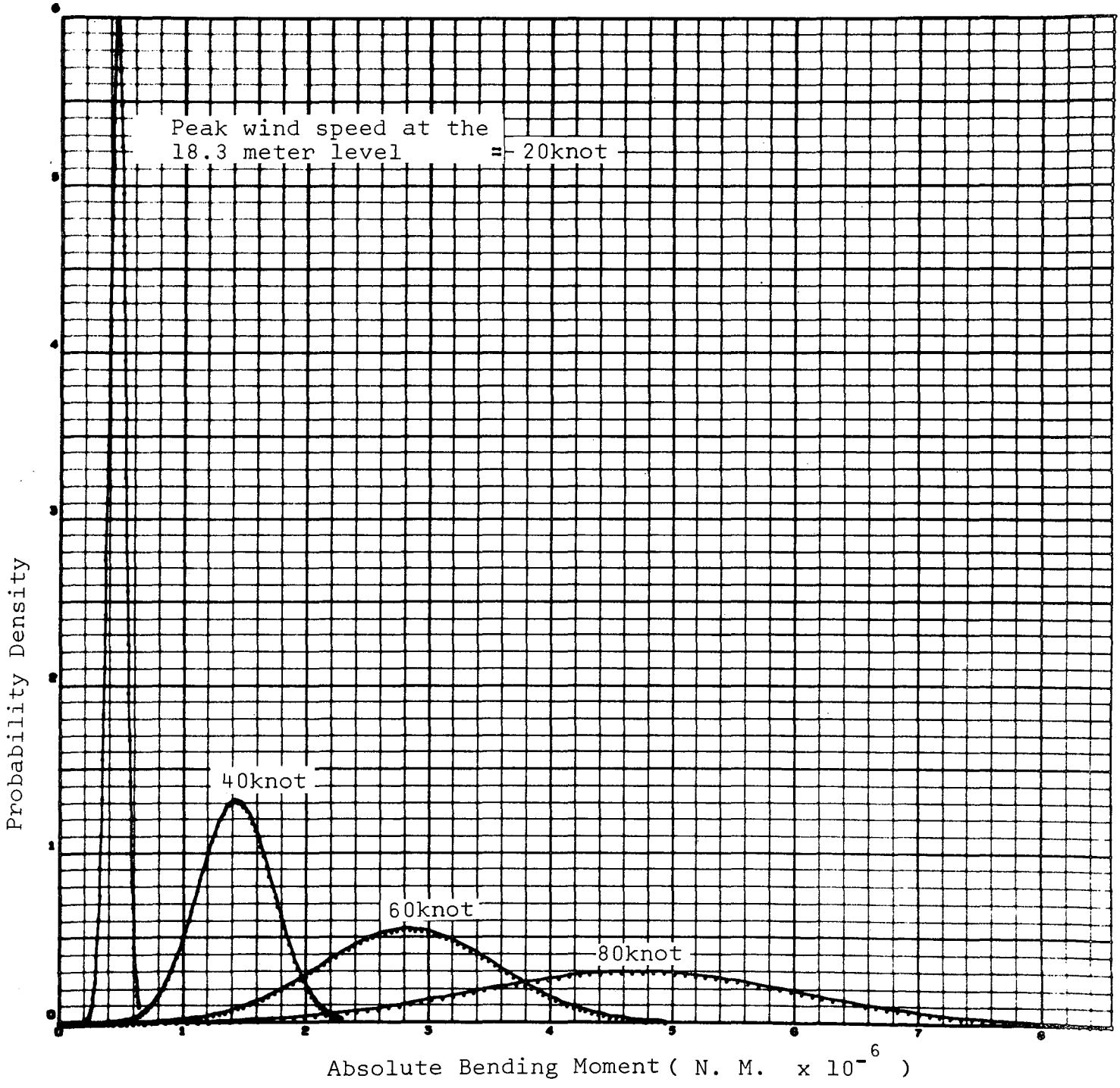

FIG. 5.5.12 PROBABILITY DENSITY VERSUS BASE BENDING MOMENT

5.6 SUMMARY OF PROPELLANT LOAD CONDITIONS AND STRUCTURAL DYNAMIC CHARACTERISTICS FOR CASE 6

Propellant Loading Configuration

Service Module	S-IB RP-1	S-IB LOX	S-IVB LOX	S-IVB LH_2
full	full	full	full	full

Structural Dynamic Characteristics

Mode No.	Natural Frequency Hz	Generalized Mass kg.(lb.sec.^{2}/in)	Structural Damping Ratio
1	0.310619	42692.04(243.789)	0.015
2	0.900213	8629.12(49.2759)	0.015
3	1.68925	16089.85(91.8846)	0.015

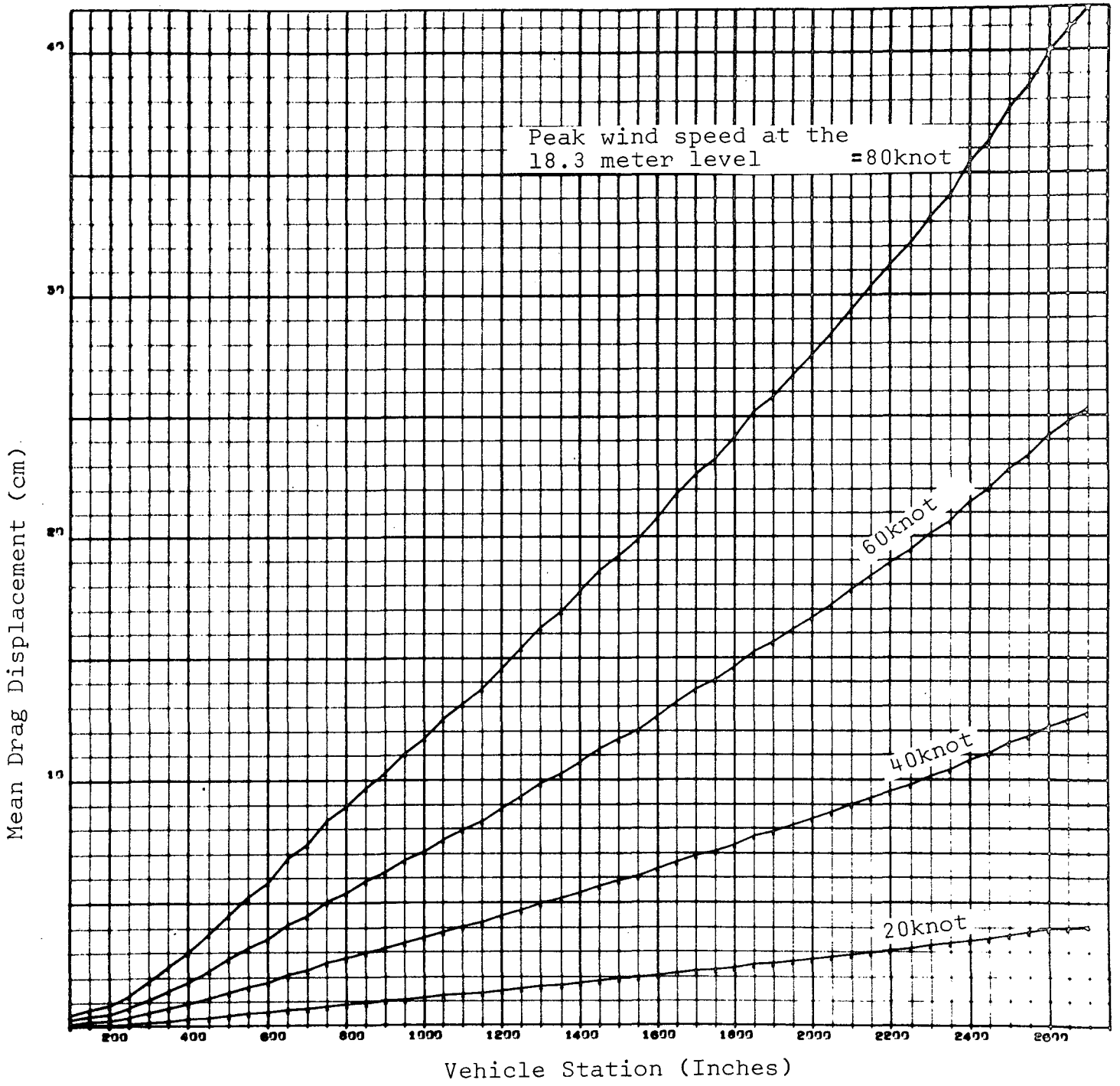

FIG. 5.6.1 MEAN DRAG DISPLACEMENT VERSUS VEHICLE STATION

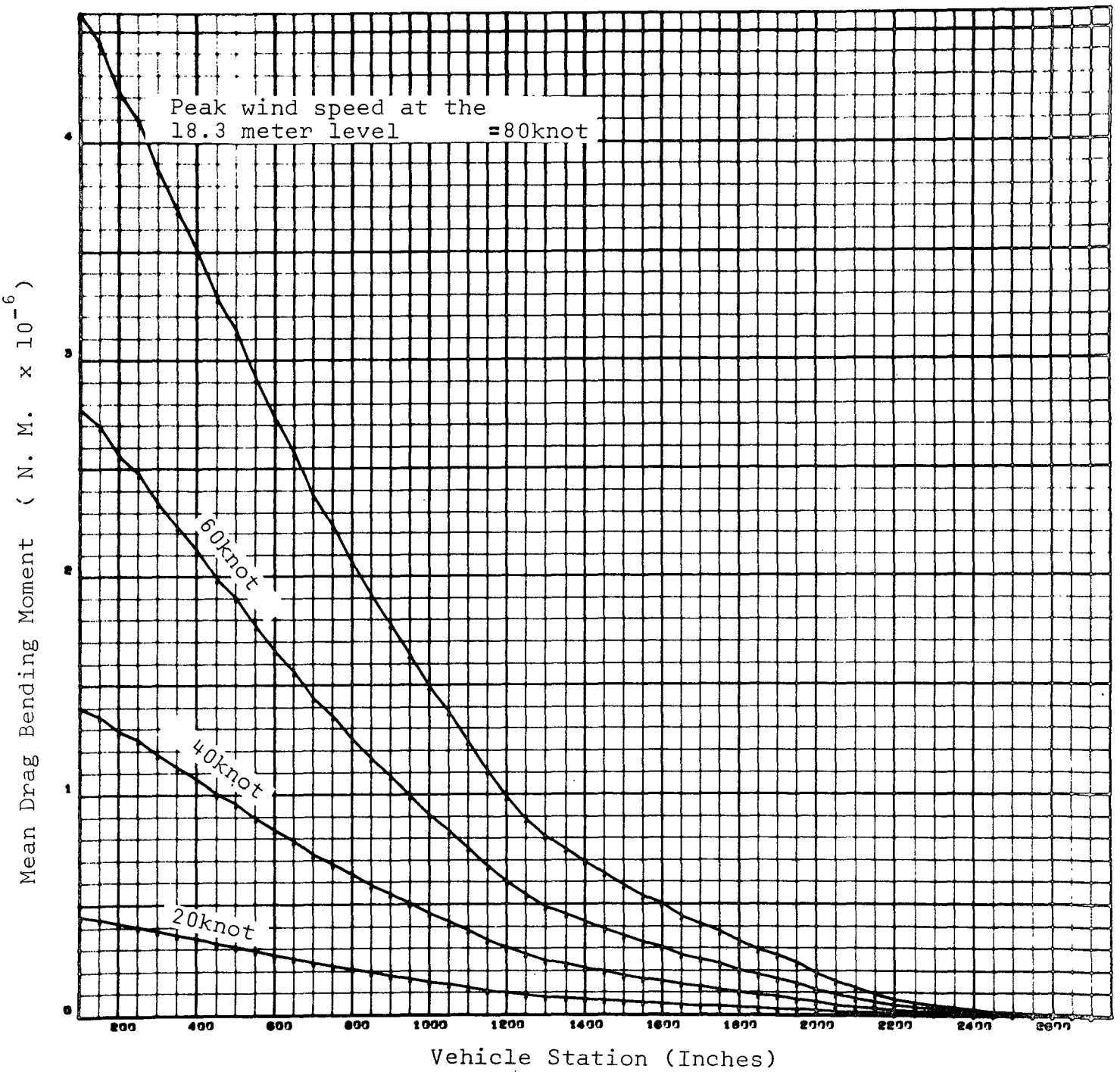

FIG. 5.6.2 MEAN DRAG BENDING MOMENT VERSUS VEHICLE STATION

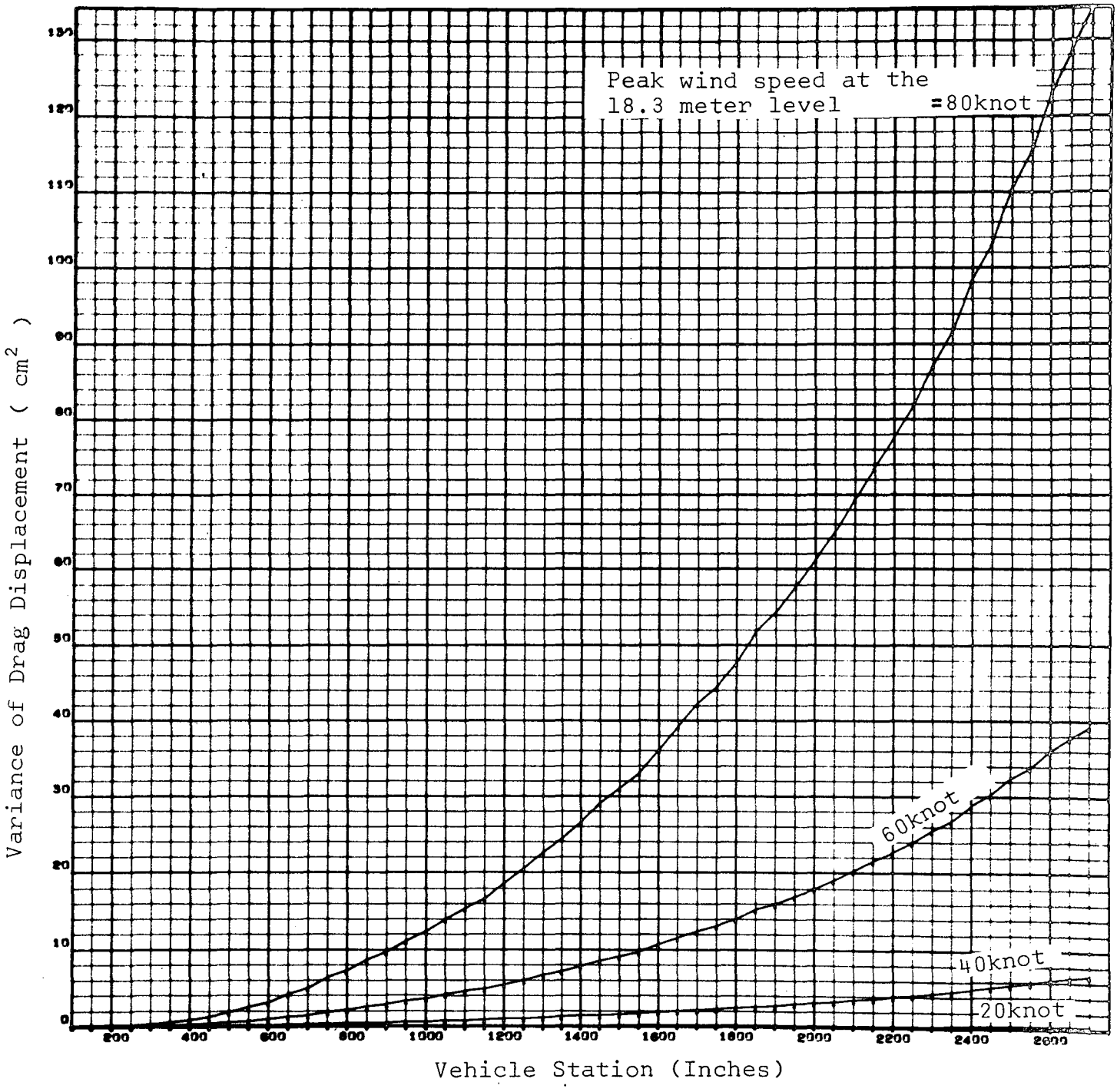

FIG. 5.6.3 VARIANCE OF DRAG DISPLACEMENT VERSUS VEHICLE STATION

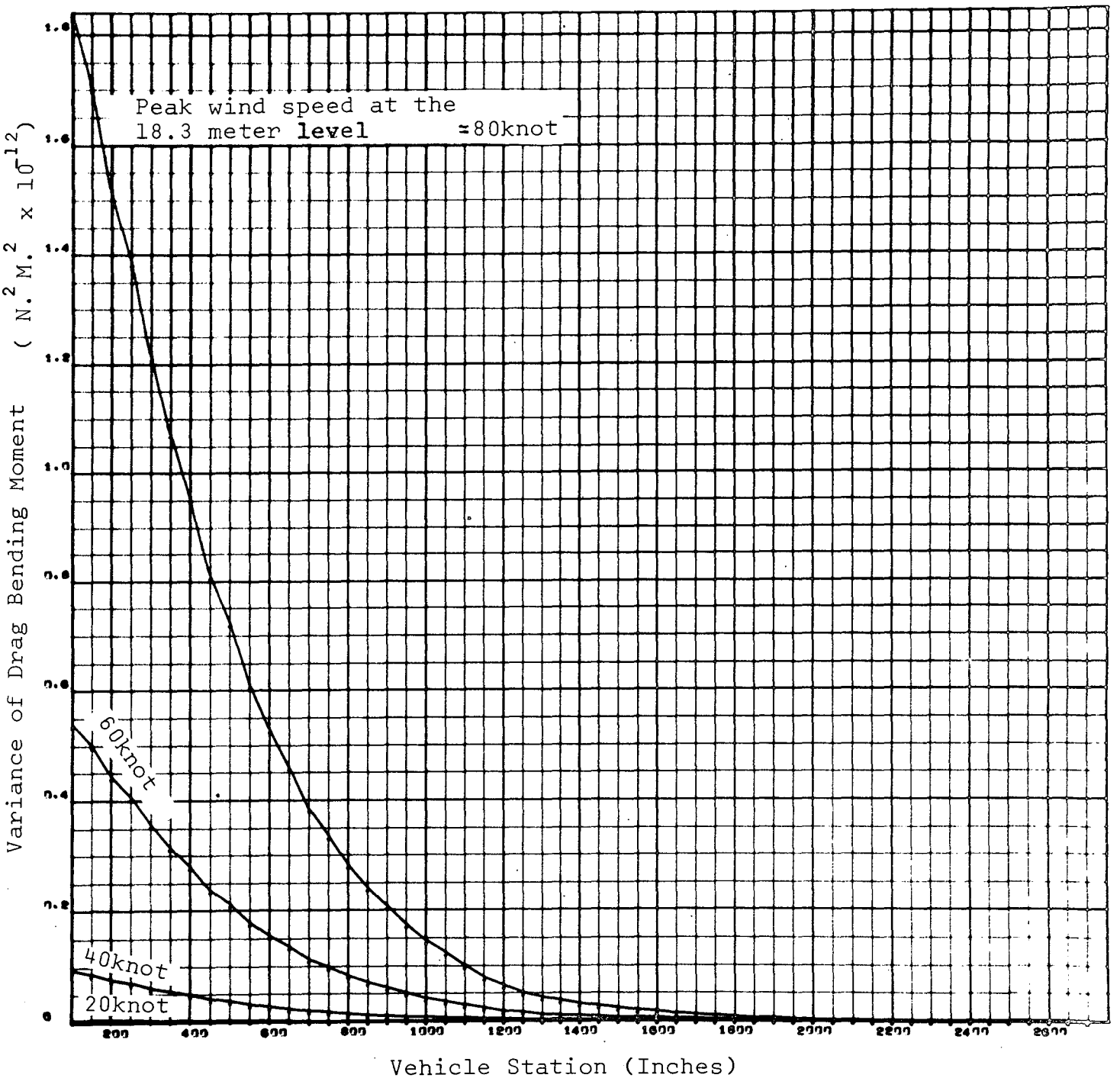

FIG. 5.6.4 VARIANCE OF DRAG BENDING MOMENT VERSUS VEHICLE STATION

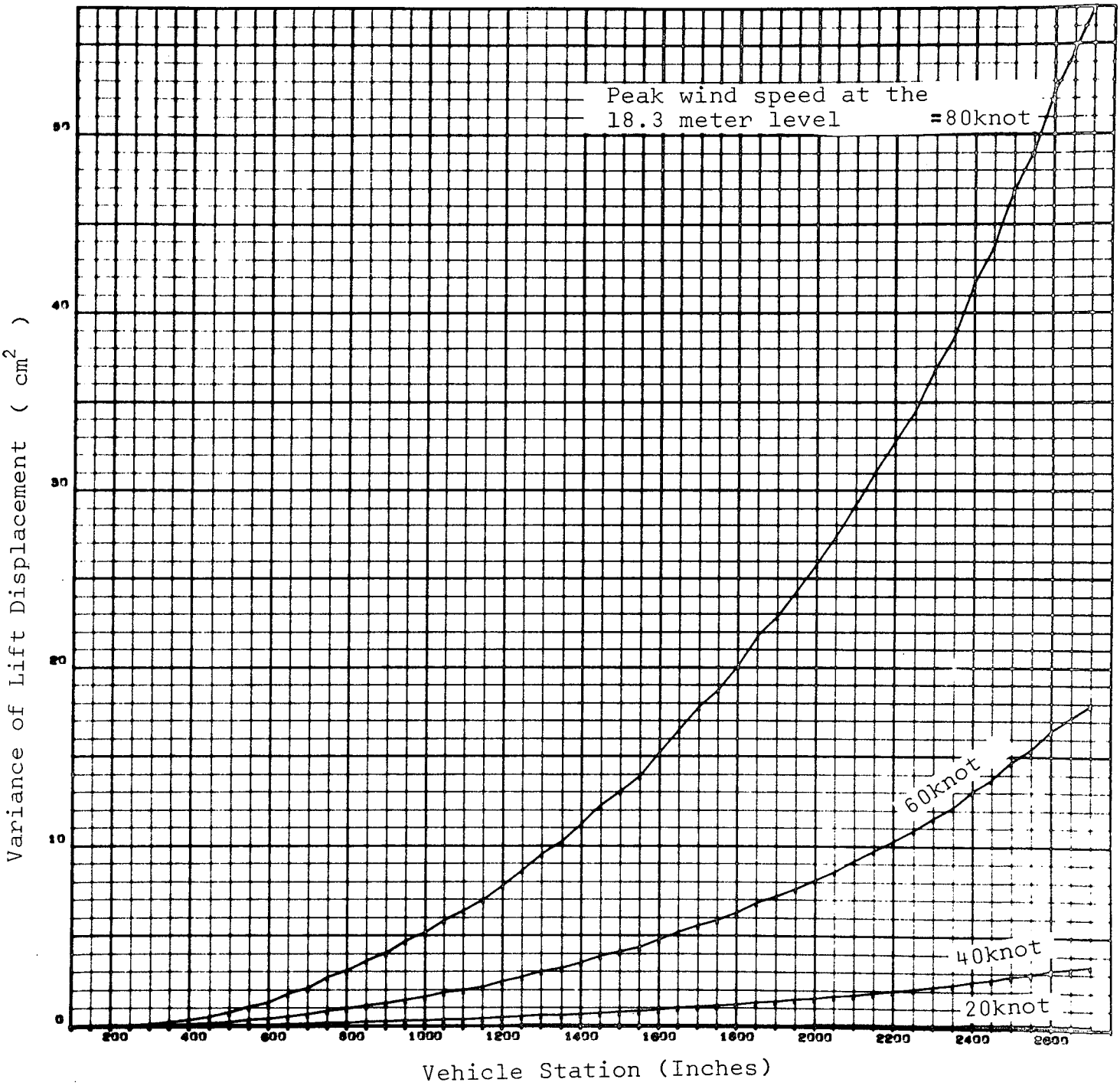

FIG. 5.6.5 VARIANCE OF LIFT DISPLACEMENT VERSUS VEHICLE STATION

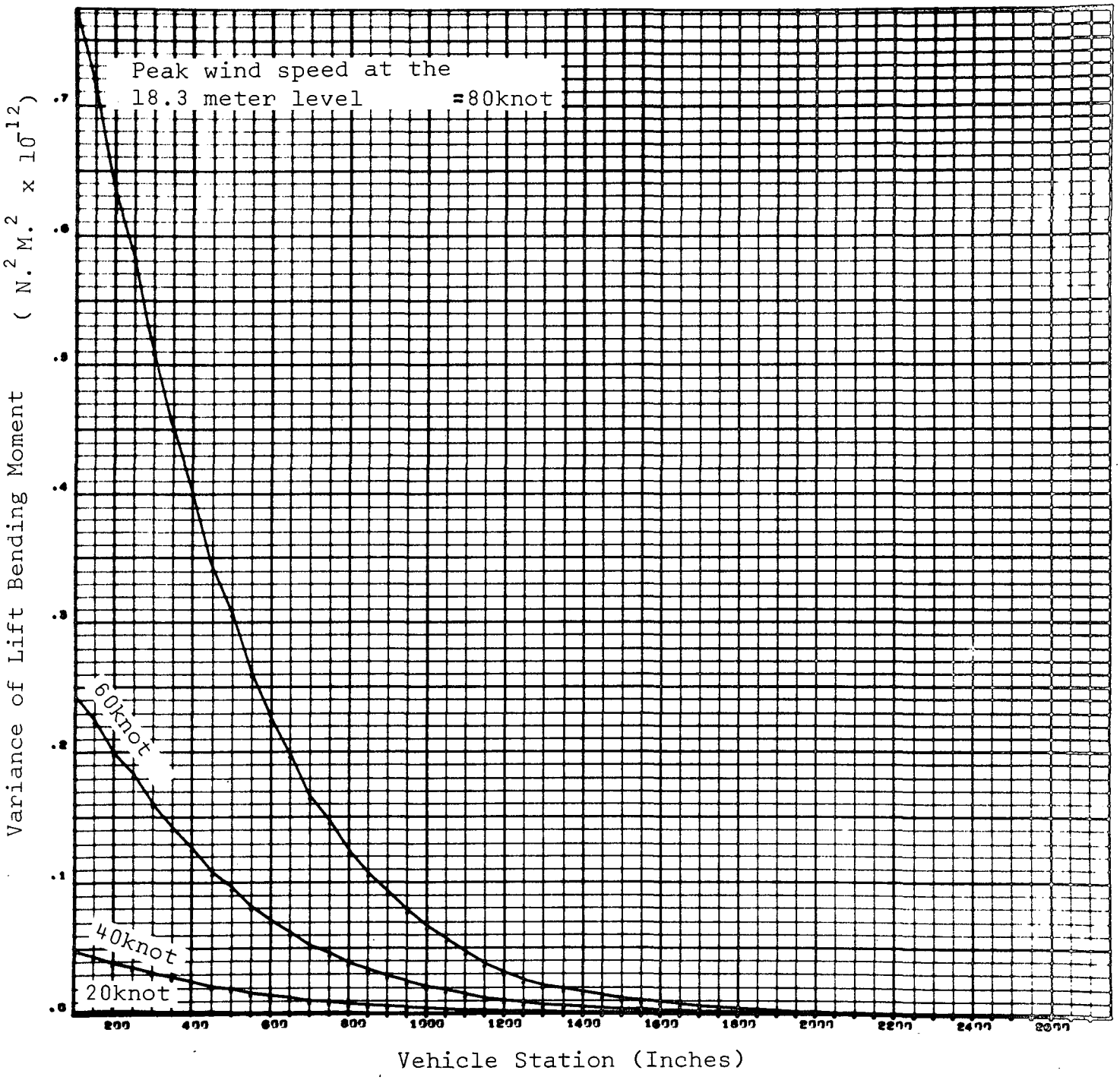

FIG. 5.6.6 VARIANCE OF LIFT BENDING MOMENT VERSUS VEHICLE STATION

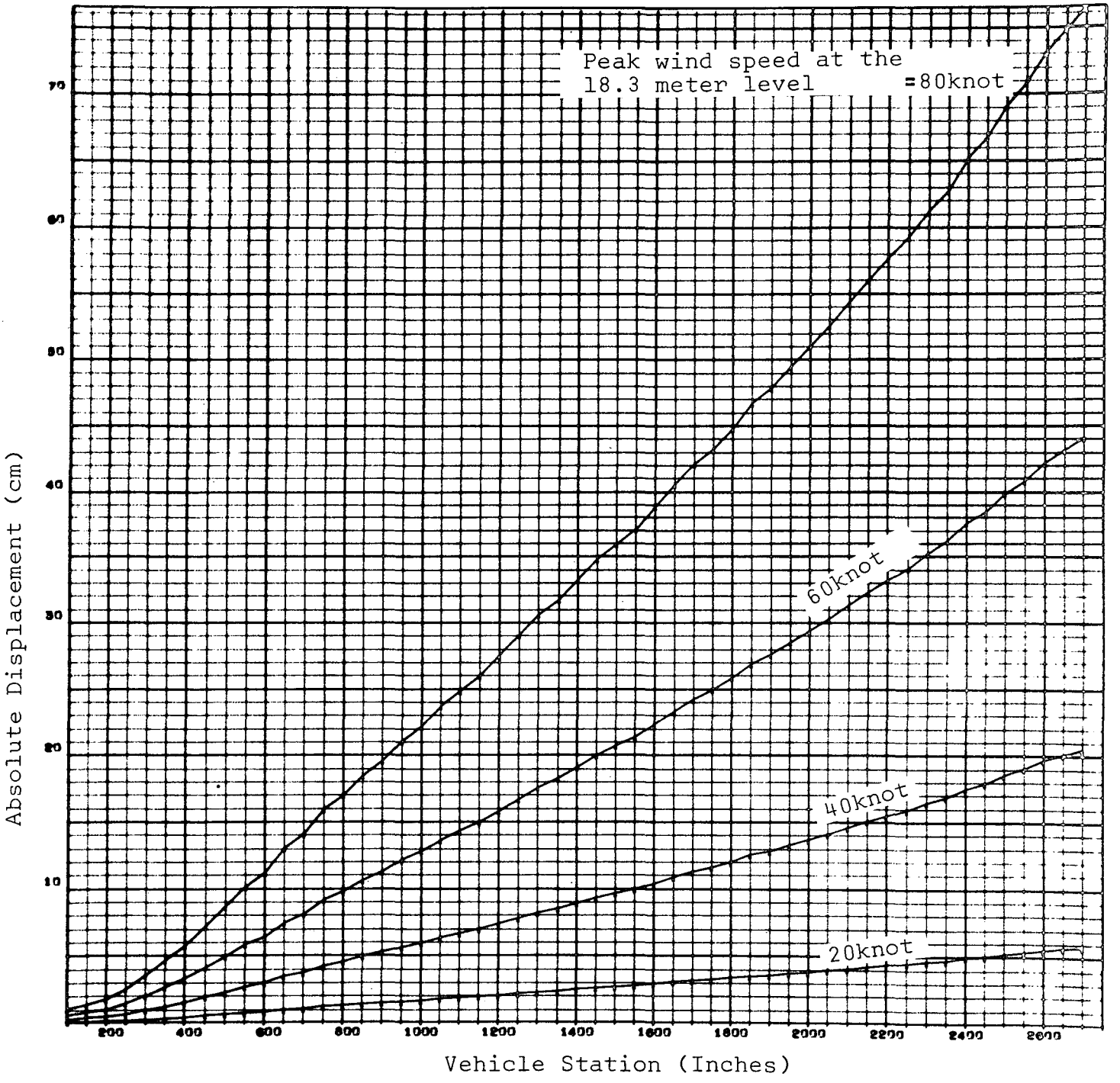

FIG. 5.6.7 ABSOLUTE DISPLACEMENT VERSUS VEHICLE STATION FOR CONCURRENT 3 SIGMA LIFT AND DRAG RESPONSE

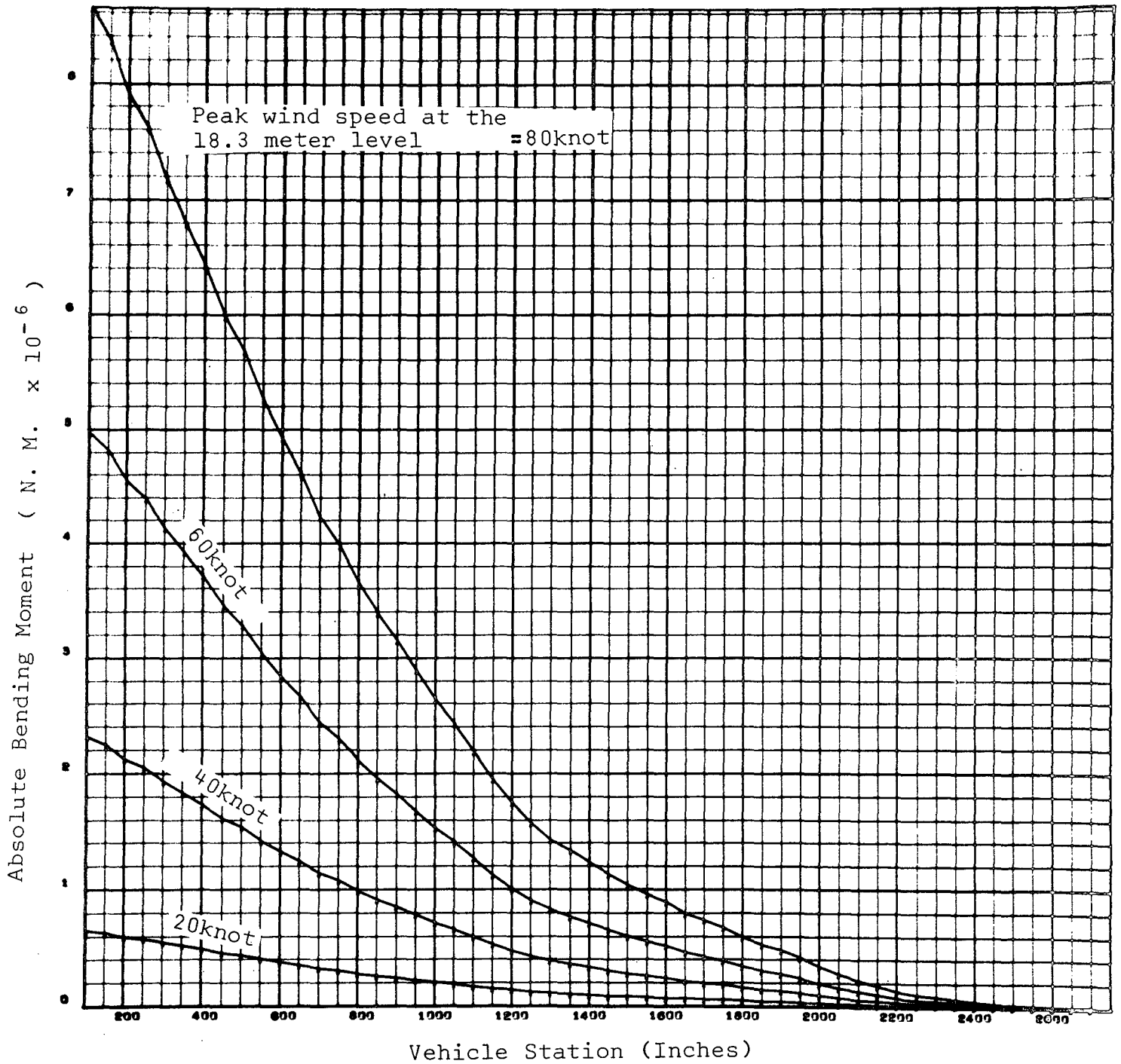

FIG. 5.6.8 ABSOLUTE BENDING MOMENT VERSUS VEHICLE STATION FOR CONCURRENT 3 SIGMA LIFT AND DRAG RESPONSE

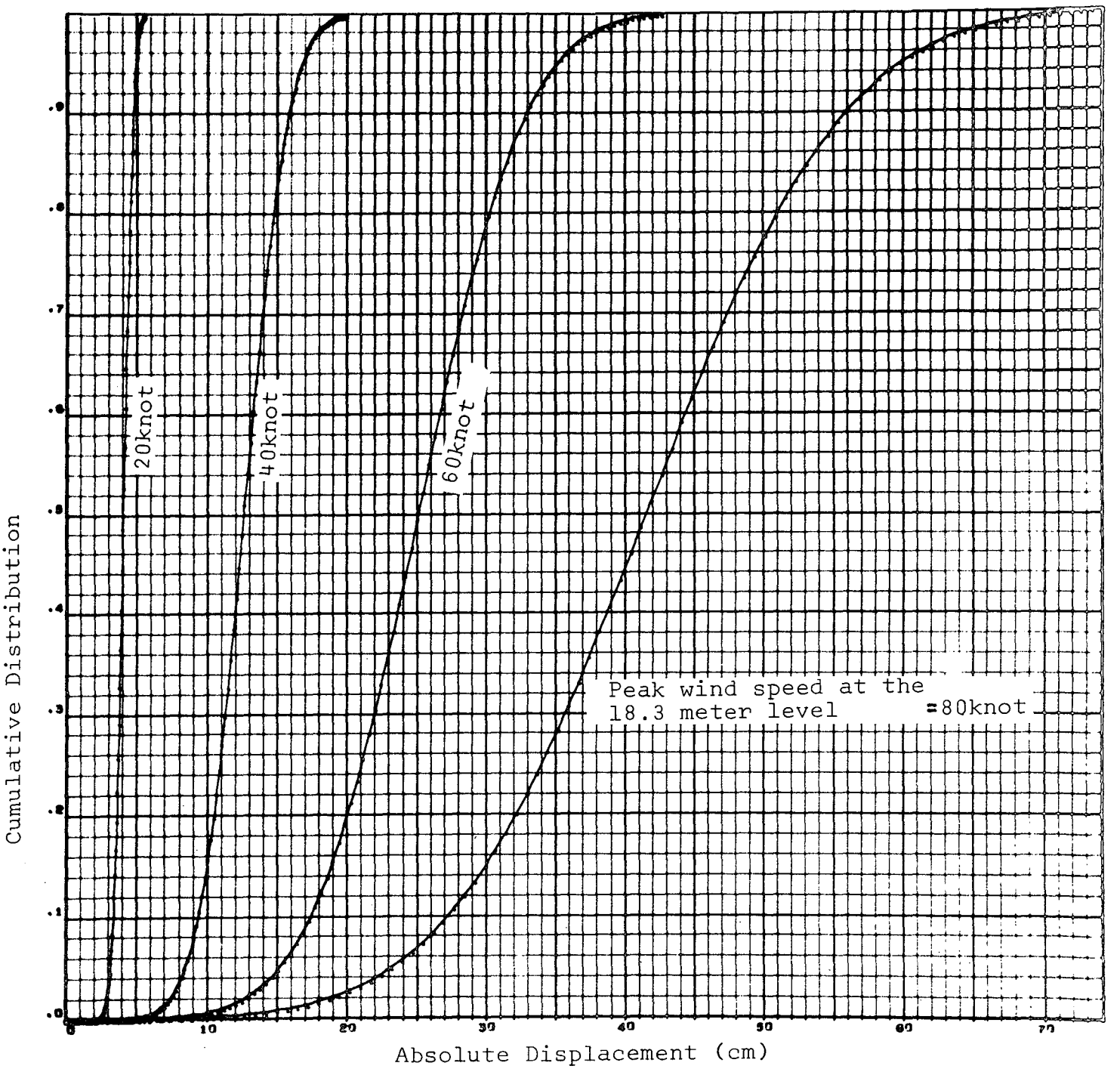

FIG. 5.6.9 CUMULATIVE DISTRIBUTION VERSUS TIP DISPLACEMENT

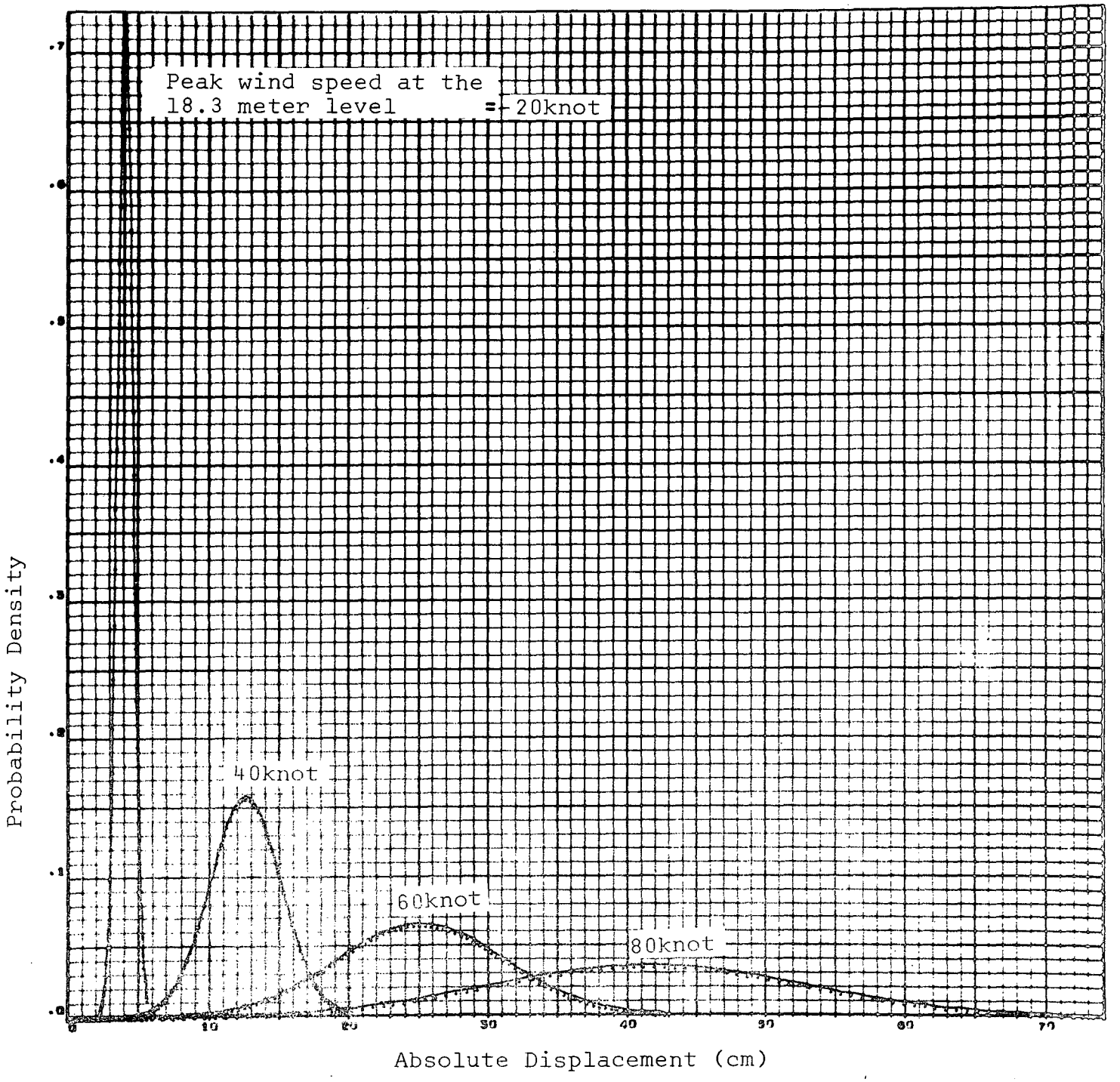

FIG. 5.6.10 PROBABILITY DENSITY VERSUS TIP DISPLACEMENT

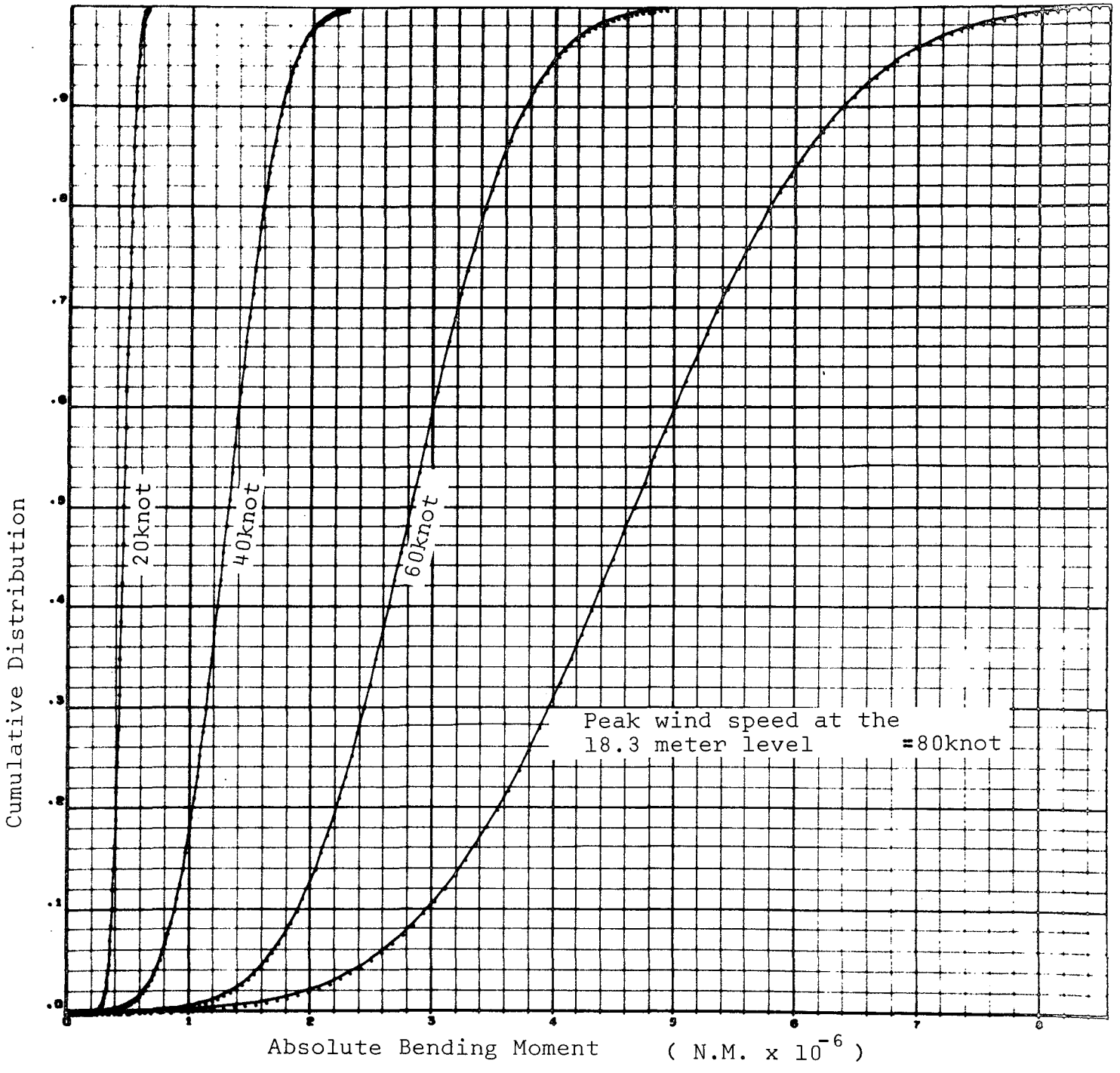

FIG. 5.6.11 CUMULATIVE DISTRIBUTION VERSUS BASE BENDING MOMENT

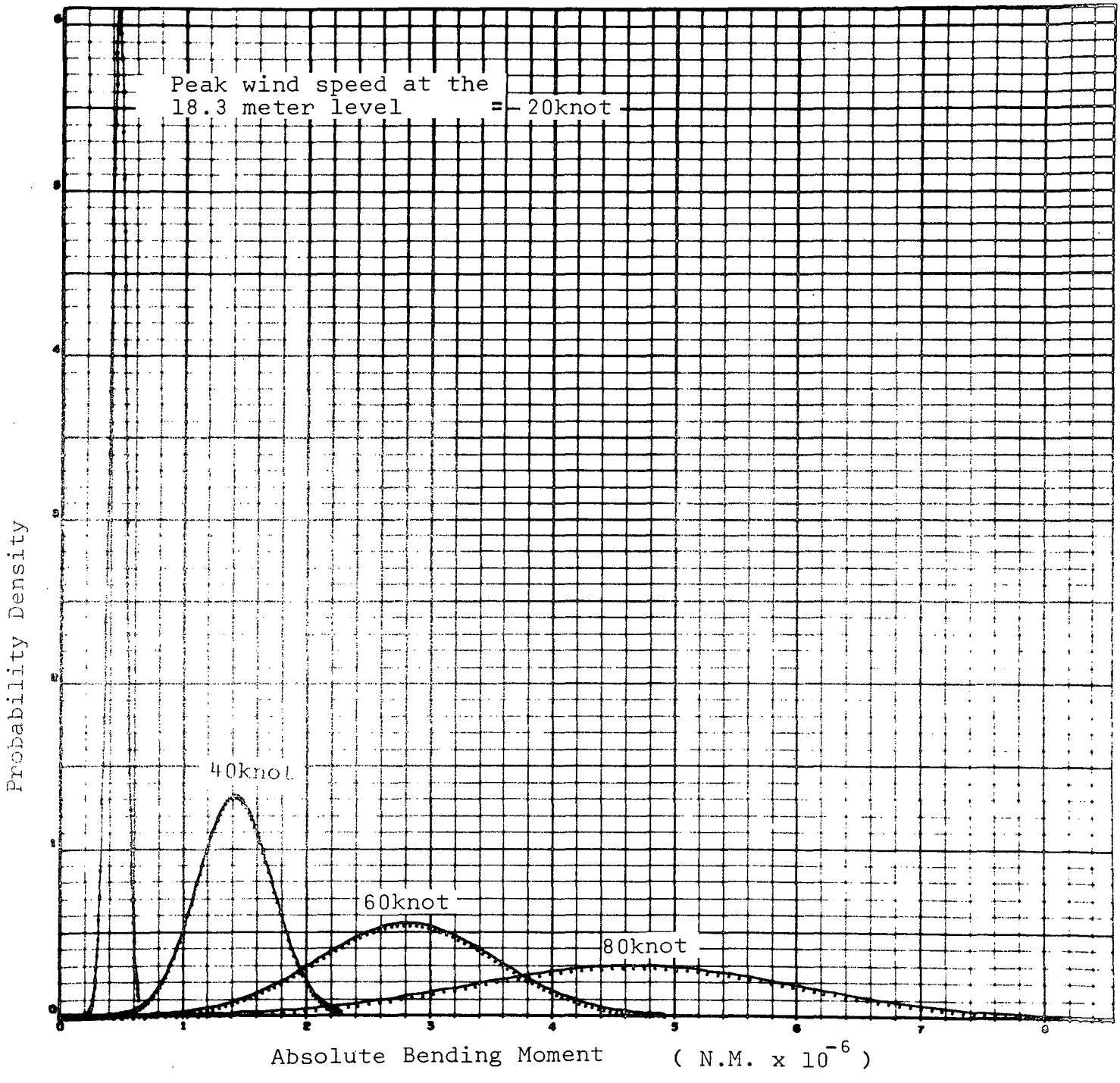

FIG. 5.6.12 PROBABILITY DENSITY VERSUS BASE BENDING MOMENT

Section VI

RESULTS OF SIMULATION FOR VARYING WIND SPEED GRADIENTS WITH A FIXED REFERENCE WIND SPEED

A cursory evaluation of SKYLAB IB sensitivity to wind speed gradients was performed by simulating a single vehicle propellant configuration and reference wind speed (18.3 m. level), with varying wind speed gradients. Propellant loading characteristics of Case 5 and a reference peak wind speed of 41.16 m/sec. (80 knots) were utilized. Peak wind speed profile distributions were obtained from /6/. Statistical characteristics of the four wind speed profiles selected are noted on each Figure presented in this Section.

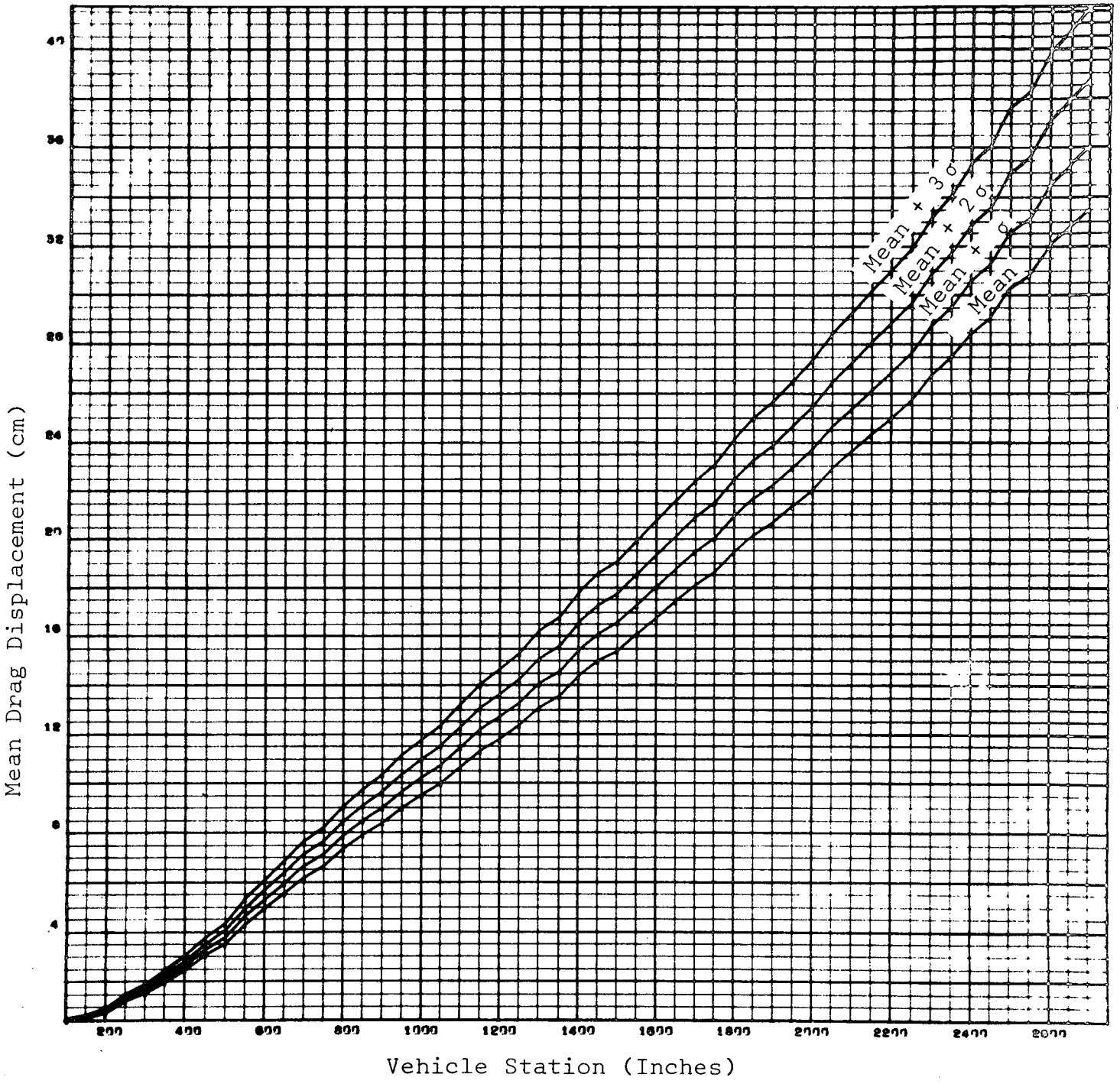

FIG. 6.1 MEAN DRAG DISPLACEMENT VERSUS VEHICLE STATION

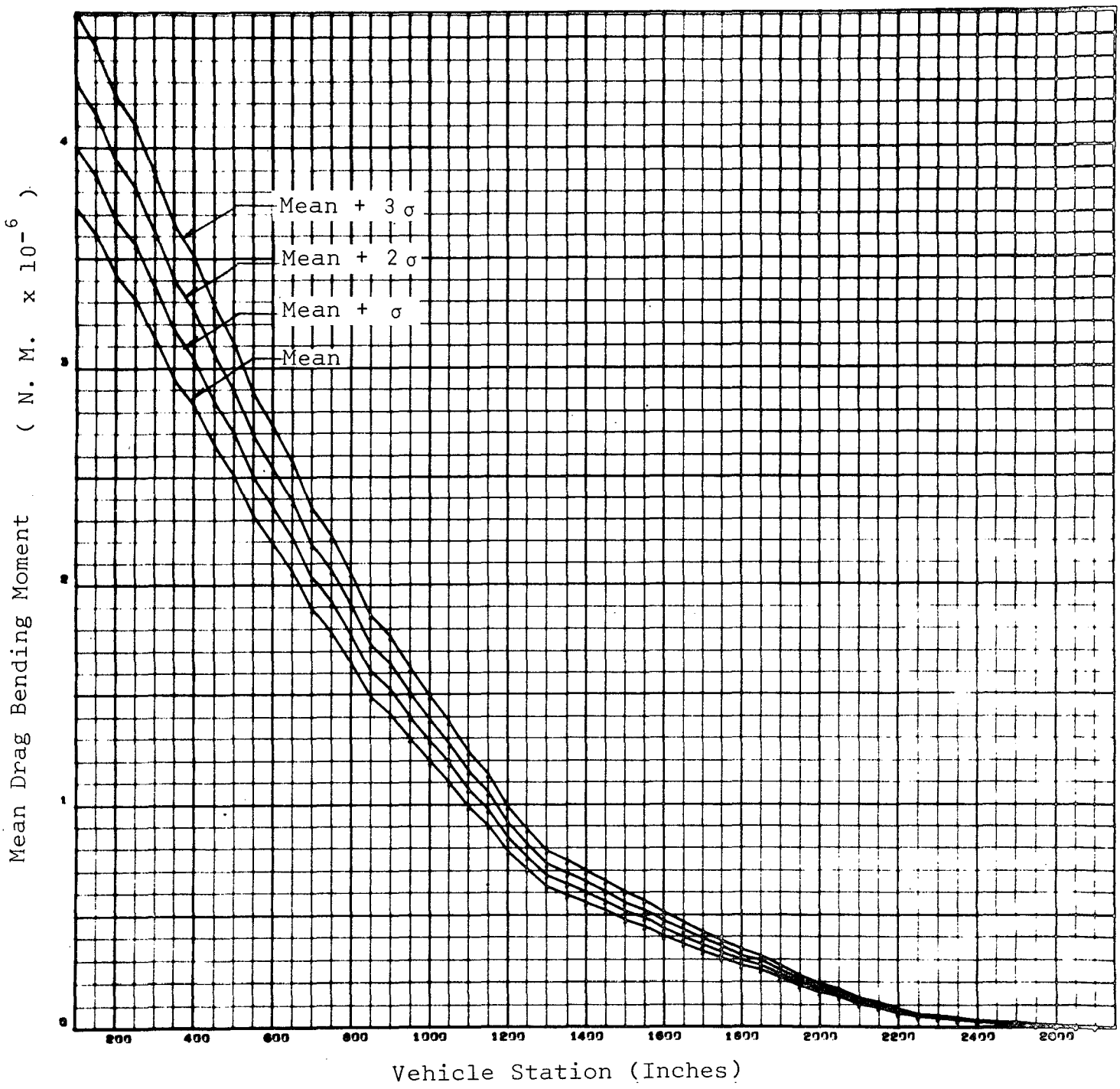

FIG. 6.2 MEAN DRAG BENDING MOMENT VERSUS VEHICLE STATION

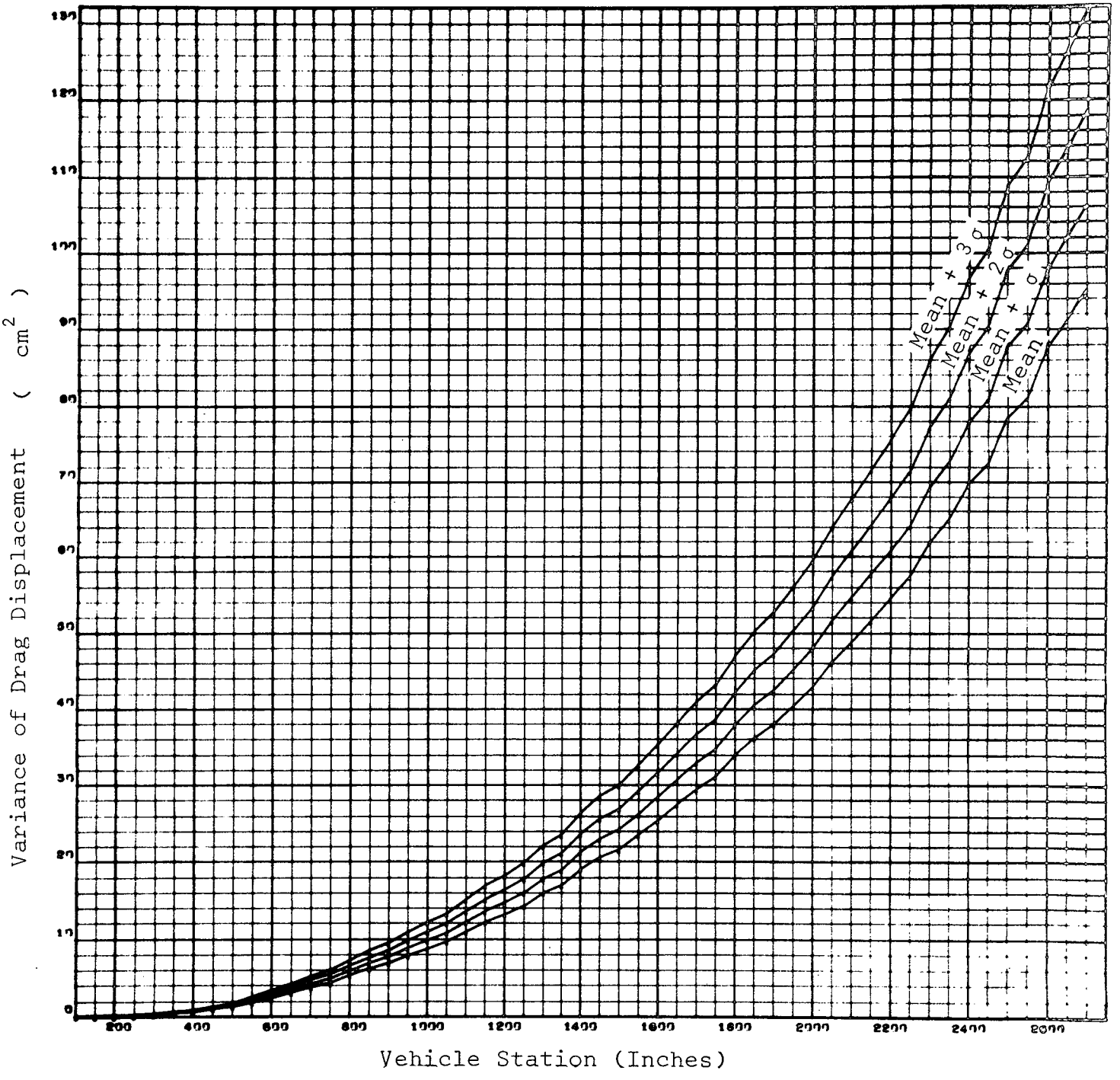

FIG. 6.3 VARIANCE OF DRAG DISPLACEMENT VERSUS VEHICLE STATION

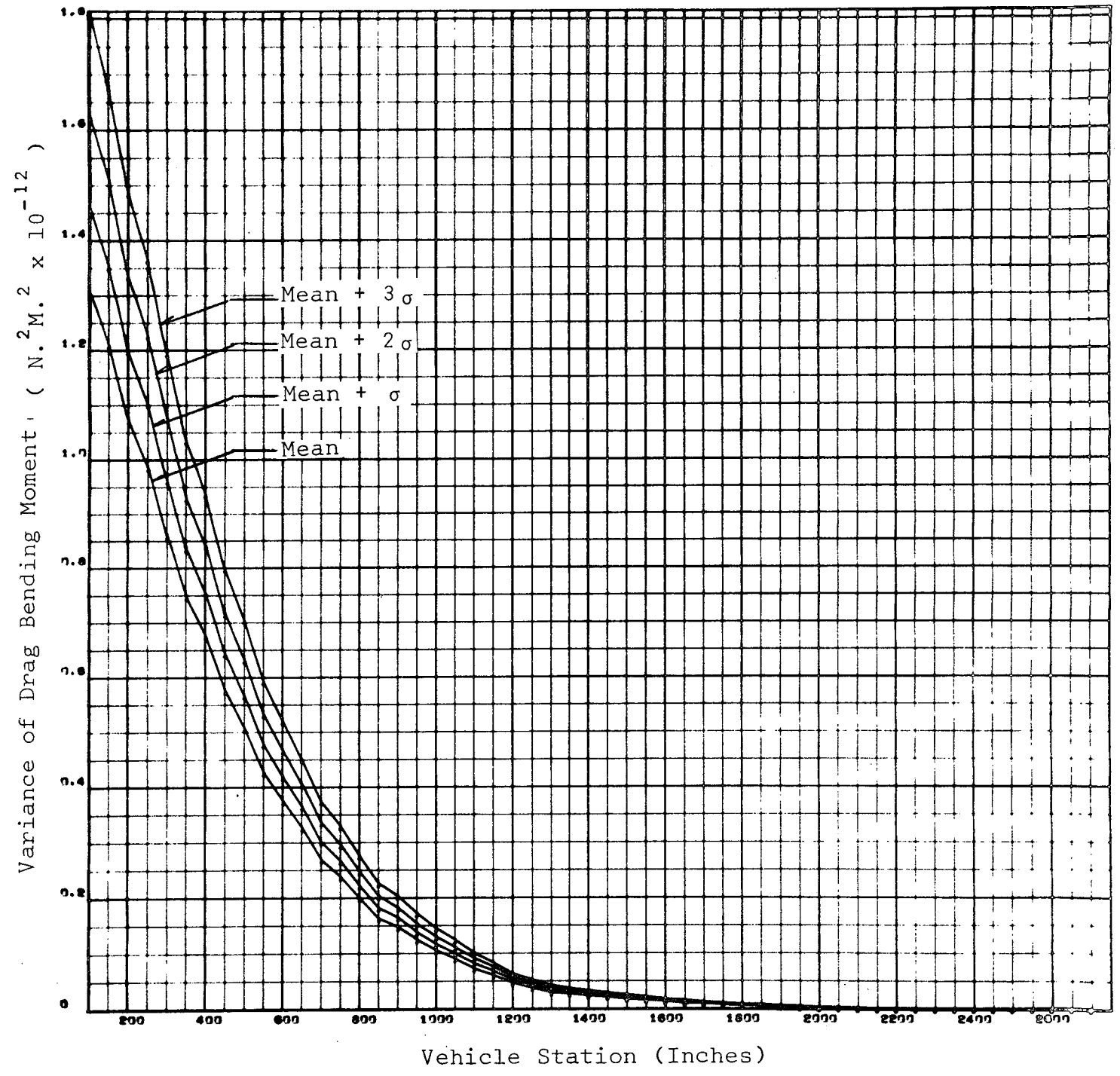

FIG. 6.4 VARIANCE OF DRAG BENDING MOMENT VERSUS VEHICLE STATION

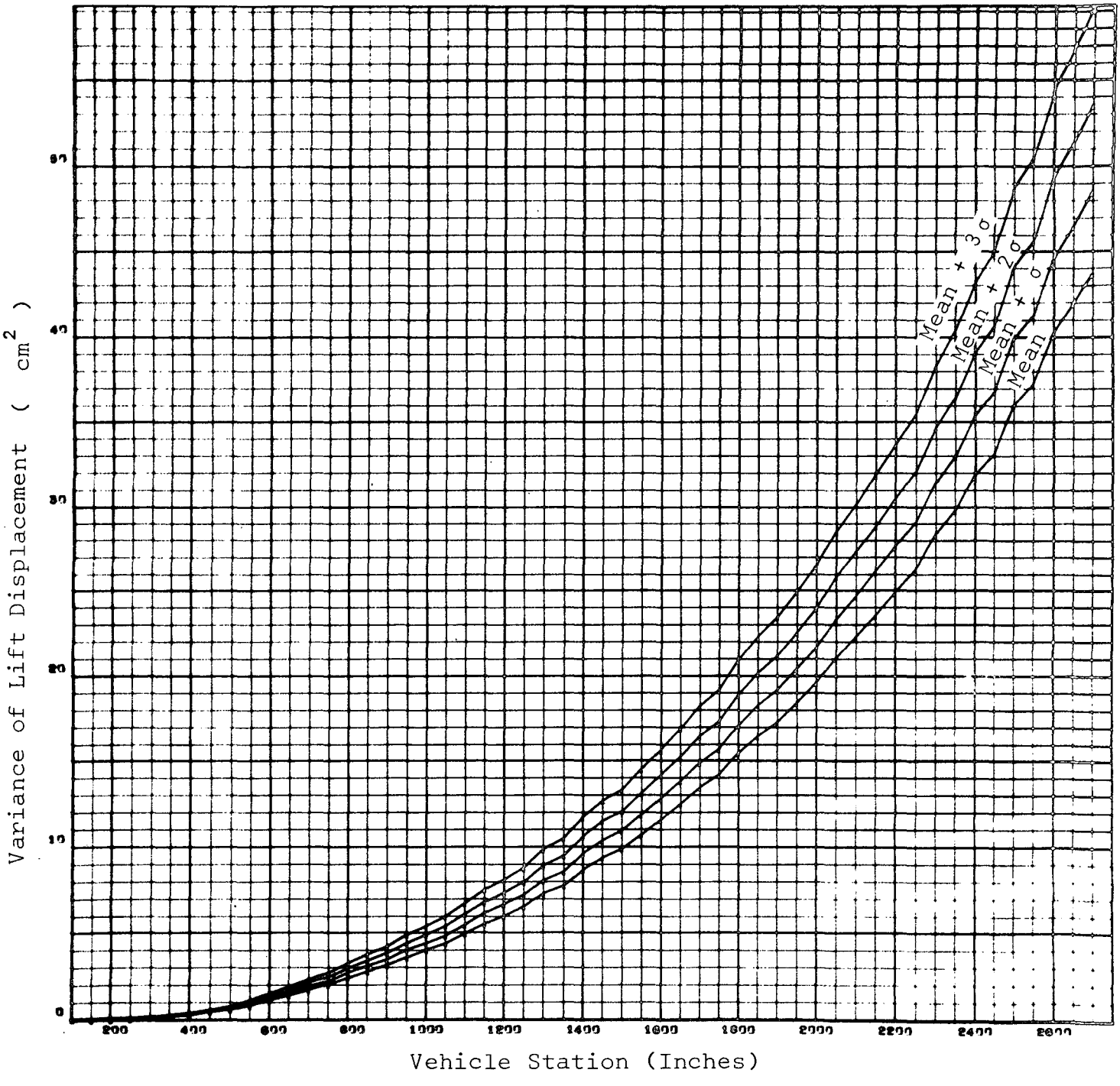

FIG. 6.5 VARIANCE OF LIFT DISPLACEMENT VERSUS VEHICLE STATION

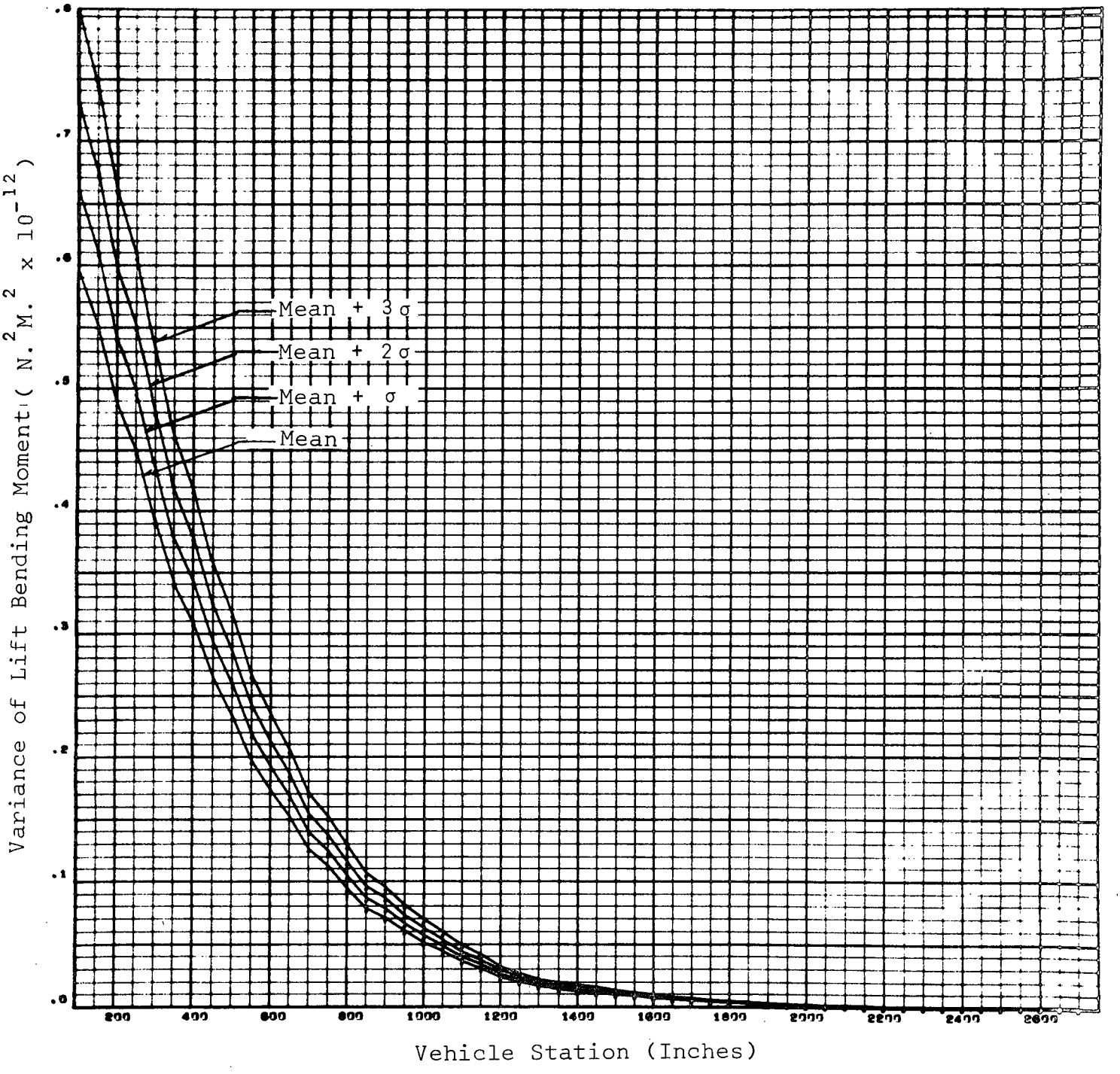

FIG. 6.6 VARIANCE OF LIFT BENDING MOMENT VERSUS VEHICLE STATION

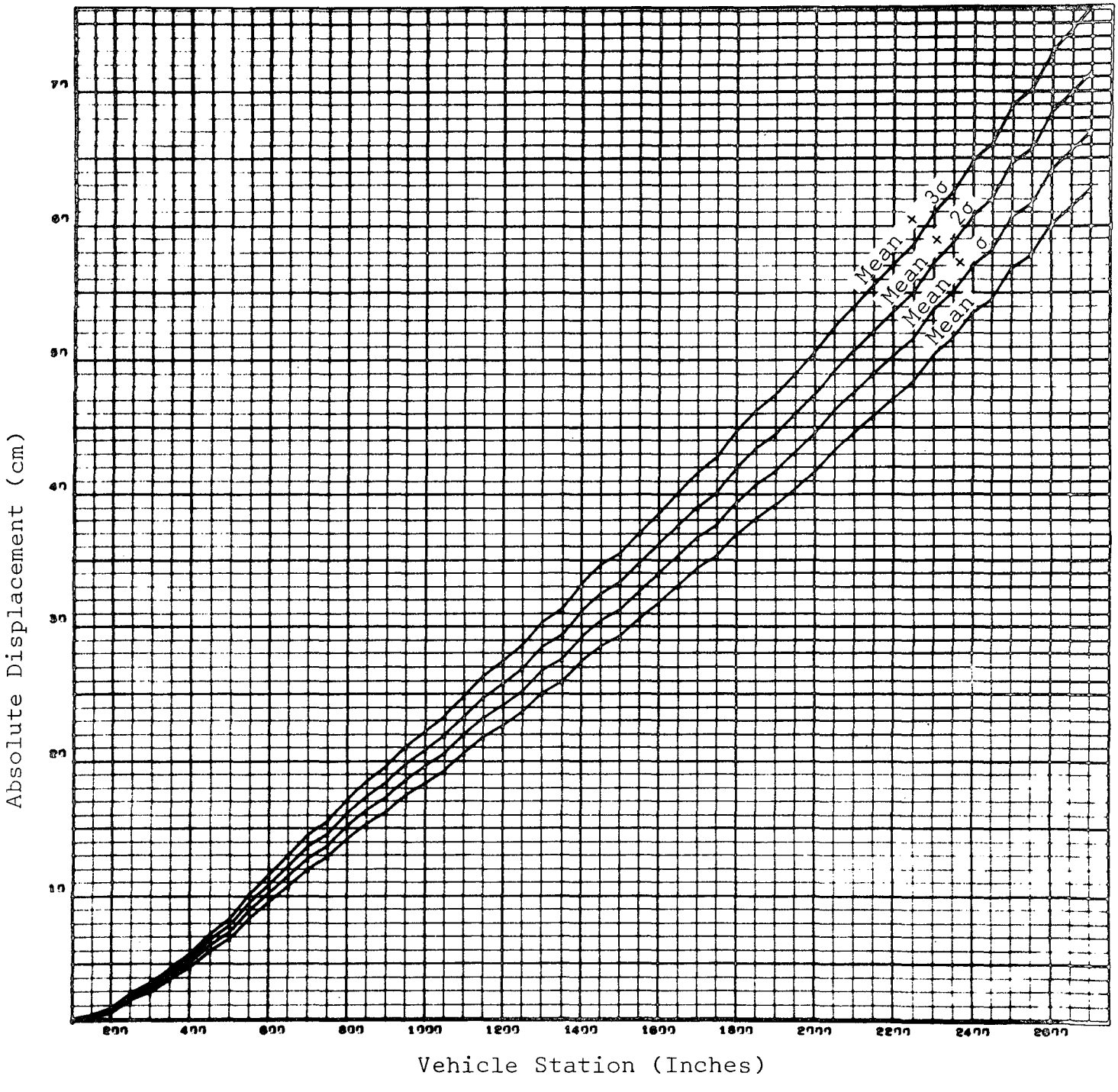

FIG. 6.7 ABSOLUTE DISPLACEMENT VERSUS VEHICLE STATION FOR CONCURRENT 3 SIGMA LIFT AND DRAG RESPONSE

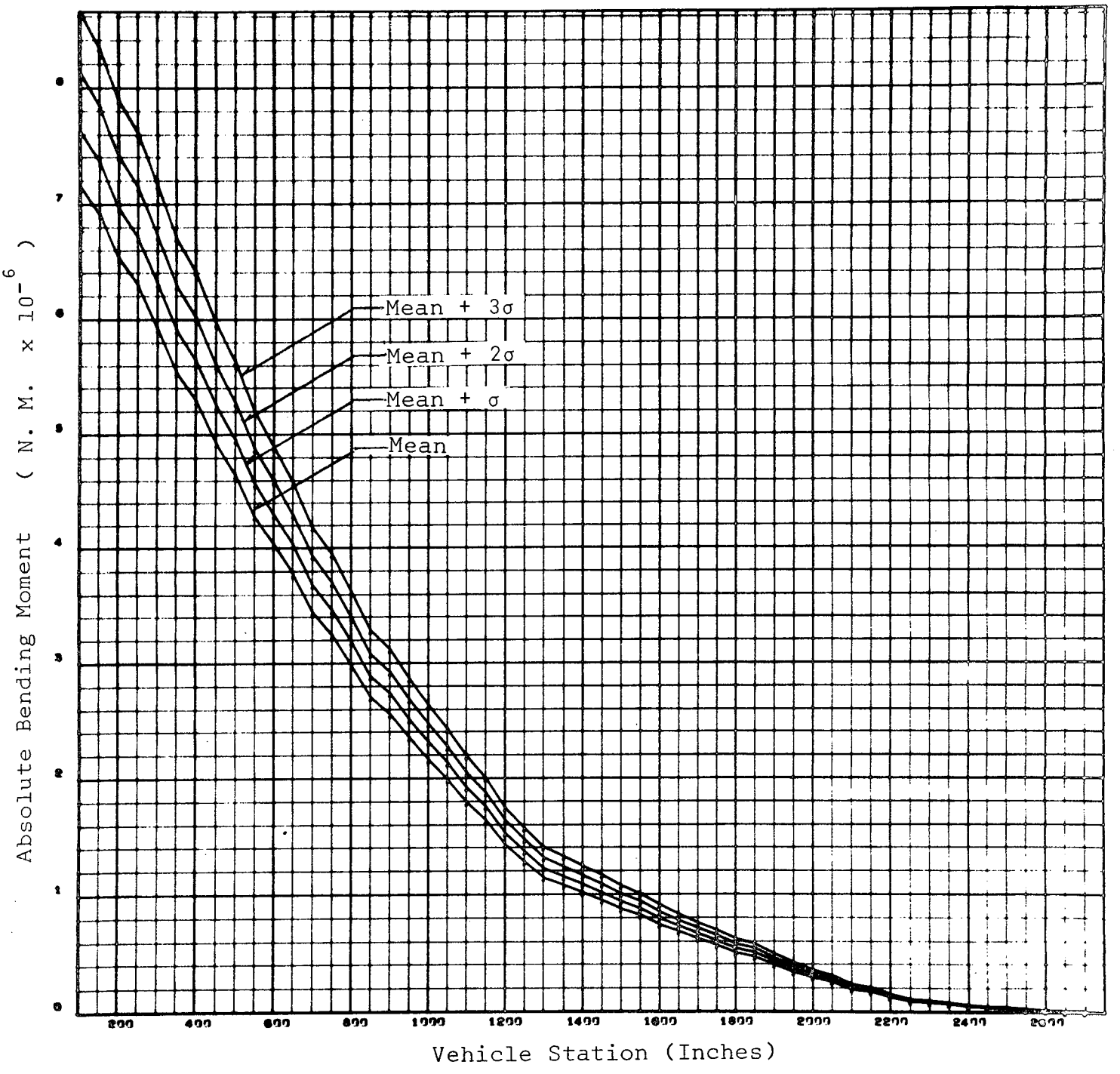

FIG. 6.8 ABSOLUTE BENDING MOMENT VERSUS VEHICLE STATION FOR CONCURRENT 3 SIGMA LIFT AND DRAG RESPONSE

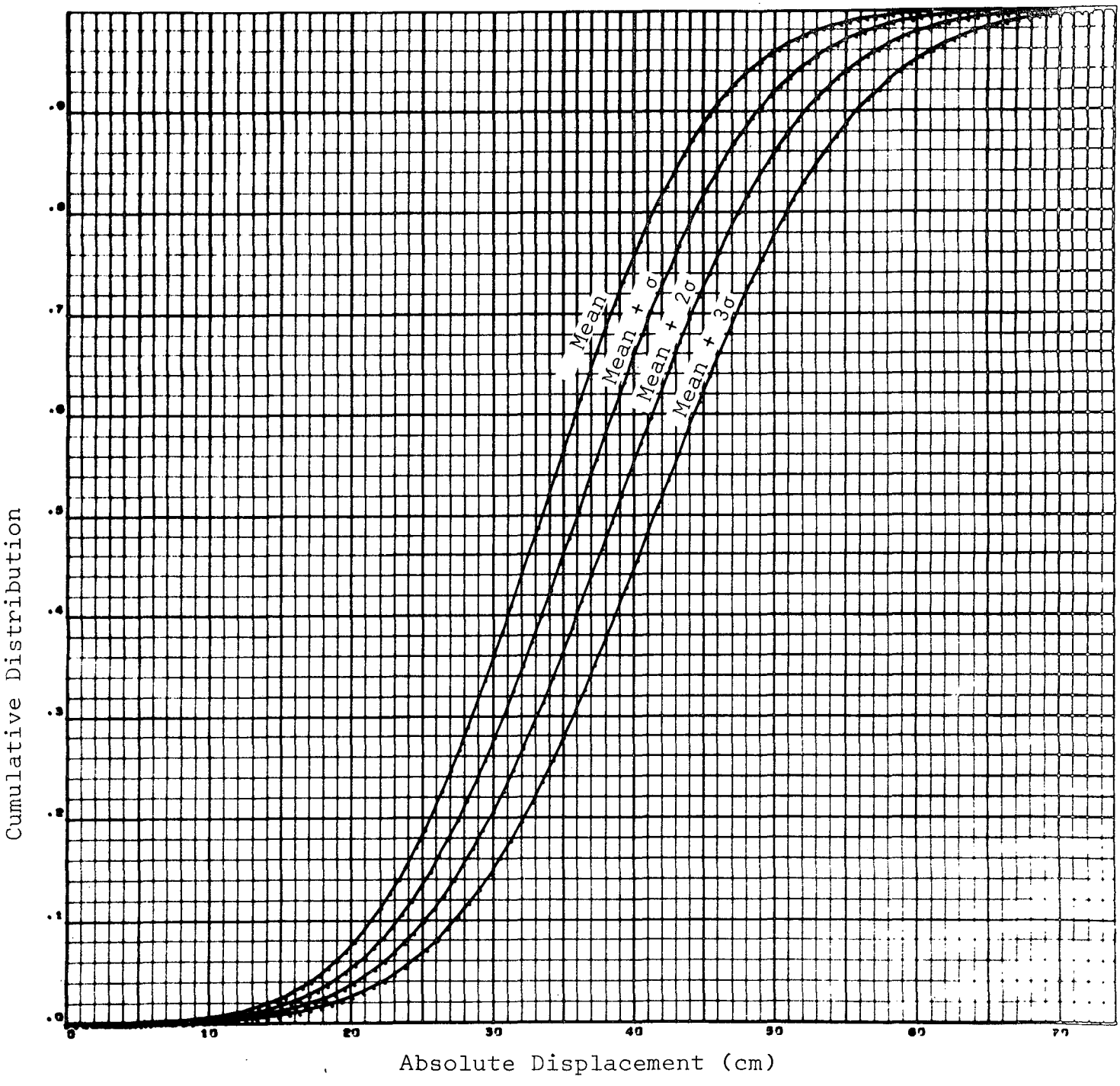

FIG. 6.9 CUMULATIVE DISTRIBUTION VERSUS TIP DISPLACEMENT

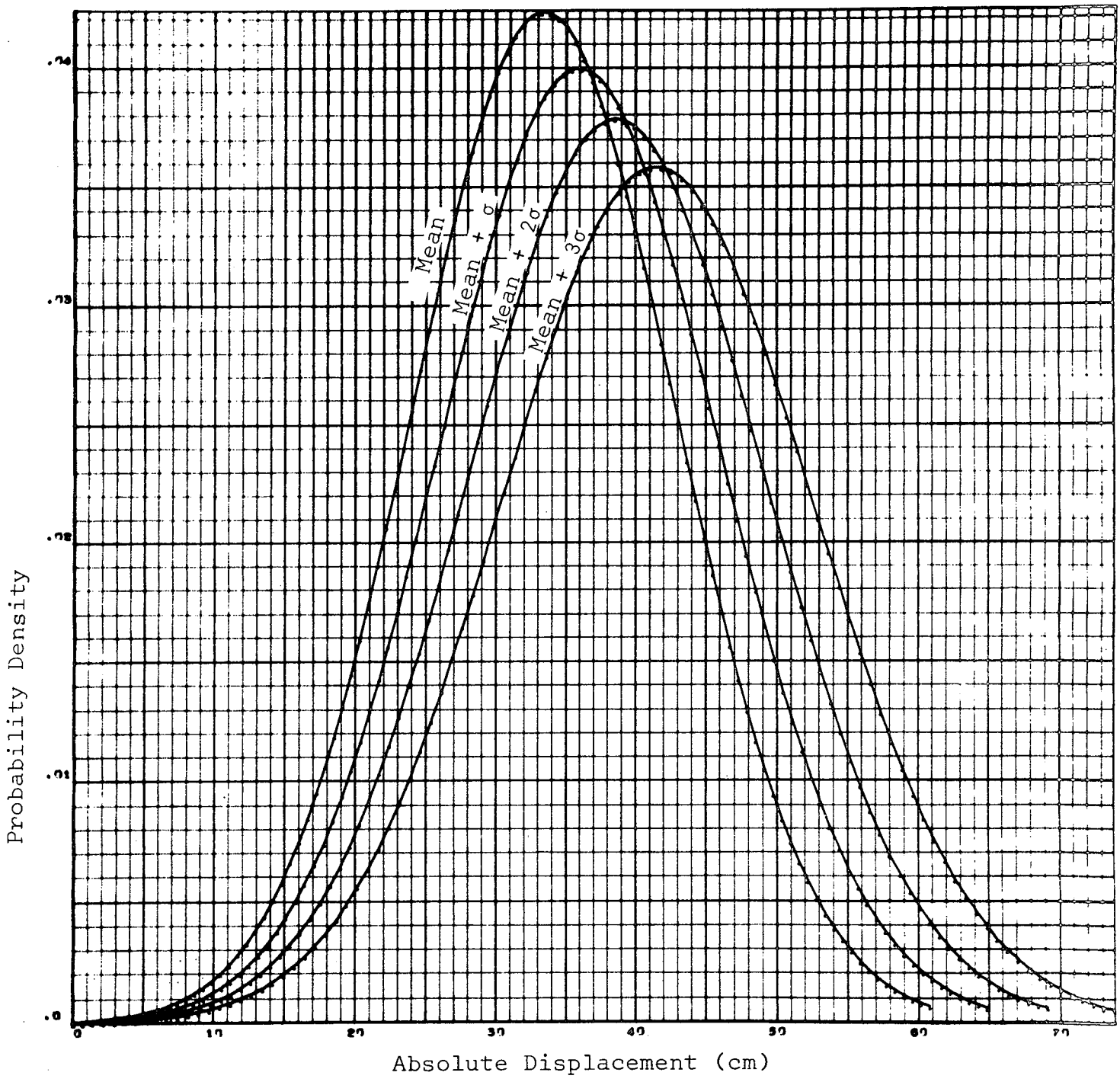

FIG. 6.10 PROBABILITY DENSITY VERSUS TIP DISPLACEMENT

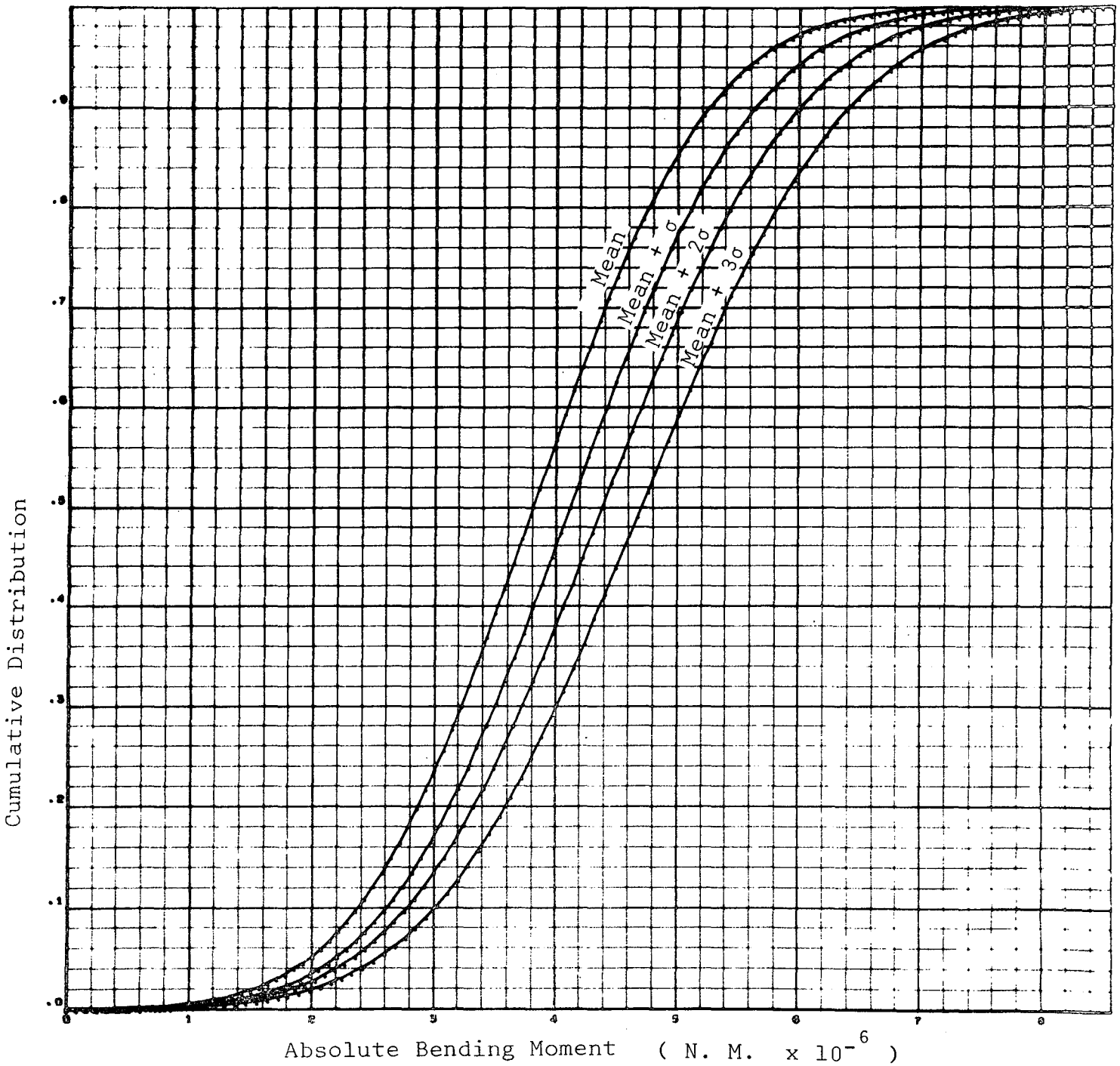

FIG. 6.11 CUMULATIVE DISTRIBUTION VERSUS BASE BENDING MOMENT

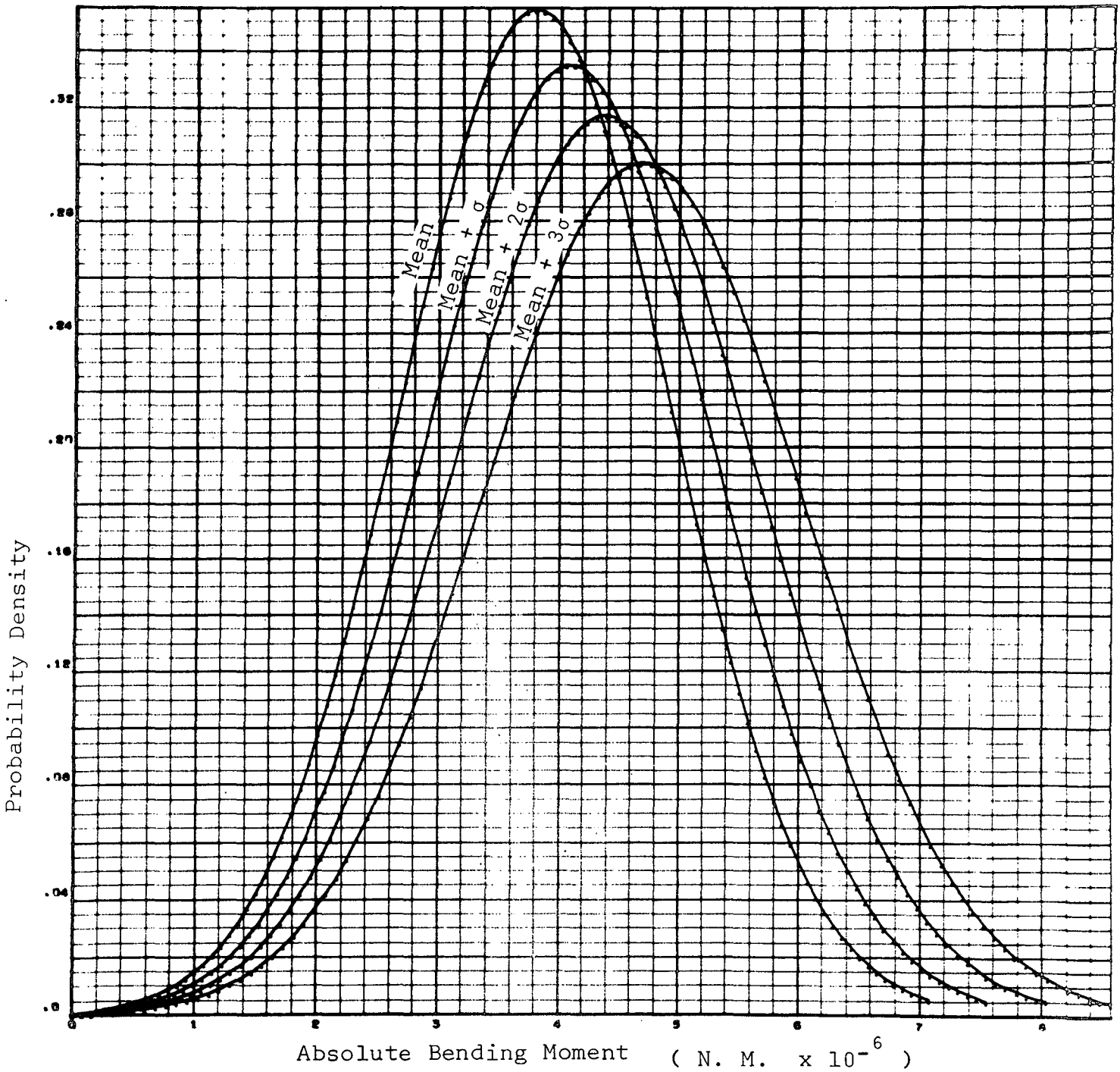

FIG. 6.12 PROBABILITY DENSITY VERSUS BASE BENDING MOMENT